Process Evaluation Tools for Enzymatic Cascades Welcome Message

Abu, Rohana

Publication date:
2016

Document Version
Publisher's PDF, also known as Version of record

Process evaluation tools for enzymatic cascades

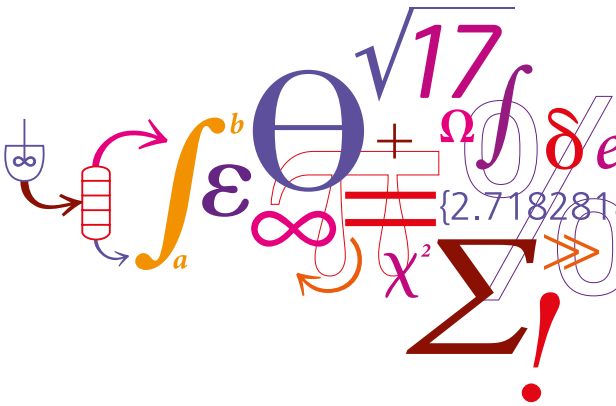

Rohana Abu

PhD Thesis

March 2017

DTU Chemical Engineering
Department of Chemical and Biochemical Engineering

PROCESS EVALUATION TOOLS FOR ENZYMATIC CASCADES

ROHANA ABU

Ph.D. Thesis

DTU Chemical Engineering
Department of Chemical and Biochemical Engineering

Address: CAPEC-PROCESS Research Center

Department of Chemical and Biochemical Engineering

Technical University of Denmark

Building 229

Dk-2800 Kgs. Lyngby

Denmark

Phone: +45 4525 2800

Web: www.capec-process.kt.dtu.dk/

Print: STEP

DTU Chemical Engineering
Department of Chemical and Biochemical Engineering

Abstract

Biocatalysis is attracting significant attention from both academic and industrial scientists due to the excellent capability of enzyme to catalyse selective reactions. Recently, much interest has been shown in the application of enzymatic cascades as a useful tool in organic synthesis to synthesize valuable compounds (e.g. chiral molecules) especially as pharmaceutical intermediates and to assist complex reactions that otherwise has problems as single step system. Despite this interest, process evaluation of many enzymatic cascades have only rarely been reported in the search for process improvement and implementation. Hence, the goal of this thesis is to evaluate the process concepts in enzymatic cascades in a systematic manner, using tools such as thermodynamic and kinetic analysis. Three relevant case studies have been used to exemplify the approach.

In the first case study, thermodynamic and kinetic studies were used to evaluate the favourability of a redox neutral cascade for the asymmetric amination of alcohols to their corresponding chiral amines. This synthetic cascade is potentially attractive since it synthesizes valuable chiral molecule from cheap raw materials as well as maximising the atom economy. The scheme consists of two primary enzymes (alcohol dehydrogenase and ω-transaminase) that are directly involved in the main synthesis. Alanine dehydrogenase was introduced as a secondary enzyme to regenerate the co-factor NAD^+ and co-substrate alanine *in situ* as well as to shift the equilibrium positions in the main syntheses. In principle, this strategy could successfully achieve high conversion, using ammonia as the sole reagent used in excess to drive the conversion. The findings herein indicate that quantitatively the possibilities for improving the conversion of thermodynamically limited reactions are not only via application of enzyme coupling reactions (coupling the unfavourable reaction with an energetically favourable reaction) but also by matching the relative reaction rates between the interconnecting enzymes.

When the reaction steps are independent in a cascade, the kinetics can be controlled in a highly efficient way to achieve a sufficiently favourable conversion to a given target product. This is exemplified in the second case study, in the kinetic modelling of one-pot cascade synthesis of 2-ketoglutarate from glucoronate, the second case study. This cascade consists of 4 enzymes (uronate dehydrogenase, glucarate dehydratase, keto-deoxy-d-galactarate dehydratase and α-ketoglutaric semialdehyde dehydrogenase) run in that order to successfully achieve high conversion.

Finally, a third case study was used to explore the effect of activity-coefficients in enzyme-catalysed reactions. Frequently, the 'apparent' or (concentration-based) equilibrium constant (K'), instead of activity-based equilibrium constant, was used to describe reaction equilibria of biological systems. It is assumed that the reactant activity is equal to the respective reactant molar concentration at equilibrium since many reactions operate in dilute aqueous solutions and thus neglect the activity coefficient effect. The effect of such assumption was therefore tested with the cyclohexanone amination with (*S*)-1-phenylethylamine catalysed by ω-transaminase. The findings showed that the activity coefficients of the components significantly deviate from unity, indicating its non-ideal behaviour in the reaction medium.

Hence, thermodynamic and kinetic analyses are powerful tools to evaluate and to achieve workable cascades for non-natural pathways. Additionally, more meaningful equilibrium data from enzyme-catalysed reactions can be a useful way to determine the effectiveness of a given cascade strategy.

Resumé

Biokatalyse tiltrækker i stigende grad opmærksomhed fra både akademiske og industrielle forskere på grund af dets evne til at katalysere meget selektive reaktioner. Der er for nyligt udvist stor interesse for anvendelsen af enzymatiske kaskader som værktøj i organisk syntese af værdifulde kemiske forbindelser (f.eks. chirale molekyler) specielt som farmaceutiske mellemprodukter og for at levere komplekse reaktioner der udviser bemærkelsesværdige fordele i forhold til ét-trins systemer. På trods af denne interesse er evalueringer af enzymatiske kaskader ud fra et procesmæssigt synspunkt kun sjældent blevet rapporteret i den videnskabelige litteratur. Målet med denne afhandling er derfor at evaluere proceskoncepterne indenfor enzymatiske kaskader ud fra en systematisk fremgangsmåde ved hjælp af værktøjer som termodynamisk og kinetisk analyse. Der er inddraget tre relevante case studier for at eksemplificere fremgangsmåden.

I det første case studie blev termodynamiske og kinetiske studier brugt til at evaluere fordelagtigheden af en redox neutral kaskade til asymmetrisk amination af alkoholer til de tilsvarende chirale aminer. Denne syntetiske kaskade er potentielt attraktiv fordi den syntetiserer værdifulde chirale molekyler fra relativt billige råmaterialer og ligeledes maksimerer atomøkonomien. Reaktionsskemaet består af to primære enzymer (alkoholdehydrogenase og ω-transaminase) der er direkte involveret i hovedsyntesen. Alanindehydrogenase blev introduceret som sekundært enzym for at regenerere co-faktor NAD og co-substrat alanin *in situ* og for at forskyde ligevægtpositionerne i hovedsyntesen. Denne strategi kunne i princippet opnå høj grad af konvertering hvor ammoniak, som eneste reagent, anvendes i overskud for at drive konverteringen. Resultaterne indikerer kvantitativt at mulighederne for at forbedre termodynamisk begrænsede reaktioner ikke kun er via anvendelsen af enzymkoblede reaktioner (at koble den ufordelagtige reaktion med en energimæssigt foretrukken reaktion) men også ved at matche de relative reaktionshastigheder mellem de forbindende enzymer.

Når reaktionstrinnene i en kaskade er uafhængige kan kinetikken kontrolleres yderst effektivt for at opnå en tilstrækkelig omdannelse til et givent slutprodukt. Dette eftervises i det andet case studie involverende kinetiskmodellering af dannelsen af 2-ketoglutarat fra glukoronat. Denne kaskade bestående af fire enzymer (uronatdehydrogenase, glucaratdehydratase, keto-deoxy-d-galactaratdehydratase og α-ketoglutaric-semialdehyde-dehydrogenase), brugt i nævnte rækkefølge, succesfuldt opnåede høj grad af omdannelse.

Endelig blev det tredje case studie brugt til at undersøge effekten af aktivitetskoefficienter i enzymkatalyserede reaktioner. Ofte er den 'oplagte' koncentrationsbaserede ligevægtskonstant (*K'*) brugt i stedet for en aktivitetsbaseret ligevægtskonstant til at beskrive reaktionsligevægte i biologiske systemer. Det blev antaget at den kemiske aktivitet for reaktanterne er ækvivalent med den respektive reaktants molære koncentration ved ligevægt, fordi reaktionen foregår i en fortyndet vandig opløsning hvorved effekten af aktivitetskoefficienten kan negligeres. På trods af dette, bliver der ofte argumenteret for at effekten burde undersøges. Derfor blev amineringen af cyclohexanon med (*S*)-1-phenyletylamin katalyseret af ω-transaminase enzymet brugt som en reaktionsmodel til at undersøge betydningen af aktivitetskoefficienterne. Resultaterne viser at værdier af aktivitetskoefficienterne for komponenterne afviger signifikant fra et, hvilket viser at reaktionssystemet ikke kan antages af opføre sig ideelt.

Det er vist at termodynamiske og kinetiske analyser er effektfulde værktøjer til af evaluere og opnå virksomme kaskader for ikke-naturlige stofskifteveje. Dog skal det siges at mere meningsfulde ligevægtsdata fra enzymkatalyserede reaktioner vil være brugbare for at fastslå effektiviteten af sådan en strategi.

List of Publications

- **Abu R** and Woodley, JM. 2015. Application of Enzyme Coupling Reactions to Shift Thermodynamically Limited Biocatalytic Reactions. *ChemCatChem*, 7, 3094–3105.
  Type: Mini-review paper

- Gundersen MT, **Abu R**, Schürmann M. and Woodley, JM. 2015. Amine donor and acceptor influence on the thermodynamics of ω-transaminase reactions. *Tetrahedron: Asymmetry*, 26, 567–570.
  Type: Research paper

- Palacio CM, Crismaru CG, Bartsch S, Navickas V, Ditrich K, Breuer M, **Abu R**, Woodley JM, Baldenius K, Wu B and Janssen DB. 2016. Enzymatic network for production of ether amines from alcohols. *Biotechnology and Bioengineering*, 113, 1853–1861.
  Type: Research paper

- **Abu R**, Gundersen MT and Woodley JM. 2015. Thermodynamic Calculations for Systems Biocatalysis. *In 12th International Symposium on Process Systems Engineering and 25th European Symposium on Computer Aided Process Engineering* Elsevier, 37, 233–238.
  Type: Conference paper & poster presentation

- **Abu R**, Lima Ramos J and Woodley JM. 2014. Thermodynamic Evaluation of the Production of Chiral Amines from Long-Chain Aliphatic Alcohols. *3rd Multistep Enzyme Catalyzed Processes Congress*, Madrid, Spain, 7–10 April 2014.
  Type: Poster and oral presentation

- **Abu R** and Woodley JM. 2014. Thermodynamic Evaluation of the Production of Chiral Amines from Long-Chain Aliphatic Alcohols. *COST Training School*, Siena, Italy, 28 May - 1 June 2014.
  Type: Poster and oral presentation

- **Abu R** and Woodley JM. 2014. Process Considerations for Systems Biocatalysis. *Bioprocess Engineering Course*, Superstar, Brac, Croatia, 21 – 27 September 2014.
  Type: Poster presentation

- **Abu R** and Woodley JM. 2014. Equilibrium study of ω-transaminase reactions. *Systems Biocatalysis: New Enzymes, New Pathways, New Products*, Siena, Italy, 27 April – 1 May 2016.
  Type: Poster and oral presentation

Acknowledgement

This thesis is submitted in partial fulfillment of the requirements for the Doctor of Philosophy (PhD) at the Technical University of Denmark (DTU). The PhD research work was carried out from October 2013 to September 2016 and was supported by the Malaysian Ministry of Education and Universiti Malaysia Pahang. This thesis was prepared at the CAPEC-PROCESS Center at the Department of Chemical and Biochemical Engineering under the main supervision of Professor John M. Woodley and co-supervision of Associate Professor Krist V. Gernaey.

I am grateful to Professor John M. Woodley, who always inspired and motivated me to believe in myself and able to grow as a person. Thank you so much for the fruitful discussions that were always stimulating and exciting. It helped me a lot to improve the research work. I could not have done this without his constant support and guidance throughout this journey.

I would also like to thank all the collaborators, Prof. Dr. Dick B. Janssen for the opportunity to contribute in an interesting industrial case study (Enzymatic network for production of ether amines from alcohols). I also thank Prof. Dr. Volker Sieber Group at Technical University of Munich for providing the experimental data used in the modelling of enzymatic cascades in the formation of 2-ketoglutarate from glucoronate and to the Prof. Dr. Gabriele Sadowski Group at TU Dortmund for the collaboration in the stimulating thermodynamic project.

Many thanks to all my friends at the CAPEC-PROCESS center for the wonderful time we had together in any occasions. Special thanks to my office mates, Catarina Sanches Seita and Maria T. Gundersen, for the fruitful discussion in academic things, but we also shared our memories together.

Finally, my deepest thanks go to all my family members and Malaysian friends for their love and support throughout this PhD journey. The three years of distance between my family (in Malaysia) and myself (here in Denmark) made me really realize how important they are in my life.

Table of Content

Abbreviations

ACP	Acetophenone
AlaDH	Alanine dehydrogenase
AlcDH	Alcohol dehydrogenase
ADH	Alcohol dehydrogenase
ALS	Acetolactate synthase
CO	cyclohexanone
CA	cyclohexylamine
COSMO-RS	Screening MOdel for Realistic Solvents
E	Enzyme
EC	Enzyme class
ePC-SAFT	Electrolyte perturbed-chain statistical fluid theory
FID	flame ionization detector
GC	Gas chromatography
GC	Group contribution method
GDH	Glucose dehydrogenase
I	Intermediate
IS	Internal standard
IPA	Isopropylamine
IScPR	*in situ* co-product removal
ISPR	*in situ* product removal
LDH	Lactate dehydrogenase
NAD	β-Nicotinamide adenine dinucleotide, oxidised form
NADP	β-Nicotinamide adenine dinucleotide phosphate, oxidised form
NADH	β-Nicotinamide adenine dinucleotide, reduced form
NADPH	β-Nicotinamide adenine dinucleotide phosphate, reduced form
NOX	NADH-oxidase
PDC	Pyruvate decarboxylase
PEA	(*S*)-Phenylethylamine
PGC	Pseudo-isomeric group contribution
PhEtOH	(*S*)-Phenylethanol
P	Product
PLP	Pyridoxal phosphate
Pyr	Pyruvate
QMM	Quantum mechanics method
S	Substrate
TEA-HCl	Triethylamine hydrochloride buffer
Tris-HCl	Tris hydrochloride buffer
ω-TA	ω-Transaminase
TECRDB	Thermodynamics of enzyme-catalysed reactions database
YADH	Yeast alcohol dehydrogenase

Nomenclature

a	Activity (–)
γ	Activity coefficient (–)
ee	Enantiomeric excess (%)
ΔG_r^o	Standard Gibbs free energy change of reaction (kJ)
$\Delta G_r'^o$	Standard Gibbs free energy change of biologically-mediated reaction (kJ)
ΔG_f^o	Standard Gibbs free energy of formation (kJ)
$\Delta G_f'^o$	Standard Gibbs free energy of formation of biologically-mediated reaction (kJ)
ΔG_r	Gibbs free energy change of reaction under non-standard-state conditions (kJ)
$\Delta G_r'$	Gibbs free energy change of biologically-mediated reaction under non-standard-state conditions (kJ)
$\Delta H_r'^o$	Standard enthalpy change of reaction (kJ/mol)
K'	Apparent equilibrium constant, concentration-based equilibrium constant (–)
K_a	Activity-based equilibrium constant (–)
K_eq	Equilibrium constant (–)
K_i	Inhibition constant (mM)
K_Si	Substrate inhibition constant (mM)
K_m	Michaelis-Menten constant (mM)
K_m	Concentration-based equilibrium constant (–)
K_γ	Concentration-based reactant and product activity coefficient (–)
m	Molal concentration (mol/kg)
c	Molar concentration (mol/L)
Q	Reaction quotient (mM)
R	Gas constant (8.314 J K^{-1} mol^{-1})
T	Temperature (^{o}C)
U	Units (μmol/min)
V_max	maximal volumetric reaction velocity (mM/min)

1 Introduction

1.1 Overview of the study

Today, the application of a single enzymes for organic synthesis is successfully established for a specific reaction (biocatalysis), especially in pharmaceutical and fine chemical industry (Turner and O'Reilly 2013). Potentially even more interesting would be the coupling one or more enzymes to catalyse several chemical reactions in the form of cascades, which is one of the strategies of choice for greener and more sustainable processes (Wenda et al. 2011; Riva and Fessner 2014). Indeed, cascades operate under relatively mild process conditions (e.g., ambient pressure (atmospheric) and temperature (20–50^{o}C), pH 5.0–8.0, aqueous solution)). The high selectivity of enzymes enables excellent atom economy as well as minimizing waste materials (Ma et al. 2010). These advantages make such processes greener and more sustainable than conventional chemical catalysis.

Although the number of interesting enzymatic cascades in the scientific literature has been increasing over the past few years (Bruggink et al. 2003; Findrik and Vasic-Racki 2009; Ricca et al. 2011; Simon et al. 2014; Riva and Fessner 2014; Köhler and Turner 2014; Muschiol et al. 2015), the full potential of implementation at an industrial scale remaining relatively limited. In general, enzymatic cascades are characterised by a high degree of complexity due to the combination of several enzyme activities (Santacoloma et al. 2011). This complexity may pose challenges, particularly related to thermodynamic limitations and enzyme kinetics.

In nature, an individual enzyme usually works as part of a larger enzymatic network (Bruggink et al. 2003). For example in microbial cells complete metabolic pathways convert simple starting molecules to complex products via multiple reaction steps. One feature of such pathways is that they are thermodynamically favourable, in part due to coupling those reactions which are thermodynamically unfavourable (positive Gibbs free energy) with those which are favourable (negative Gibbs fee energy). In some cases, reactions which can be very useful synthetically *in vitro* will need to be run in the opposite direction to that found *in vivo*. Hence, in principle by coupling an unfavourable reaction with a more favourable one, as in nature, a given synthetic scheme can also be made to work. While these principles are already established, the actual values of Gibbs free energy for individual reactions are rarely reported. Hence understanding the precise role of coupling reactions in the network is often not possible. Besides, many studies, to some extent, have successfully

overcome thermodynamic constraints in the application of coupling cascades (Abu and Woodley 2015). Remarkably, very little information on thermodynamics was quantified in such studies.

Additionally, the enzymatic cascades typically involve a combination of several engineered enzymes (which may come from different hosts) *in vitro* for the conversion of a non-natural substrate. However, the results, the substrate scope and kinetic profile of the coupling enzymes need to be matched. For example, unbalanced rates between the interconnecting enzymes (low activity of one enzyme compared to the other), will contribute to the accumulation of intermediate compounds or by-products in the reaction mixture and thus renders the synthesis inefficient. To date, process and kinetic modelling of enzymatic cascades has been less explored, due to the complexities of incorporating kinetic models of individual enzymes with such many kinetic parameters involved (Xue and Woodley 2012).

In the long term, many examples of enzymatic cascades will be forthcoming as one of the valuable tools in organic synthesis (Muschiol et al. 2015). It would be therefore valuable to evaluate the process concept of enzymatic cascades in a systematic manner. By using a set of existing tools such as, thermodynamic and kinetic analysis, the favourability (by improving the target conversion) and the efficiency (by improving the enzyme kinetics) of enzymatic coupling in a given case can be evaluated.

1.2 Objective of the Study

The objective of this study is to evaluate the process concepts of enzymatic cascades in a systematic manner, by the use of tools, thermodynamic and kinetic analysis, in the search for process improvement and implementation.

1.3 Scope of the Study

The scope of this study is drawn in order to achieve the objective:

1. **Thermodynamic study:** Obtaining thermodynamically meaningful equilibrium data for enzyme-catalysed reactions (e.g. equilibrium constant, Gibbs free energy of reactions). Such properties, can be used to evaluate the favourability of enzyme coupling, for example, to what extend the thermodynamically favoured reactions can drive the unproductive equilibrium reactions towards achieving the target equilibrium conversion for a cascade system. Moreover, the influence of activity coefficient on the concentration-based equilibrium constant in aqueous solution was also studied for a transamination reaction. This study was also targeted

to understand how the equilibrium position changes with varying physical reaction conditions such as pH, temperature, concentration and solvents.

2. **Kinetic study:** Developing kinetic models to evaluate the enzymatic cascades. Besides, understanding the process behaviour of the cascade, the mathematical modelling was used to predict the performance of the cascades (e.g. to find the suitable enzyme activity and substrate concentrations) under the required conditions and to predict the relevant kinetic parameters.

3. **Case studies:** Using relevant case studies, the process concepts in the enzymatic cascades can be evaluated via tools, thermodynamic and kinetic analysis.
    i. Case study 1: Thermodynamics and kinetics of ω-transaminase-based cascades for the production of chiral amines from alcohols. In this case study, thermodynamics and kinetics of the cascade were investigated.
    ii. Case study 2: One-pot cascade synthesis of 2-ketoglutarate from glucuronate. The kinetic modelling was developed to describe and understand the dynamic behaviour of the cascade.
    iii. Case study 3: Use of activity coefficients in determining the equilibrium constant in the ω-transamination of (*S*)-phenylethylamine. The question of whether the activity coefficients should to be taken into account in calculating the equilibrium constants was addressed in this study.

1.4 Thesis Outline

This section describes the overview of the overall thesis.

Chapter 1 (Introduction)

This chapter introduces the overall thesis and the objective to be met within the scope of the study.

Chapter 2 (Biocatalysis and enzymatic cascades)

This chapter introduces the basic concepts and a new emerging concept of enzymatic cascade as well as the limitations and challenges in this area.

Chapter 3 (Thermodynamics of enzymatic cascades)

This chapter covers the background of the application of enzyme coupling reactions to shift thermodynamically limited biocatalytic reactions. The chapter emphasizes the ω-transaminase-catalysed reactions and also discusses the advantages and disadvantages of such a strategy and its implications for process implementation.

This chapter was written for the paper publication: Abu R and Woodley, JM. 2015. Application of Enzyme Coupling Reactions to Shift Thermodynamically Limited Biocatalytic Reactions. ChemCatChem, 7, 3094–3105.

Chapter 4 (Process evaluation tools)

This chapter describes the tools used for the process evaluation throughout this study and summarized in **Figure 4.1**. The chapter starts from how to obtain the thermodynamic data (thermodynamic database, experimental measurement and property prediction methods) and how to balance with the kinetic measurement and modelling.

Chapter 5 (Thermodynamics and kinetics of ω-transaminase-based cascades for the production of chiral amines from alcohols)

This chapter explains the first case study in the thesis. The thermodynamic and kinetic analyses were used to evaluate the ω-transaminase-based cascade for the production of (*S*)-phenylethylamine.

*This chapter was written for the paper publication: **Abu R**, Gundersen MT and Woodley JM. 2015. Thermodynamic Calculations for Systems Biocatalysis. In 12th International Symposium on Process Systems Engineering and 25th European Symposium on Computer Aided Process Engineering Elsevier, 37, 233–238.*

Chapter 6 (One-pot Cascade Synthesis of 2-Ketoglutarate from Glucuronate)

This chapter covers the kinetic modelling of enzymatic cascade in the formation of 2-ketoglutarate from glucoronate. This cascade consists of 4 enzymes (uronate dehydrogenase, glucarate dehydratase, keto-deoxy-d-galactarate dehydratase and α-ketoglutaric semialdehyde dehydrogenase) run sequentially in a cascade system.

The kinetic data were kindly provided from Professor Dr. Volker Sieber Group at Technical University of Munich.

Chapter 7 (The use of activity coefficients in determining the equilibrium constant in the ω-transamination of (*S*)-phenylethylamine)

This chapter shows the role of activity coefficients in determining the equilibrium constant in enzyme-catalysed reaction. The cyclohexanone amination with (*S*)-1-phenylethylamine catalysed by the ω-transaminase enzyme was used as a model reaction.

This chapter was written for the manuscript in collaboration with Professor Dr. Sadowski Group at TU Dortmund.

Chapter 8, 9 and 10 (Discussions, Conclusions and Future works)

The central discussion of the thesis is presented in Chapter 8 and concludes with the significant contributions in Chapter 9 and recommendation for future research in Chapter 10.

2 Biocatalysis and Enzymatic Cascades

2.1 Biocatalysis

Today, biocatalysis is established as a powerful tool for organic synthesis, especially for the synthesis of high value products (e.g. chiral molecules and intermediates compounds) in the pharmaceutical industry (Pollard and Woodley 2007; Wenda et al. 2011; Lalonde 2016). The scope of biocatalysis has been growing in the last few years, beyond the production of fine chemicals, to include fuels and bulk chemicals (Illanes et al. 2012). Many of the opportunities have been driven by the excellent selectivity of enzymes. This key feature of enzymes outperforms conventional chemical catalysts, particularly in producing high yields of enantiomerically pure chiral molecules such as, amines, alcohols, amino acids, epoxides and lactones (**Table 2.1**).

Additionally, the key developments in protein engineering also play a significant role, due to improved enzymes properties to suit the requirement for industrial applications. Problems that are frequently encountered in biocatalysis such as, low operational stability, and insufficient activity, can now be improved by the advanced protein engineering techniques. The techniques such as, directed evolution, rational design, molecular and computational modelling, gene shuffling and screening methods (Turner 2009; Illanes et al. 2012; Singh et al. 2013; Woodley 2013; Reetz 2013; Adrio and Demain 2014), are used to improve properties (**Table 2.2**) as well as to develop more efficient and cost-effective biocatalysts (Jemli et al. 2016). Following the discovery of more novel enzymes such as, C–C, C–N, and C–O bond- forming biocatalysts, new opportunities are also growing in the synthesis of functionalized and complex molecules with multiple chiral centres for example, amino alcohols (Sehl et al. 2014; Nestl et al. 2014). Although protein engineering offers huge potential as a very useful and efficient tool to tailor the biocatalyst, such methods to some extent cannot justify and make an ideal biocatalyst for industrial purposes. Integrating with reaction engineering solutions such as, feeding strategies, *in situ* product removal and multi-phase operations, can guide protein engineering to fit the process demands, thus avoiding 'over'-engineering enzymes (Ringborg and Woodley 2016).

Table 2.1: Examples of synthesis of enantiomerically pure chiral molecules, for pharmaceutical applications

Enantiomerically pure molecules	Reaction scheme	Example of process & biocatalyst challenges	References
Chiral amines	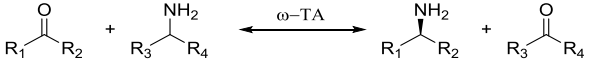 ω-transaminase (EC 2.6.1.18)	• unfavorable equilibrium • low substrate solubility in aqueous solution • substrate & product inhibition	(Tufvesson et al. 2011)
	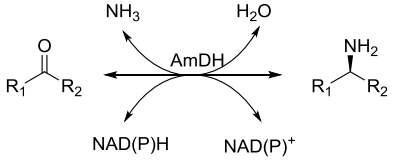 Amine Dehydrogenase (EC 1.4.99.3)	• low substrate specificity • lack of stereospecificity	(Abrahamson et al. 2012; Bommarius et al. 2014)
	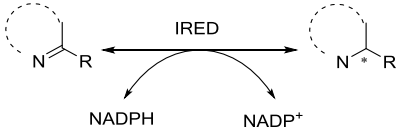 Imine reductase (EC 1.5.1.X) (example, chiral indolines)	• low substrate specificity • lack of stereospecificity	(Hussain et al. 2015; Li et al. 2015)

Chiral amines	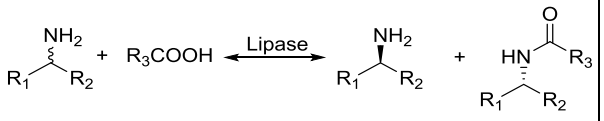 Lipase (EC 3.1.1.3)	• unfavourable equilibrium	(Balkenhohl et al. 1997)
Chiral alcohols	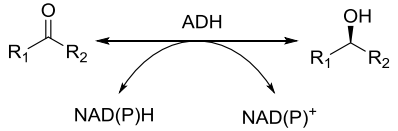 Alcohol dehydrogenases (EC 1.1.1.1, NAD-dependent) and (EC 1.1.1.2, NADP-dependent)	• co-factor recycling • low substrate solubility in aqueous solution	(Höllrigl et al. 2008; Leuchs and Greiner 2011)
Chiral amino acids	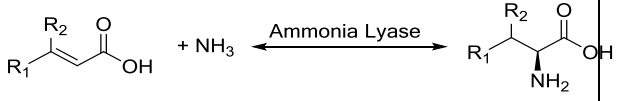 Ammonia Lyases (EC 4.3.1.X)	• unfavorable equilibrium • low substrate specificity	(Tewari 1990; Turner 2011)
Two chiral carbon centers	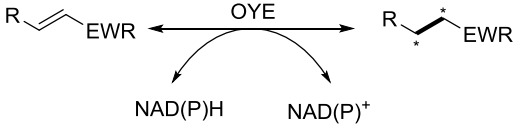 Ene-reductases (EC 1.3.1.31)	• co-factor recycling • enzyme stability in the presence of enone substrate	(Flickinger 2009; Tauber et al. 2011)

Chiral epoxides	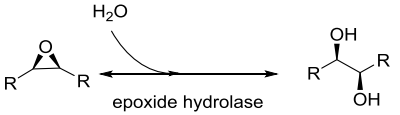 epoxide hydrolase (EC 3.3.2.9)	• co-factor recycling • lack of stereospecificity	(Kotik et al. 2011)
Chiral lactones, (e.g. chiral enol- and ene-lactones)	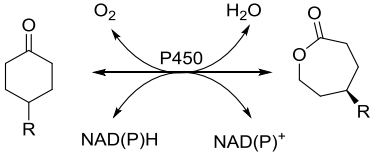 Baeyer–villiger monooxygenases (EC 1.14.13.X)	• co-factor recycling • substrate & product inhibition • poor oxygen-transfer rates • degradation of the product	(Torres Pazmiño et al. 2008)

Table 2.2: Improved enzyme properties via protein engineering

Enzyme properties	Improved enzyme properties
Activity	• increase activity at given process conditions
Specificity	• high stereoselectivity, regioselectivity and enantioselectivity
Stability	• long-term stability • tolerant to the extreme pH, temperature, high concentration of substrate/product, presence organic solvents

In the challenge to develop process cost-effectively, metrics for biocatalytic processes such as, pharmaceutical, fine and bulk chemicals have been developed to give quantitative values and to identify and remove bottlenecks (Tufvesson et al. 2011; Lima-Ramos et al. 2014). Engineering tools can be used to evaluate the process feasibility including process and kinetic modelling (Santacoloma et al. 2011), and economic and environmental analysis (Lima-Ramos et al. 2014). The successful approach in reaction engineering is not new in biocatalysis, which is an effective way in minimising the product and substrate inhibition by *in situ* product removal and substrate feeding strategies, respectively. Besides, the equilibrium of unfavourable thermodynamic reactions can be improved successfully (independent to biocatalyst) by using an excess of a co-substrate (to push the equilibrium position) or removing one of the products during the reaction by *in situ* product removal (to pull the equilibrium position) towards the target product (Abu and Woodley 2015). Additionally, ISPR techniques can be applied by either evaporation under reduced pressure (for volatile products) or extraction into an organic solvent phase (for hydrophobic products). Another emerging process concept, so-called "coupling enzymes" can also be used to assist thermodynamically limited reactions. Moreover, the concept of a 'one-pot' reaction consists of enzymatic cascades as for example, can substantially decrease the amount of reactants used and the down-stream processing steps as well as minimised the waste production, to further improving the sustainability of enzymatic processes. Besides the benefits, enzymatic cascades are also one of important tools nowadays for organic synthesis in making more valuable compounds (e.g. multi-chiral centres) which even more interesting the use of cheap materials as the starting materials. This process concept of cascade biocatalysis is the

central topic in this thesis where the process consideration and evaluation are essential for implementation of such processes as for a new generation of biocatalysis.

2.2 Enzymatic Cascades

In recent years, much interest has been shown in the application of enzymatic cascades in many chemical syntheses. 'Enzymatic cascades' has been broadly used as a term to describe the use of more than one enzyme in a synthetic scheme *in vitro*. Several synthetic schemes have been proposed to produce valuable chemicals, by providing valuable alternative routes, since in most cases, enzymes operate under relatively similar reaction conditions (e.g., mild pressure (atmospheric) and temperature (20–50^{o}C), pH 5.0–8.0, aqueous solution), which ease the combination of enzymes into the synthetic scheme (Riva and Fessner 2014). Besides, the enzymatic cascades can provide added value to a synthetic scheme by starting from cheaper raw materials or making more valuable products (e.g. chiral compounds, multiple–chiral centres). Additionally, it is possible to combine several enzymes as in **Table 2.1**, in order to make a new synthesis route. For example, ene-reductase combined with ω-transaminase-catalysed reaction to synthesis chiral amines whereas the combination of ene-reductase with alcohol dehydrogenase to produce chiral alcohols.

2.2.1 Basic concept of enzymatic cascades

Three basic concepts can be found in the scientific literature, specifically, linear-, parallel-, and orthogonal enzymatic cascades as shown in **Figure 2.1** (Simon et al. 2014). Such synthetic cascades are arranged in such a way to meet the process requirements, for example, the need to recycle co-factors or co-substrates, to overcome thermodynamic equilibrium limitations, to remove toxic compounds, and or to minimize kinetic inhibitions.

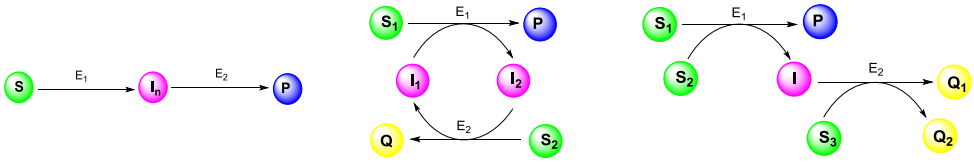

(a) Linear cascade

(b) Parallel cascade

(c) Orthogonal cascade

Figure 2.1: The classifications of enzymatic cascades; enzyme (E), substrate (S), product (P), by-product (Q), intermediate (I), and number of compounds (*n*)

2.2.1.1 Linear cascade

In a linear cascade, a sequence of enzymes is arranged in a way to convert substrates to intermediate(s) and subsequently to the target products **(Figure 2.1a).** In some cases, it is not necessary to isolate and purify the intermediates for each conversion step. The decision is made dependent on enzyme activity and stability, particularly when the cost of each enzyme is not critical. For example, in the two-step reactions in a one-pot system in the conversion of aromatic amino alcohols to cyclic amides (**Figure 2.2**). Here, the pH-sensitive galactose oxidase M_{3-5} variants (GOase M_{3-5}) can be operated sequentially in a one-pot at pH 7 with *E. coli* xanthine dehydrogenase (XDH, able to work in a wide pH range between 7.0 to 8.5) to give viable conversion >99% (Herter et al. 2015). A recent example is in the production of multiple chiral centres such as, the preparative synthesis of chiral amino alcohols from achiral starting materials using a two-step reaction of transketolase/transaminase cascade system (Rios-Solis et al. 2015).

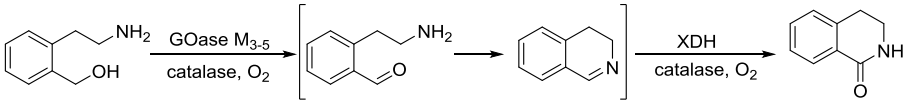

Figure 2.2: GOase M_{3-5}/XDH system in the synthesis of 3,4-dihydroisoquinolin-1(2H)-one

2.2.1.2 Parallel cascades

Parallel cascades are the most typical scheme found in the scientific literature (**Figure 2.1b**). One of the important examples is in the co-factor regeneration system. Cofactors are crucial for the functionality of certain enzymes, particularly in the enzyme-catalysed redox reactions (Voss et al. 2008). Feeding cofactors into a reactor is expensive if added in stoichiometric amounts (Kratzer et al. 2015) and it is therefore necessary to regenerate the cofactor *in situ* using a regeneration enzyme e.g. (glucose dehydrogenase, formate dehydrogenase and alcohol dehydrogenase) (Hall and Bommarius 2011; Paul et al. 2014). For example in the enantioselective reduction of aliphatic ketones (**Figure 2.3**), the NADPH-dependent alcohol dehydrogenase (*Lb*ADH, *Lactobacillus brevis*) and the NADP-dependent glucose dehydrogenase (GDH, *Bacillus sp*.) must run simultaneously in parallel at catalytic amounts for efficient cofactor regeneration (Leuchs et al. 2012).

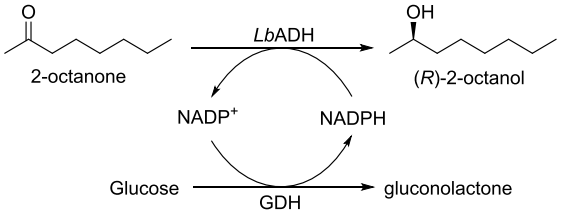

Figure 2.3: *In situ* redox-cofactor recycling. ADH (*Lactobacillus brevis*)/GDH (*Bacillus sp.)* system

2.2.1.3 Orthogonal cascade

An orthogonal cascade is one in which the intermediate(s) such as, by-product or inhibitory product, is removed *in situ* by an additional enzyme that is not directly involved in the main synthesis (**Figure 2.1c**). In some cases, the intermediate(s) is removed in order to improve the yield of thermodynamically challenged reactions (Abu and Woodley 2015). The main synthesis of enzyme-catalysed reactions is frequently restricted due to the unfavourable thermodynamics that can cause a low yield. By coupling an unfavourable reaction with a more energetically favourable reaction in the form of a cascade, the overall equilibrium reaction can be shifted towards the target product, thus increasing the reaction yield. Such techniques are very well studied in the synthesis of chiral amines using ω-transaminase (EC 2.6.1.18) (Abu and Woodley 2015). The equilibrium displacement reaction such as, the pyruvate decarboxylase (PDC, EC1.2.4.1) as shown in **Figure 2.4,** is coupled with an

amine transaminase in order to remove the co-product pyruvate and consequently shift the overall equilibrium position towards the product side, achieving >99% conversion (Höhne et al. 2008). The application of enzyme coupling reactions to shift thermodynamically limited enzymatic reactions is further discussed in Section 3**.**

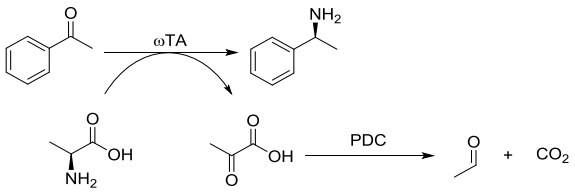

Figure 2.4: Equilibrium displacement reaction system: ω-TA/PDC system

In enzymatic cascades, there are some cases involving the formation of toxic or unstable intermediate that need to be removed immediately in the following reactions. Such cascade reactions can be represented either in parallel or orthogonal schemes. This approach is aimed of keeping such inhibitory compounds below their inhibitory concentration. If the compound has a high potential to accumulate during the course of the reaction, it is therefore necessary to balance the activity between the enzyme in the main reaction and the enzyme that is used to remove the toxic compounds. In this way the rate of formation of the inhibitory product is similar to the rate of consumption of this compound so as to keep the inhibitory concentration at a low level (Muschiol et al. 2015). An interesting example is the oxidation of benzyl alcohol to benzaldehyde as shown in **Figure 2.5**. The presence of catalase is used to minimise the toxic concentration of hydrogen peroxidase (H_2O_2) and to avoid enzyme deactivation in the main synthesis (Toftgaard Pedersen et al. 2015).

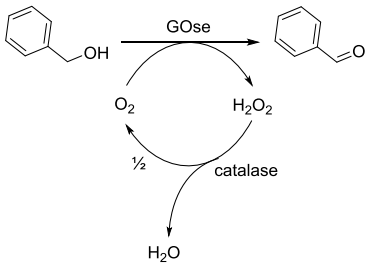

Figure 2.5: the oxidation of benzyl alcohol into benzaldehyde

2.2.2 New concept of enzymatic cascade

Some new concepts in applying a synthetic cascade scheme are shown in **Figure 2.6**. The schemes complement the basic schemes and are aimed at minimising waste generation. Additionally, the atom efficiency can also be maximised, for example in the cyclic (**Figure 2.6a**) and closed-loop cascades (**Figure 2.6c**). Besides making new synthetic pathways, these new generations of enzymatic cascades exploit cheap raw material (e.g. renewable sources) as the starting substrates to synthesize valuable compounds.

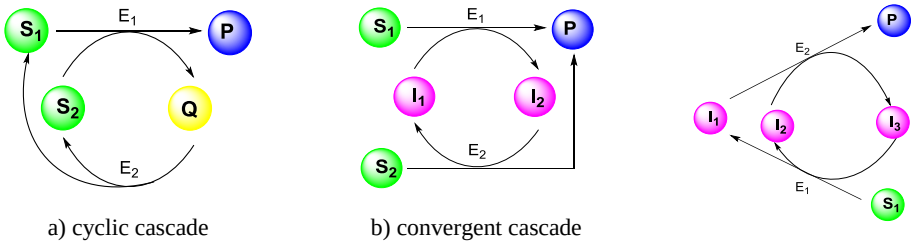

a) cyclic cascade b) convergent cascade c) closed-loop cascades

Figure 2.6: New concept of enzymatic cascades

2.2.2.1 Cyclic cascades

Recently, there is an increasing trend to convert a co-substrate back to the starting material(s) which has been found as cyclic cascade (**Figure 2.6a**). This scheme is limited to certain applications such as, in the deracemisation processes to produce high enantiopure compounds. Here, one enantiomer of the racemic compounds is selectively oxidised to a prochiral product which is later reduced back to the racemic starting material. Interesting example is in the deracemisation of racemic α-chiral primary amines employing of ω-transaminase ATA-117 and ATA-113 (selectively towards *R* and *S*-enantiomer respectively) which were combined in two-step one-pot process, resulting >99% optically pure amine (*S*-product) with isolated yield up to 95% (Koszelewski et al. 2009). Recently, in the deracemisation of racemic benzylic amines employing a one-pot monoamine oxidase/ω-transaminase cascade system, allowing to produce >99% optically pure (*R*)-amines with excellent conversion (O'Reilly et al. 2014).

2.2.2.2 Convergent cascades

Recently, "a double co-substrate" was introduced by the Kara's group through a redox-neutral convergent cascade as shown in **Figure 2.6b** (Bornadel et al. 2015). The first co-substrate allows the formation of a thermodynamically stable co-product that shifts the overall equilibrium towards the desired product, whereas the presence of a 'double-smart co-substrate' allows the coupling to a secondary enzyme to converge to the same target product and give a higher conversion. This new strategy also improves the atom efficiency of the synthesis route. A recent example from the same research group, is in the synthesis of ε-caprolactone through a Baeyer–Villiger monooxygenase/alcohol dehydrogenase, a convergent cascade (Bornadel et al. 2015). This cascade system allows to utilise two molar equivalents of cyclohexanone and one equivalent of 1,6-hexanediol as a 'double-smart co-substrate' to converge to the same target product with only water as sole by-product.

2.2.2.3 Closed-loop cascades

Recently, there is an increasing trend to apply the 'self-sufficient' or 'closed-loop' cascades as shown in **Figure 2.6c** (Torres Pazmiño et al. 2008; Mutti et al. 2012; Sattler et al. 2012; Tauber et al. 2013; Mallin et al. 2013; Hummel and Gröger 2014; Mutti et al. 2015; Chen et al. 2015). An interesting example is the synthesis of ε-caprolactone from cyclohexanol (**Figure 2.7**). In this self-sufficient redox cascade, cyclohexanol is oxidized into ketone by an alcohol dehydrogenase (*Lb*ADH, *Lactobacillus brevis*) and subsequently the ketone is consumed by Baeyer–Villiger monooxygenase (engineered BVMO, C376 LM400I double mutant) to produce ε-caprolactone. Additionally, both involved in the main synthesis and are NADP-dependent with the capability to regenerate *in situ* cofactors between them in the absence of another regeneration enzyme. Results indicate the cascade successfully reached 98% conversion at 200 mM substrate concentration (Sattler et al. 2014). In another study using a similar cascade system, 83% conversion was achieved at preparative scale using wild-type BVMO *Acinetobacter calcoaceticus* (Mallin et al. 2013).

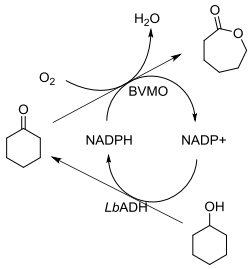

Figure 2.7: Closed-loop enzymatic cascade for the synthesis of ε-caprolactone with lbADH/BVMO

Another example of a closed loop cascade is in the asymmetric amination of alcohols which was developed by Kroutil's group (Sattler et al. 2012). This is interesting since in general, there is no enzyme that is able to directly convert an alcohol into an amine. This artificial system consists of three redox enzymes that provide a way to convert the alcohols to their corresponding amines. One of the schemes is shown in **Figure 2.8a**. Interestingly, the introduction of alanine dehydrogenase (AlaDH) in the cascade serves dual purposes. Besides recycling the co-factor and co-substrate *in situ*, AlaDH reaction is energetically favourable that can therefore also be used to shift both unfavourable reactions (oxidation of alcohols as well as the amination of ketone) achieving a high conversion. However, the major challenge in this cascade is to run the oxidation and amination steps simultaneously, since it is known that ω-transaminase reaction is often hindered by an adverse equilibrium position, particularly using alanine as the amino donor (Shin and Kim 1998; Tufvesson et al. 2011; Abu and Woodley 2015), giving a low conversion. Alternatively, a redox-neutral two-enzyme cascade process for the preparation of chiral amines from alcohols has recently been constructed (Mutti et al. 2015; Chen et al. 2015). Here, the alcohols are oxidized by an alcohol dehydrogenase to ketones and subsequently aminated by an amine dehydrogenase (AmDH) to produce the corresponding chiral amines. Interestingly, this approach only requires ammonia as the amino donor and water as the by-product without the addition of alanine and an external reducing agent as in **Figure 2.8b**.

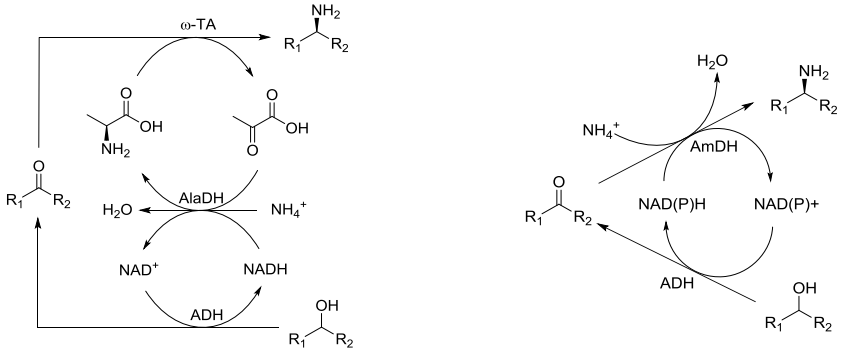

Figure 2.8: Closed-loop cascades in the synthesis of chiral amines. (a) ADH/ω-TA/AlaDH and (b) ADH/AmDH coupled system. ADH: alcohol dehydrogenase, ω-TA: ω-transaminase, AlaDH: alanine dehydrogenase, AmDH: Amine dehydrogenase.

2.2.3 Challenges in enzymatic cascades

Despite great interest in the application of enzymatic cascades, the feasibility of many enzymatic cascades (as described in the previous subsections) has not been reported and is therefore difficult for process evaluation and improvement. Although guidelines for evaluating such process concepts in enzymatic cascades have not yet been established, several engineering tools are available such as process and kinetic modelling, thermodynamic modelling, sensitivity and uncertainty analysis, windows of operation and bottleneck analysis. The tools can help the process evaluation of a given enzymatic cascade under defined process conditions. Besides, such tools are most useful in understanding the process behaviour as well as the effects of process variables of coupling techniques on kinetic and thermodynamic parameters. Therefore the process challenges and solutions for enzymatic cascades should be identified and solved for further process development of such processes.

The main challenge in enzymatic cascades is to identify suitable compatible reaction conditions since often involve many interactions between enzymes, substrate(s), co-factors, intermediates, reagents and product(s). For example, the complexity of reactions increases when more than one co-factor recycling system is present in a cascade. In the conversion of (1*S*,5*R*)-Carveol (**a**) shown in **Figure 2.9**, cyclohexanone monooxygenase-catalysed (CHMO, *Acinetobacter sp.*) reaction became a rate limiting step due to the competition of NADH with the enoate reductase-catalysed reaction (ERED). Thus, favouring the alcohol oxidation step (LhADH, *Lactobacillus kefi*) in the self-sufficient redox cascade. Besides, it is clearly important to choose the specific type of cofactors (e.g. NAD-

specific or NADP-specific) that can be accepted for the enzymes in order to avoid competing activities among the cofactor-dependent reactions, or otherwise separating between the competing reactions, *Lb*ADH/ERED and CHMO/G6PDH, would be necessary. The viability of such cascades was achieved only at 4 mM substrate, giving the 88% conversion of target product **(d),** due to the substrate inhibition >10 mM (Oberleitner et al. 2014).

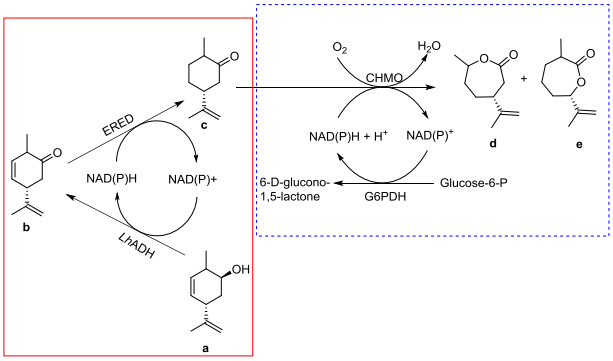

Figure 2.9: Potential competition of NADH in a redox cascade *in vitro* (Oberleitner et al. 2014)

Another example of a complex cascade was performed by Sattler and co-workers (Sattler et al. 2014). The system consists of 7 enzymes with two closed-loop redox cascades where the choice of enzymes and cofactors were carefully selected in order to avoid cross interferences. Another interesting example is in the conversion of aliphatic primary alcohols to the corresponding amines (Pickl et al. 2015). In this cascade, two primary enzymes (long-chain alcohol oxidase from *A. fumigatus* and ω-transaminase from *C. violaceum*) and three secondary enzymes (alanine dehydrogenase, glucose dehydrogenase, and catalase) with the optimized reaction conditions (pH 10, oxygen pressure of 2 bars, cofactors and co-substrate regeneration, substrate concentrations and enzyme ratio). However, such an elegant cascade cannot tolerate at high substrate concentration (>10 mM) due to the complex interactions between enzymes and various compounds and reagents in a one-pot system.

3 Thermodynamics of Enzymatic Cascades

This chapter was written for the paper publication: Abu R and Woodley, JM. 2015. Application of Enzyme Coupling Reactions to Shift Thermodynamically Limited Biocatalytic Reactions. *ChemCatChem*, 7, 3094–3105.

3.1 Introduction

Today biocatalysis has been established as a valuable tool in organic synthesis, especially for the synthesis of optically pure chiral molecules, both at preparative and industrial scale (Liese et al. 2006). While several hundred industrial examples have now been reported, many more have failed to make the transition from laboratory to the process plant. One reason for this is that the most interesting syntheses are not usually found already existing in nature, meaning that it is necessary to engineer enzymes to carry out such conversions at a sufficient rate. Likewise the investment in protein engineering required means that expanding the substrate repertoire becomes equally important to justify implementation of a given biocatalyst. A second reason for the failure of reactions to make the transition from laboratory to process plant is the limitation often imposed by enzymes operating at low concentrations of substrate and product. Indeed it is this very feature that has been evolved in enzymes over millions of years. Here too, protein engineering can provide part of the solution, if screens can be adequately designed. The use of substrate feeding and continuous product removal technologies can also be beneficial. A final challenge to be overcome is that in some cases the thermodynamics of a reaction means that running the synthesis in the desired direction is not energetically favourable. This problem arises surprisingly frequently and while use of an excess substrate or alternatively continuous product removal technologies can be used here also, this remains a major challenge. Recently it was argued that the use of so called ‘coupling enzymes’ to assist thermodynamically limited reactions could also be employed to overcome this problem.

To date, several promising multi-enzyme cascade reaction schemes have been reported in the scientific literature for the synthesis of interesting chemical products (Riva and Fessner 2014). Unlike chemical catalysts, most enzymes operate under relatively similar reaction conditions to each other (e.g. mild pressure (atmospheric) and temperature (20 to 50°C), pH 5.0–8.0, aqueous solution), that

facilitates the sequential combination of enzymes into a synthetic scheme and thereby allows effective reaction engineering strategies to shift the equilibrium, in an analogous way to that done in nature.

Here, the advantages and disadvantages of such a methodology and its implications for process implementation were discussed. The chapter was divided into several sections including an overview of the relevant thermodynamic properties, suitable strategies for shifting equilibria (including the addition of excess of co-substrates, the application of *in situ* product removal and *in situ* co-product removal, as well as enzyme coupling reactions (which is the main focus)) as summarised in **Figure 3.1**. These principles are exemplified with a case-study**.**

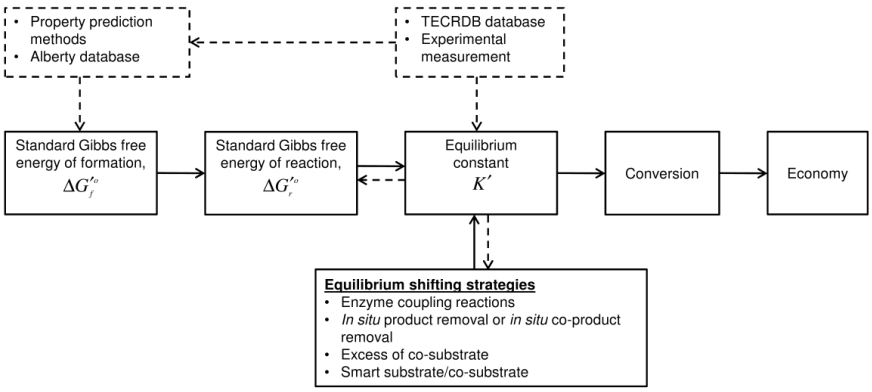

Figure 3.1: Summary of potential process solutions to improve the productivity of thermodynamically challenged biocatalytic reactions. The knowledge of equilibrium constant determines the suitable operating strategies for achieving maximum conversion of thermodynamically-challenged biocatalytic reactions.

3.2 Theoretical Background

The thermodynamic favourability of a chemical reaction can be calculated from the standard Gibbs free energy change of reaction (usually denoted as ΔG_r^o) using Equation 3.1:

$$\Delta G_r^o = \sum_j^p n_j \Delta G_{f,j}^o - \sum_i^r n_i \Delta G_{f,i}^o \tag{3.1}$$

In Equation 3.1, ΔG_r^o is measured under the standard state conditions (1 atm, 298 K, 1 M substrate (reactant) thermodynamic activity; $[H^+]$ is also defined to be 1 M (i.e. pH = 0)). Additionally, in

Equation 3.1, ΔG_r^o is the standard Gibbs free energy of formation of substrate(s) *r* and product(s) *p*. The subscript *i* denotes species of substrate(s), and *j* species of product(s), while *n* is the stoichiometric coefficient of a given species. ΔG_f^o is the change in free energy that occurs when a compound is formed from its elements in their most thermodynamically stable state at standard-state conditions. Usually, for biologically-mediated reactions, the standard Gibbs free energy of reaction is denoted as $\Delta G_r'^o$ to indicate that it is defined at slightly different standard-state conditions (1 atm, 298 K, 1 M substrate activity, while $[H^+]$ is defined to be 10^{-7} M (i.e. pH 7)). In order to calculate the Gibbs free energy in Equation 3.1, the $\Delta G_f'^o$ is needed and this value can be obtained from the Alberty database (Alberty 2003) if the compound is listed. For many metabolites this is very useful, but in the case of a *de novo* pathway (synthetic network), many of the compounds are not listed. As a second approach, such values could also be predicted using computational property prediction tools such as the group contribution method. To complicate further, in practice, biocatalytic reactions rarely operate at the standard-state conditions, and therefore, Equation 3.2 may be used to calculate the Gibbs free energy change of the reaction under non-standard-state conditions (termed ΔG_r). This allows for deviations from standard-state both in temperature and also more importantly concentration.

$$\Delta G_r = \Delta G_r'^o + RT \ln \frac{\prod_j^p c_j^{n_j}}{\prod_i^r c_i^{n_i}} \tag{3.2}$$

In Equation 3.2, *R* is the gas constant, *T* is the temperature, c_i and c_j are the concentrations of substrate and product species, respectively, and *n* is the stoichiometric coefficient of a given species. As indicated in Equation 3.2, usually in a biologically-mediated reaction, the substrate thermodynamic activities are assumed to be equal to the respective substrate molar concentrations (Mavrovouniotis 1991; Villadsen et al. 2011) since the solutions are in general dilute, although the precise influence of such assumptions remain the subject of ongoing research (Hoffmann et al. 2013).

The favourability of a given reaction can be determined by the sign of ΔG_r, where a negative ΔG_r means that the reaction will be driven spontaneously towards the products, and a positive ΔG_r means the reaction is unfavourable. When the system is at equilibrium the ΔG_r is equal to zero, which in turn, by rearrangement of Equation 3.2, gives the (concentration-based) equilibrium constant, K' (Equation 3.3).

$$\Delta G_r'^{o} = -RT\ln K' \tag{3.3}$$

To complement and validate predictions, experimental values can also be obtained. For metabolic reactions, many previously determined experimental values of K' can be obtained from the Thermodynamics of Enzyme-Catalysed Reactions Database (TECRDB), (Goldberg et al. 2004) while, in other cases, experimental measurements need to be made using a suitable approach (Tewari et al. 2000; Tufvesson et al. 2012) to obtain such data.

3.3 Strategies for Shifting Equilibria

3.3.1 Conventional strategies for shifting equilibria

Thermodynamic data such as, the equilibrium constant K' (either obtained via prediction or experiments) can be used to find suitable operating strategies in order to achieve sufficiently high conversion of an energetically unfavourable reaction. Achieving sufficiently high conversion is essential in order that the value added by the reaction (difference in economic value between products and substrates) can be fully exploited (see **Figure 3.1**). Examples of strategies to shift equilibria include the addition of co-substrate in excess to 'push' the equilibrium position or the application of *in situ* product or co-product removal (ISPR or IScPR) by 'pulling' the equilibrium position towards the target product (**Figure 3.2**).

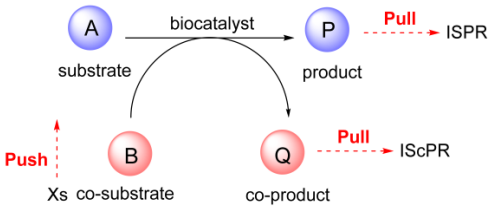

Figure 3.2: Conventional strategies for shifting equilibria based on Le Châtelier's Principal: (a) Pushing the equilibrium position by addition of excess of co-substrate (Xs) and (b) pulling the equilibrium position by either in situ product removal (ISPR) or in situ co-product removal (IScPR) towards the target product.

3.3.1.1 Addition of excess co-substrate

A frequently employed technique to shift equilibrium position, for reactions with more than one substrate, is to use one of the substrates in stoichiometric excess (Tufvesson et al. 2011). The extent to

which this excess is required to achieve a given conversion can be determined by the equilibrium constant, *K'* of the reaction. For example, for a reversible reaction with *K'* less than 1, a 50% conversion is the best achievable (**Figure 3.3a**).

In principle, by 'pushing' the reaction using an excess of co-substrate, the equilibrium position of such an unfavourable reaction can be driven up to 100% conversion. However, if the *K'* is too low, for instance <0.01, more than 100 molar equivalents of excess co-substrate would be required (**Figure 3.3**b). Clearly too high a concentration of the co-substrate could exceed the solubility of the substance in solution (Halling 1990). Therefore, it is essential to know the solubility limit of a substance if this technique is chosen or other reaction engineering strategies such as substrate feeding techniques (Woodley 2012) should be considered. Likewise, too high an amount of co-substrate can cause inhibition and/or instability of the enzyme (Kroutil et al. 2004) although this can be partially solved (at least) by protein engineering (Bommarius et al. 2011; Bornscheuer et al. 2012) or enzyme immobilization (Polizzi et al. 2007).

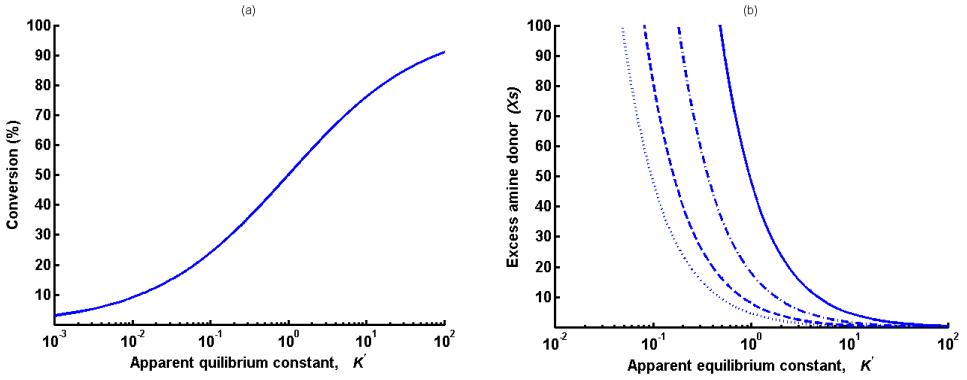

Figure 3.3: (a) The maximum conversion of a reversible reaction with two substrates and (b) use of excess co-substrate as a function of equilibrium constant, with 85% (dot), 90% (dash), 95% (dash dot) and 98% (solid) line.

3.3.1.2 Application of in situ product removal or in situ co-product removal

In situ product removal or *in situ* co-product removal is one of the technologies that in principle can 'pull' products from the reaction mixture in order to shift the equilibrium (Woodley et al. 2008). The products are removed during the reaction using such technologies as evaporation under reduced pressure (for volatile products) or extraction into an organic solvent phase (for hydrophobic products)

(Freeman et al. 1993). Using the thermodynamic properties such as, equilibrium constant *K'* for a given target conversion, the maximum allowable concentration of product (or co-product) in the solution to achieve a given conversion can be determined. For example, using IScPR, if the value of *K'* for a reaction is 0.01, and one of the substrates is the limiting substrate at a concentration of 50 mM, then the maximum concentration of co-product in the solution would be 0.001 mM in order to achieve 95% conversion (**Figure 3.4a**), which is clearly very low. However, by manipulating the value of *K'* by simultaneously using an excess of co-substrate, for instance 100 molar equivalents of that limiting reagent, the maximum co-product allowable in the solution would be 0.1 mM, 100-fold higher (**Figure 3.4b**). Thus, the information on *K'* is very useful in order to predict the feasibility of such strategies. Obviously, there are other physico-chemical properties of substrate and product that also need to be considered when selecting IScPR or ISPR dependent upon on the separation principle, such as the volatility, solubility, molecular weight or size, charge and hydrophobicity (Lye and Woodley 1999).

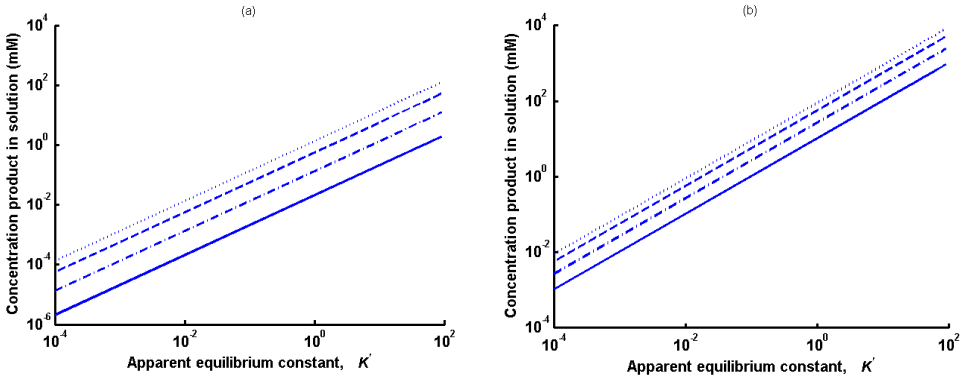

Figure 3.4: IScPR or ISPR (a) without excess of co-substrate and (b) with excess of co-substrate, 85% (dot), 90% (dash), 95% (dash dot) and 98% (solid) line.

Use of extraction technologies are of particular interest since a common problem when using enzymes as biocatalysts is the poor water-solubility of many of the interesting compounds. For that reason, the use of a biphasic system is particularly useful for some hydrophobic substrates in order to increase the solubility of such substrates and to improve the reaction conversion, by also extracting product or co-product. Frequently used co-solvents include tert-butyl methyl ether (MTBE) and dimethylformamide (DMF) (Richter et al. 2014). In all cases the selectivity of the ISPR or IScPR method (of product or co-product over substrate and so-substrate) is essential in order to shift equilibrium effectively.

3.3.2 Smart substrate or co-substrate - Spontaneous equilibrium shift

An alternative approach could be to shift the thermodynamically unfavourable reaction by using a so-called 'smart' substrate or co-substrate (Simon et al. 2014). A smart co-substrate is one that is converted into a thermodynamically stable co-product (Ni et al. 2014) and, a smart substrate (Truppo et al. 2010) is one that is converted to a thermodynamically stable product, which both simultaneously drives the reaction to completion. Helpfully, these techniques avoid the use of co-substrate in excess which simultaneously minimises waste products. Recently, 'a double co-substrate' was introduced by Bornadel and co-workers via a redox-neutral convergent cascade (Bornadel et al. 2015). The first co-substrate allows the formation of a thermodynamically stable co-product which shifts the overall equilibrium towards the desired product, while the presence of a 'double-smart co-substrate' allows the coupling with a secondary enzyme to converge to the same target product, yielding higher conversion. This new strategy successfully also improves the atom-efficiency of the synthesis route.

3.3.3 Enzyme coupling reactions

An alternative to these conventional approaches is to use a coupling enzyme to shift the equilibrium position of unfavourable reactions. This approach can be applied to improve the conversion of otherwise thermodynamically limited reactions, by coupling an unfavourable reaction with an energetically favourable one. This mimics the approach taken in nature in metabolic pathways. In nature, an individual enzyme usually works as part of a larger enzymatic network (Bruggink et al. 2003). For example, in microbial cells complete metabolic pathways convert simple (sugar) starting molecules to complex products via multiple steps. One feature of such pathways is that they are thermodynamically favourable, in part due to coupling those reactions which are unfavourable (positive Gibbs free energy), with those which are favourable (negative Gibbs free energy). Such coupling can be done in either in orthogonally (**Figure 3.5a**) or sequentially (**Figure 3.5b**).

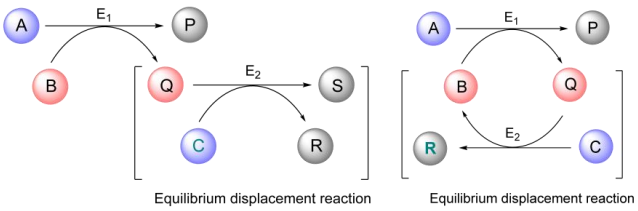

Figure 3.5: Possible strategies to shift the equilibrium position of unfavourable reaction (E_1). The energetically favourable reaction (E_2) can be arranged either (a) in orthogonally or (b) in parallel to drive the overall reaction towards the product. Substrate (*A*), co-substrates (*B, C*), product (*P*), and co-products (*Q, S, R*).

However, not all *in vitro* reactions in a scheme will be of thermodynamically favourable. For example, some unfavourable reactions *in vitro* may not be automatically coupled in an initial proposal for a synthetic scheme. Likewise, some reactions which can be very useful synthetically will need to be run in the opposite direction to that found *in vivo*. Such inconsistencies mean that in many cases the preliminary synthetic scheme is not thermodynamically favourable. Although protein engineering offers the opportunity to improve the kinetic profile of a network of enzymes, unfavourable thermodynamics requires a different approach. In principle by coupling an unfavourable reaction with a more favourable one, as in nature, a given synthetic scheme can be made to work. While these principles are already established, the actual values of Gibbs free energy for individual reactions are rarely reported. Hence understanding the precise role of coupling reactions in the network is often not possible.

Although several methodologies have been proposed to analyse the thermodynamic favourability of existing natural pathways in microbial cells, (Mavrovouniotis et al. 1992; Mavrovouniotis 1996; Henry et al. 2007; Villadsen et al. 2011; Noor et al. 2014) these analyses are usually only helpful to understand metabolic networks of *in vivo* systems, (Pissarra and Nielsen 1997; Efe et al. 2008) since *in vitro* compartmentalization can be controlled at will and the concentration of components are frequently very different. While there are several academic examples of enzymatic cascade reactions *in vitro* to shift equilibria, to our knowledge, rather few detail the thermodynamics with which to support such claims.

3.4 Case study

The concept of using alternative strategies to shift an unfavourable equilibrium is very well exemplified by the well-studied aminotransferase reaction (Simon et al. 2014). There are many other enzymatic reactions of current (and potential) industrial interest where equilibrium considerations play an important role such as, dehydrogenases, ammonia lyases, amine dehydrogenases and aldolase catalysed reactions (see **Table 3.1**).

Table 3.1: Thermodynamic-limited enzymatic reactions of current (and potential) industrial interest

Reaction scheme	Comments	Example of equilibrium shifting strategies
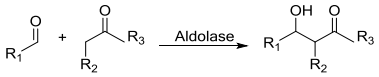 N-acetylneuraminic acid aldolase (EC 4.1.3.3)	N-acetylneuraminic acid aldolase catalyses the aldol condensation of N-acetyl-D-mannosamine with pyruvate in the synthesis of N-acetylneuraminic acid (Neu5Ac) and suffers from unfavourable equilibrium thermodynamics	• Excess of pyruvate (Zimmermann et al. 2007; García García et al. 2012) • Enzyme coupling reaction – removing pyruvate via LDH
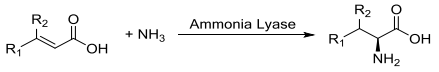 Ammonia Lyases (EC 4.3.1.X)	Phenylalanine (PAL, EC 4.3.1.5),aspartate (AspA, EC 4.3.1.1) and 3-methylaspartate (MAL, EC 4.3.1.2) ammonia lyase catalyses the unfavourable thermodynamic reaction in the amination of α,β−unsaturated carboxylic acid.	• Excess of ammonia (Tewari 1990; Raj et al. 2012; Parmeggiani et al. 2015)
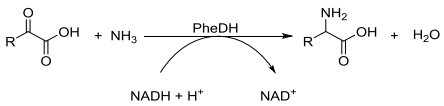 Phenylalanine dehydrogenase (EC 1.4.1.20)	PheDH-based amine dehydrogenase catalyses *para*-fluorophenyl-acetone to (*R*)-1-(4-fluorophenyl)-propyl-2-amine.	• Excess of ammonia and cofactors regeneration via enzyme-coupled approach (coupled with GDH (Abrahamson et al. 2013)
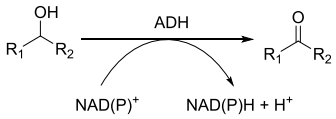 Alcohol dehydrogenases (EC 1.1.1.1, NAD-dependent) and (EC 1.1.1.2, NADP-dependent)	Alcohol dehydrogenase catalyses the oxidation of alcohol to ketone (more unfavored towards ketone).	• Cofactors regeneration by either substrate-coupled approach (often a high excess of alcohol (e.g. 2-propanol (Leuchs et al. 2012) or enzyme-coupled approach (e.g. enoate reductase (Gargiulo et al. 2012; Oberleitner et

Table 3.1: Thermodynamic-limited enzymatic reactions of current (and potential) industrial interest

Reaction scheme	Comments	Example of equilibrium shifting strategies
		al. 2014), GDH (Leuchs et al. 2012))
		• ISPR (Goldberg et al. 2006)

The ω-transaminase (ω-TAs) (E.C. 2.6.1.18) class of aminotransferase enzymes is of particular value for the synthesis of chiral amines, especially secondary and more complex amines. Due to the superb selectivity of these enzymes the chiral amine is rendered optically pure. Such molecules have great interest for the pharmaceutical industry and although this is not the only way to make such molecules there have been several interesting industrial examples reported in the scientific literature (e.g. synthesis of Sitagliptin (Savile et al. 2010). The enzyme catalyses the transfer or an amine group from a donor molecule to a carbonyl acceptor. One feature of running the enzyme in the synthetic direction to create a chiral center is that the products are often less energetically stable than the substrates, resulting in a thermodynamically unfavourable equilibrium, giving a poor conversion.

For example in the synthesis of (*S*)-1-phenylethylamine (PEA), a pharmaceutical compound used as an antiemetic agent, (Zhang 2000) the ω-transaminase catalyses the transfer of an amine group from L-alanine (L-Ala) to acetophenone (ACP), yielding the target amine and the co-product pyruvate (**Figure 3.6**).

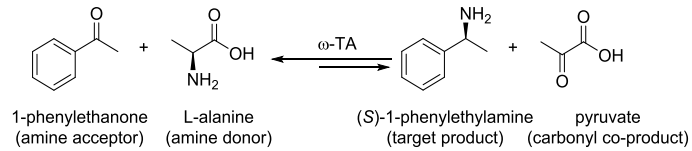

Figure 3.6: The example of thermodynamically-limited reaction. The aminotransferase (ω-TA) catalyses the transfer of an amine group from L-alanine (L-Ala) to an amine acceptor, acetophenone (ACP), yielding the target amine ((S)-1-phenylethylamine, PEA) and the co-product pyruvate (Pyr).

In this synthetic direction, the equilibrium constant for this transamination has been reported to be rather low (Shin and Kim 1998; Tufvesson et al. 2012). The products are less energetically stable than the reactants and thus a low conversion is expected. Indeed, this is supported by the calculations using the available experimental data of the equilibrium constant (K'=4.03*10^{-5}) (Tufvesson et al. 2012) which predicts that a maximum of 10% conversion would be expected. A frequently employed technique to increase conversion of reactions of this type is to use L-Ala in stoichiometric excess. However, reports using an excess of the amine donor L-Ala do not indicate much success (**Table 3.2**). In fact, based on our calculations, this technique is not a feasible option, since in principle it requires an excess of 10,000 molar equivalents of L-Ala to achieve a 90% conversion, which is clearly impractical. Additionally, the solubility of L-Ala will also become an issue since the solubility of the L-Ala is limited to 1.9 M in aqueous solution.

Table 3.2: The addition of excess co-substrate (*Xs*) in the synthesis of 1-phenylethylamine from acetophenone

Process conditions	Substrate (mM)	*Xs*	Kinetic Conv.	Expected eq. conv.	Ref.
ATA-113, pH 7.5, 30 ^{o}C, 24 h	416	L-Ala (2.4 equiv.)	<1%(*S*)	5%	Truppo et al. (2010)
Vibrio fluvialis, pH 7, 30 ^{o}C, 24 h, 15% v/v DMSO	20	L-Ala (10 equiv.)	<1%(*S*)	9%	Koszelewski et al. (2008)
ATA-103, pH 7.5, 30 ^{o}C, 10 h	50	L-Ala (10 equiv.)	3%(*S*)	9%	Truppo et al. (2009)
ATA-117 (ArRmut11-ω-TA), pH 7, 30 ^{o}C, 20% v/v DMSO	50	IPA (20 equiv.)	25%(*R*)	55%	Mutti et al., (2011)

Interestingly, in the aminotransferase reaction, the couples of amine donor/carbonyl co-product can be flexibly selected, since the structure of the target product is determined by its amine acceptor. For instance, instead of L-Ala, isopropylamine (IPA) is frequently considered as an alternative amine donor for this type of reaction (Cassimjee et al. 2010; Park et al. 2013a; Richter et al. 2014). The experimentally-determined equilibrium constant for **Figure 3.6** using IPA (instead of L-Ala) as the amine donor is 0.033 (Tufvesson et al. 2012). Although the equilibrium constant in significantly increased, perhaps surprisingly, neither IPA nor L-Ala is really a good choice of amine donor for the synthesis of such products when an excess of donor alone is used as the equilibrium shifting method.

For IPA, still 240 molar equivalents are needed to push the equilibrium position to achieve 90% conversion (**Figure 3.7**). Although IPA requires a lower excess than L-Ala, nevertheless, the excess is still large, which also generates waste owing to the unused reagent and creates separation problems downstream (Ni et al. 2014). So, while the choice of the amine donor in this particular type of reaction plays a significant role in determining the equilibrium conversion of the target product, it may not be sufficient to enable such an approach. In fact to understand this further we recently measured the apparent equilibrium constant for several donor/acceptor combinations for better implementation of such reactions (Gundersen et al. 2015).

Alternatively, the commercially available amine donors (e.g. *ortho*-xylylenediamine dihydrochloride (Green et al. 2014) and 3-aminocyclohexa-1,5-dienecarboxylic acid (Wang et al. 2013)) which spontaneously favour the tautomerization process could be used. This smart co-substrate approach can successfully shift the equilibrium position towards products where the unstable co-product ketone is spontaneously converted to a more stable molecule, giving >99% conversion of PEA. However, this approach is limited by the expensive amine donor which has to be added in equimolar amounts to achieve a high conversion (Park et al. 2013b).

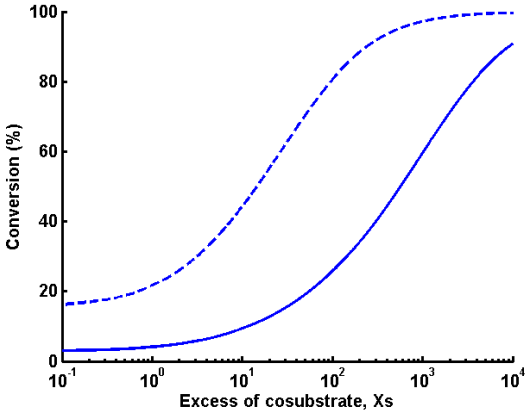

Figure 3.7: The equilibrium constant (K') determines the maximum theoretical conversion of a reaction. With an excess of co-substrate L-alanine (K' = 4.03*10^{-5}, solid line) or isopropylamine (K' = 0.033, dash line).

Interestingly however, the use of IPA as an amine donor also allows the removal of its volatile co-product, acetone (Park et al. 2013a), by IScPR using technologies such as stripping (Goldberg et al. 2006), sparging (Tufvesson et al. 2013), adsorbing resins (Truppo et al. 2010) or membrane technologies (Leuchs and Greiner 2011; Rehn et al. 2014). In an analogous manner to the previous calculations, the maximum acetone concentration allowable in solution to give a required conversion, can be determined using *K'*. For example, if the *K'* is 0.033, and if the target conversion is 95%, the required acetone concentration in solution should be less than 1 mM if the limiting reagent of 50 mM ACP is used (**Figure 3.8a**). It is also common to couple the use of excess of IPA with IScPR. The calculation is now much better. For example, if the ACP concentration of 50 mM is used, with the target of 90% conversion, using 100-fold excess of IPA, the acetone in solution is 18.5 mM (**Figure 3.8b**). Still probably the 100-fold excess is unrealistic but in practice even more of a problem is that when using IScPR and/or ISPR either using solvent or resin extraction, as in this example, the IPA competes with the PEA to bind onto the resins or to co-extract into the solvent, resulting in ineffective *in situ* product removal (Truppo et al. 2010). Indeed as mentioned previously, selectivity of ISPR or IScPR is an essential requirement to shift equilibrium using this technique.

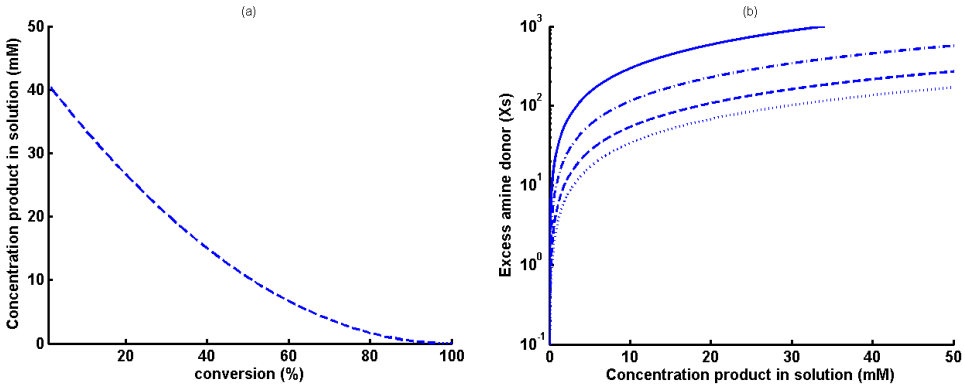

Figure 3.8: (a) IScPR without excess IPA. ISPR gives the same trend. Data not shown. (b) IScPR or ISPR combine, with excess, 85% (dot), 90% (dash), 95% (dash dot) and 98% (solid) conversion.

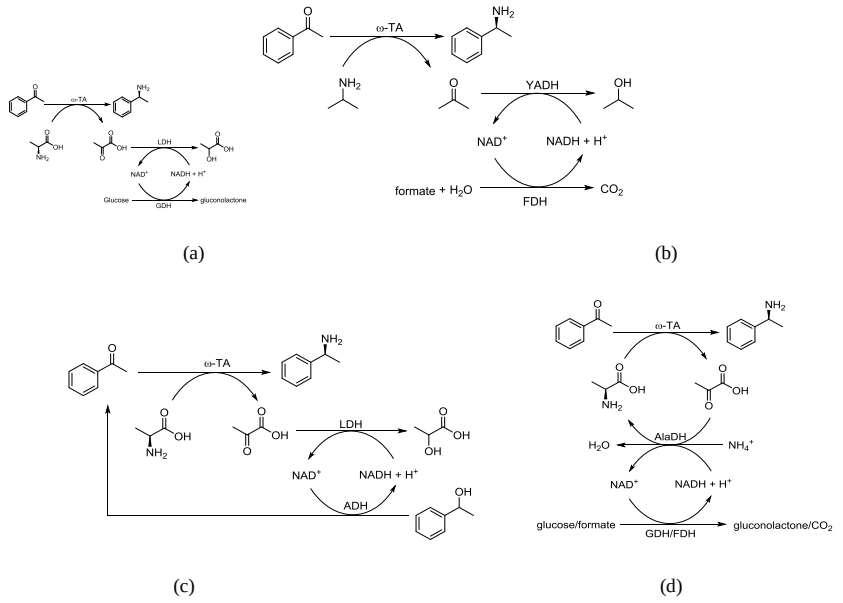

Figure 3.9: Equilibrium displacement reaction with co-factor regeneration system: ω-TA/AlaDH/GDH (Truppo et al., 2009), ω-TA/AlaDH/FDH (Koszelewski et al., 2008; Mutti et al., 2012; Mutti et al., 2011), ADH/ω-TA/LDH system (Tauber et al., 2013), ω-TA/LDH/GDH system (Mutti et al., 2012, 2011; Truppo et al., 2009; Truppo et al., 2010), ω-TA/YADH/FDH (Cassimjee et al., 2010), ω-TA/AlaDH/GDH (Truppo et al., 2009), ω-TA/AlaDH/FDH (Koszelewski et al., 2008; Mutti et al., 2012, 2011) system.

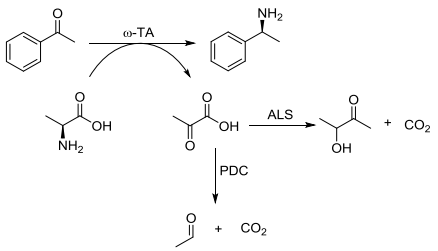

Figure 3.10: Equilibrium displacement reaction without co-factor regeneration system: ω-TA/ALS system (Yun and Kim, 2008) or ω-TA/PDC system (Höhne et al., 2008).

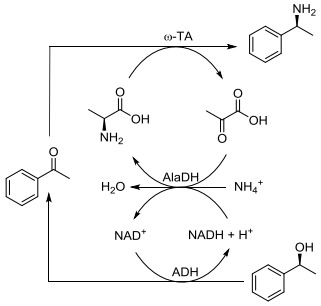

Figure 3.11: Redox-neutral cascade: ADH/ω-TA/AlaDH system (Tauber et al., 2013)

For all these reasons therefore the use of co-substrate excess and/or co-product removal is limited using the previously mentioned techniques and this has been the driver towards an alternative approach using coupling reactions. To date, several cascade reaction schemes to couple with the ω-transaminase as a means of overcoming thermodynamic limitations have been proposed (Simon et al. 2014). For instance, some cascade schemes for assisting the synthesis of PEA have been reported and are summarized in **Figure 3.9.** Frequently, the equilibrium displacement reactions use secondary enzymes such as lactate dehydrogenase (LDH, E.C. 1.1.1.27), alanine dehydrogenase (AlaDH, EC.1.4.1.1), pyruvate decarboxylase (PDC, EC1.2.4.1) (Höhne et al. 2008), acetolactate synthase (ALS, EC 2.2.1.6) (Yun and Kim 2008) and yeast alcohol dehydrogenase (YADH, EC1.1.1.2) (Cassimjee et al. 2010). The reaction is coupled either to remove the co-product or regenerate the co-substrate, both with the objective to shift the equilibrium position towards the product. Notably, the amine donor L-Ala was frequently used in enzymatic cascades due to its selective reactivity towards other enzymes (e.g. AlaDH for regeneration) as well as its corresponding product pyruvate (e.g. LDH for IScPR).

In the same example, an approach of potentially even greater interest would be to use alcohols as the starting material rather than ketones to produce the corresponding amines using an alcohol dehydrogenase, (AlcDH, EC.1.1.1.2) (Sattler et al. 2012; Tauber et al. 2013). However, both reactions (AlcDH and ω-TA) are reversible and need to be coupled with energetically favourable reactions in order to pull the reaction towards the target product.

In this example of a multi-enzyme cascade, LDH, AlaDH and YADH all require a cofactor (e.g. NADH) which is essential for the functionality of these enzymes. Due to the cost of such co-factors, it is necessary to re-generate them in-situ. To date, in the required direction, the most common co-factor regeneration systems are glucose dehydrogenase (GDH, E.C.1.1.1.1) and formate dehydrogenase (FDH, EC 1.2.1.2). Both GDH and FDH are thermodynamically favourable in the required direction where the apparent equilibrium constant is 3.1 (Brink et al. 1953) and 420 (Ruschig et al. 1976), respectively. Other co-factor regeneration enzymes are also available such as glucose-6-phosphate dehydrogenase (G6PH, E.C.1.1.1.49) (Hall et al. 2008) and glutamate dehydrogenase (EC 1.4.1.2). A number of previous reviews have been published on the co-factor regeneration system (Wichmann and Vasic-Racki 2005; Weckbecker et al. 2010). Recently, a [Ni-Fe]-hydrogenase has been successfully coupled with ω-TA/AlaDH using H_2 as the reducing equivalent as an alternative option, giving high efficiency co-factor regeneration in comparison to the NH_3/formate or glucose system (Holzer et al. 2015).

An alternative elegant method to overcome such problems would be the use of a self-sufficient redox cascade (Tauber et al. 2013) as shown in **Figure 3.11** where alanine dehydrogenase (AlaDH)

was used to shift both unfavourable reactions towards PEA and at simultaneously regenerate the amine donor L-Ala and nicotinamide cofactor (NAD+) *in situ*. Although the study did not report the equilibrium constant or indicate that the equilibrium conversion was achieved, since AlaDH reaction is energetically favourable (with the $K' = 1.30 \times 10^5$, pH 7.98), this in principle should provide the energy to make the reaction go forward (Piérard and Wiame 1960). Nevertheless, the extent to which such a reaction can drive the cascade is unknown. A final conversion of 25% was obtained. Nevertheless, such an elegant cascade might be beneficial for industrial practice, as the use of external source of a hydride (from glucose or formate) can be eliminated can also be used as a co-solvent which would be beneficial from an environmental perspective (Ni et al. 2014).

We also note that frequently reports of enzymatic cascades (rather than single reactions) have been operated experimentally using an excess of co-substrate (**Table 3.2**). However the effectiveness of such a strategy is not yet proven since a full thermodynamic analysis is not currently available. The key to maximize the equilibrium conversion of a cascade is determined by a single net reaction that controls the favorability of that cascade. For example, in the synthesis of PEA, 0.5 molar equivalents of pyruvate (co-substrate) were used in the ω-TA/AlaDH/GDH system and a conversion of 96% achieved Interestingly, when compared to the ω-TA/LDH/GDH system, 10 molar equivalents of L-Ala were required to achieve the same conversion (Truppo et al. 2009). This might due to the net reaction which requires the excess in order to achieve the high conversion, and since for the same system, 5 molar equivalents of L-Ala did not achieve such values (Koszelewski et al. 2008). Hence some enzymatic cascades coupled with the addition of an excess of co-substrate show good results while others do not show significant improvement of the conversion (**Table 3.3**). Analysis of the thermodynamics should allow the excess of reagents to be minimized and the enzyme coupling used to its full potential.

Using the coupling techniques involving engineered enzymes, the substrate scope and kinetic profile of the enzymes of course also needs to be matched, which for a conversion of a non-natural substrate can be challenging. Nevertheless, protein engineers have made great progress in achieving workable cascades of non-natural pathways able to convert non-natural substrates. In order to carefully control such systems, it has been argued that *in vitro* systems are particularly attractive since the required enzyme activities can relatively easily be manipulated by altering protein concentration, rather than by adjusting expression levels inside the cell. Regardless of the cascade system, the interactions and compatibility of each of the enzymes and their associated reagents need to be considered. For instance, the introduction of high concentrations of co-substrates (e.g. L-Ala, NH_3) is likely to affect the activity and stability of the other enzymes.

Table 3.3: Available experimental data for aminotransferase-catalysed reaction in the synthesis of (*S*)-1-phenylethylamine (kinetic conversion)

System	Process conditions	ACP (mM)	Ratio (co-substrate/ACP)	*ee* (%) conv. (%)	Ref.
ω-TA/LDH/GDH	ω-TA (ATA-103), pH 7, 30 ^{o}C, 24 h, 15% v/v DMSO	50	L-Ala (5 equiv) glucose (~2 equiv)	*ee* >99% conv. 21%	Koszelewski et al., (2008)
	ω-TA (ATA-113), pH 7, 30 ^{o}C, 24 h 15% v/v DMSO	50	L-Ala (5 equiv) glucose (~2 equiv)	*ee* >99% conv. 5%	
	ω-TA (ATA-103), pH 7.5, 30 ^{o}C, 10 h	50	L-Ala (10 equiv) glucose (2 equiv)	*ee* >99% conv. >96%	Truppo et al., (2009)
	ω-TA (His *Vibrio fluvialis*), pH 7, 30 ^{o}C, 24 h, 15% v/v DMSO	50	L-Ala (5 equiv) glucose (3 equiv)	*ee* >99% conv. 38%	Mutti et al., (2012)
ω-TA/AlaDH/FDH	ω-TA, (ATA-113), pH 7, 30 ^{o}C, 24 h	50	L-Ala (5 equiv) NH_4HCO_2 (3 equiv)	*ee* >99% conv. 6%	Truppo et al., (2009)
	ω-TA (His-*Vibrio fluvialis*), pH 7, 30 ^{o}C, 24 h, 15% v/v DMSO	50	L-Ala (5 equiv), NH_4HCO_2 (3 equiv)	*ee* >99% conv. 23%	
	ω-TA (His-*Vibrio fluvialis*), pH 7, 30 ^{o}C, 24 h	50	L-Ala (5 equiv), NH_4HCO_2 (3 equiv)	*ee* >99% conv. 65%	
	ω-TA (His-*Vibrio fluvialis*), pH 7, 30 ^{o}C, 24 h	50	L-Ala (5 equiv), NH_4HCO_2 (3 equiv)	*ee* >99% conv. 97%	Mutti et al., (2012)
ω-TA/AlaDH/GDH	ω-TA (ATA-103), AlaDH (LAADH-117), pH 7.5, 30 ^{o}C, 48 h	50	Pyr (0.5 equiv) NH_4Cl (2 equiv) glucose (2 equiv)	conv. 96%	Truppo et al., (2009)
ω-TA/YADH/FDH	ω-TA (*Arthrobacter citreus*), YADH (*Saccharamyces* cerevisiae), FDH (*Candida boidinii*), pH 7, 30 ^{o}C, 24 h	1.8	IPA (311 equiv)	*ee* >99% conv. 99%	Cassimjee et al., (2010)
ADH/ω–TA/AlaDH	ADH (*Rhodococcus* ruber), ω-TA (*Vibrio fluvialis*), AlaDH (*Rhodococcus ruber*), pH 7, 30 ^{o}C, 24 h	50[a]	L-Ala (5 equiv) NH_4Cl (4 equiv)	*ee* >98% conv. 47% (ACP) conv. 25% (PEA)	Tauber et al., (2013)

equiv. = molar equivalent, [a] 1-phenylethanol

3.5 Future Perspectives

In this chapter, the several options to shift the equilibrium position, such as the use of excess co-substrate, ISPR, IScPR and smart substrate/co-substrate have been discussed. Nevertheless, each of the methods has practical limitations. Such challenges can be (at least) partly improved via the application of enzymatic cascades (coupling an energetically unfavourable reaction with a more favourable one) to achieve a sufficiently high conversion of an otherwise thermodynamically-limited reaction. In the long term it is clear that further examples of multi-enzyme cascades will be forthcoming as one of a number of new tools to help the synthetic and process chemist.

4 Process Evaluation Tools

4.1 Introduction

As previously discussed, it is clear that not all *in vitro* biocatalytic reactions will be thermodynamically and kinetically favourable. The problems in running biocatalytic processes are frequently restricted by thermodynamically unfavourable yields as well as limited enzymatic rates. Thus, it is necessary to evaluate and to identify the potential of enzymatic cascades by thermodynamic and kinetic studies in order to successfully apply the concept. In this chapter, several engineering tools will be discussed (and summarised in **Figure 4.1**).

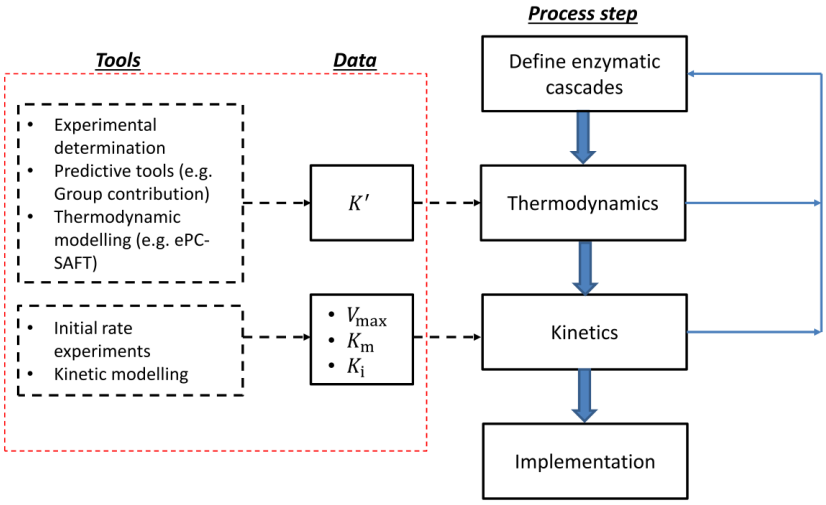

Figure 4.1: Summary of process evaluation tools used in this study.

4.2 Obtaining Thermodynamic Data on Biochemical Reactions

It is important to obtain meaningful thermodynamic data to find the suitable operating strategies for biocatalytic processes. For example, the equilibrium constant is a critical parameter for making rational design choices to improve conversion of a thermodynamically-limited reaction (see section 4). Several ways to obtain such properties are discussed here.

4.2.1 Thermodynamics database

Thermodynamics of Enzyme-Catalysed Reactions Database (TECRDB) is a data collection of experimentally-determined apparent equilibrium constants, *K'* and calorimetrically-measured enthalpy changes, ΔH_r^o that can be found in the scientific literature (Goldberg et al. 2004). To date, there are 400 biocatalytic reactions available in this database with various measurement conditions (temperature, pH, ionic strength, buffer(s) and cofactor(s)). Although, Goldberg and co-workers (1993–2007) have critically evaluated the quality of these data (Goldberg et al. 2004), some data were highly scattered. Therefore, process feasibility and economic viability for the reaction of interest could not be assessed directly due to data uncertainties. However, to some extent, the data could be used to identify the favourability of a reversible reaction, under given conditions.

On the other hand, the Alberty database has 131 biochemical compounds with thermodynamic values of ΔH_r^o and $\Delta G_f'^o$ (Alberty 2003). These values are basically derived from TECRDB via correlation with the *K'* values of various reaction conditions found in the TECRDB. The data of Alberty can be further used to calculate the standard molar transformed properties (e.g. enthalpies of reaction $\Delta H_r'^o$, Gibbs energy formations, $\Delta G_f'^o$) under specified conditions of temperature, pH and ionic strength, using Legendre transformation (Goldberg et al. 2007). This approach allows the calculation of *K'* values that are not available in the TECRDB. Interestingly, the mathematical function of Legendre transforms can be quantitatively calculated using Mathematica® (a computational software program) (Alberty 2006). However, Alberty's starting point for the calculations depend on the TECRDB, where the reliability of the experimental results is unknown, which is a clear disadvantage using this approach.

4.2.2 Experimental measurements

Thermodynamic properties can of course also be obtained through experimental measurements. In order to get more reliable and accurate experimental data, Alberty and his colleagues have developed guidelines and recommendations for data measurement and data representation for biochemical thermodynamics (Alberty et al. 2011). However, to our knowledge, there is no standard protocol available to measure such properties. One of the available methods (which can be found in much scientific literature) is to allow reactants to reach equilibrium from both directions of the reaction as for example in work done by Tewari and co-workers (2000) and Gundersen and co-workers (2015). A recent approach was developed by Tufvesson and co-workers for the aminotransferase reaction (Tufvesson et al. 2012). This method is based on the measurements of the reaction rate using a variety of substrate and product concentrations in order to find the point where the forward and reverse

reactions converge to a zero net reaction (Equation 4.1). However, this method requires a lot of data points to reach the solution where the relative quotient (Q) at zero net reaction is equal to 1 and thus Q is assumed to be K'.

$$Q = \frac{[C][D]}{[A][B]} \xrightarrow{t=\infty} K' \tag{4.1}$$

The equilibrium constant can also be calculated via experimentally-determined kinetic parameters according to the Haldane relationship (Shin and Kim 1998; Zimmermann et al. 2007; Seo et al. 2011). This equation represents the kinetic parameters of reversible enzymatic reaction. Each kinetic parameter is independent of one another and is limited by the thermodynamic equilibrium constant of the overall reaction (Leskovac 2004).

4.2.3 Property prediction methods

Not all thermodynamic properties are available for the compounds of interest in the scientific literature or databases. Likewise, it is also probably unrealistic to measure the data when it is needed if time constraints are a major problem. Thus computational estimation methods such as, the group contribution method and quantum chemical calculations are the best alternative, they may also serve as a useful complement to experimental methods.

The group contribution (GC) method is the most commonly used tool to quickly estimate the required properties without a large computational effort. The method was developed based on the molecular structures of compounds where the structure of a single compound is decomposed into a set of smaller molecular sub-structures (different sub-molecules for different GC-methods) where each model parameter is associated with one of the constituent molecular sub-structures (or so-called 'groups') that combine to form the compound. Mavrovouniotis was among the first to use the GC-method to estimate the standard Gibbs free energies of formation of biochemical compounds in aqueous solutions (Mavrovouniotis 1990).

However, this method has limited applicability due to the over-simplification of the represented molecular sub-structures, in particularly for molecules involving sulphur, nitrogen, and halogens. Building on this work, Jankowski and his colleagues introduced those sub-structures in their GC-method combined with various new interaction factors (conjugated double bonds, thioester bonds, and vicinal chlorine atoms) to give better accuracy (Jankowski et al. 2008). However, we have found that the Jankowski-GC method does not consider the stereochemistry of chiral compounds. For instance, in an aminotransferase reaction, the structural similarity between reactants and products may end up to

have the same energy value, thus limiting the applicability of this method. Recently, Noor and co-workers have developed a new and updated version of the GC-method, using an integrated framework from TECRDB, Alberty's and Jankowski's work, known as Pseudo-isomeric Group Contribution (PGC) (Noor et al. 2012). In this approach, a biochemical compound is divided into its pseudo-isomers (e.g. for example L-Ala has three protonation states ($C_3H_5O_2-NH_3^+$, $C_3H_5O_2-NH_2$ and $C_3H_4O_2^- - NH_3^+$) given by its acid dissociation constant (pKa)), where each pseudo-isomer has its own group contribution energy, giving better predictions.

The properties of standard Gibbs free energy of reaction ($\Delta G_r'^o$) were calculated for the transamination of PEA from ACP using L-alanine as the amino donor, using each of the group contribution (GC) methods discussed here (**Table 4.1**). The values were then compared with the $\Delta G_r'^o$ values obtained from the experimental *K'* values from Tufvesson et al. (2012) and Shin and Kim (1998), using the Equation 4.2, where *R* is the gas constant and *T* is the absolute temperature.

$$\Delta G_r'^o = -RTlnK' \tag{4.2}$$

Interestingly, there are significant deviations between the experimentally-determined $\Delta G_r'^o$ and the predicted values from the various GC-methods (**Table 4.1**). Additionally, the excellent GC-method that is used to predict the pure and uncharged chemical compounds (Marrero and Gani 2001; Hukkerikar et al. 2012), cannot be used in such cases, since the $\Delta G_r'^o$ calculated here have negative value. Thus, it was not possible to estimate accurately the $\Delta G_r'^o$ for such a synthesis, giving an energetically favourable value compared to the other GC methods. This might be due to the pH-dependent charges of biochemical compounds since biocatalytic reactions usually operate in aqueous solutions (von Stockar and van der Wielen 2003).

Another emerging tool to estimate thermodynamic properties is the use of quantum mechanics (QM). This method solves the quantum mechanical Schrödinger equation (Hehre 2003) to predict the properties of the molecules. For instance, the quantum chemistry Screening MOdel for Realistic Solvents (COSMO-RS) is a quantum mechanical based method to calculate the chemical potential of a compound either in pure fluid or in mixtures (Letcher 2007). From this method the values of ΔG_f^o in any type of solvent, can be determined (Eckstein et al. 2006; Peters et al. 2007). Like COSMO-RS, *ab initio* quantum mechanics can also be used to predict the values of thermodynamic properties (e.g. standard molar enthalpies H_m^o, entropies S_m^o, Gibbs free energies G_m^o) using the Hartree–Fock model of geometry-optimized structures (Eckstein et al. 2006). In this method, the total energies of reactions can be calculated based on the optimal energy of molecular structure of the components involved.

Recently, a simple and fast approach has been proposed to predict the thermodynamic favourability of a transaminase reaction (Meier et al. 2015). This method was developed based on *ab initio* calculations of the total energies of the molecules involved and validated with the experimental values obtained from the scientific literature review and our laboratory.

Table 4.1: Comparison between the experimental $\Delta G_r'^o$ values and the $\Delta G_r'^o$ values calculated using the Group contribution (GC) methods for the synthesis of (*S*)-1-phenylethylamine (see **Figure 3.6**).

Methods	$\Delta G_r'^o$ **(kJ/mol)**	**References**
Experimental measurement	+25.50	Tufvesson et al. (2012)
Haldane relationship via experimental (kinetic) measurement	+17.73	Shin and Kim (1998)
Mavrovouniotis GC	+0.42	Mavrovouniotis, (1990)
Jankowski GC	+16.78	Jankowski et al., (2008)
Pseudo-isomeric GC	+7.3	Noor et al. (2012)
GC for pure compounds	–27.76	Hukkerikar et al. (2012); Marrero and Gani (2001)

GC=group contribution

4.2.4 ePC-SAFT modelling

The mathematical modelling might be a useful tool to evaluate thermodynamic data for specific case studies. Using an equation of state such as, Electrolyte Perturbed-Chain Statistical Fluid Theory (ePC-SAFT) (Cameretti et al. 2005), it is possible to estimate the values of component activity coefficients of biochemical compounds in aqueous solution (Held et al. 2011; Hoffmann et al. 2013; Hoffmann et al. 2014). Interestingly, a recent study by Hoffmann and co-workers found that the activity coefficient correlates strongly with pH for a thermodynamically favourable reaction (Hoffmann et al. 2013). Further work is clearly required especially since the kinetics of the aminotransaminase reaction is known to be affected by the protonation state of the amine reactant (itself dependent upon the pKa).

4.3 Kinetic study

A mathematical model of a multi-enzyme cascade was constructed based on the kinetic mechanism of individual enzymes (Santacoloma et al. 2011). The important parameters to perform such a calculation are:

- Michaelis-Menten kinetics (K_m, V_{max})
- substrate/product inhibition (K_i)
- biocatalyst activity (turnover frequency, $1/K_{cat}$)
- biocatalyst stability (deactivation rate constant, K_d)

In most cases, Michaelis-Menten parameters vary in the literature reports, due to different types of host organisms and experimental conditions (temperature, pH, ionic strength, buffer, and etc.). Thus, mathematical modelling often developed based on specific case studies and the robustness of the models is still questionable especially for multi-enzyme cascades. However, mechanistic modelling is still a good tool to understand the behaviour of enzymatic reaction, especially in the multi-enzyme cascades since the interaction between enzyme and components is of importance.

Table 4.2: The effect of inhibition (I) on the Michaelis-Menten equation model

Type of inhibition	Rate Equations
None	$V = \frac{V_{\max}[S]}{K_m + [S]}$
Competitive	$V = \frac{V_{\max}[S]}{K_m\left(1 + \frac{[I]}{K_i}\right) + [S]}$
Uncompetitive	$V = \frac{V_{\max}[S]}{K_m + [S]\left(1 + \frac{[I]}{K_i}\right)}$
None competitive	$V = \frac{V_{\max}[S]}{(K_m + [s])\left(1 + \frac{[I]}{K_i}\right)}$

Table 4.3: Summary of process considerations for implementation of enzymatic cascades

Thermodynamics	Kinetics	Process metric

Evaluation
• Equilibrium constant
• Gibbs free energy of reactions
 	
Strategy to shift equilibria
1. cascade coupling
  • have energetically downhill equilibria
  • coupling with high energy substrate (e.g. oxygen, phosphate)
2. Thermodynamic control (based on Le Chatelier's principle)
  • pH, temperature, solvent consideration/solubility, excess of co-substrate concentration
3. Process engineering
  • ISPR or IcSPR – volatile compound removal
  • Phase transfer (e.g. multi-phase operations)
  • Spontaneous equilibrium shift with substrate choice
	Evaluation
	• enzyme activity
	• enzyme stability
	• enzyme selectivity (purity)
	• inhibition
	• selectivity toward substrate/co-factor
	
	Strategy to improve catalytic properties
	1. Immobilization to modify the active site of enzymes (e.g. polarities, pH, metals, oxidation states, etc.)
	2. Protein engineering to modify the substrate selectivity (e.g. regio/chemo/stereo-selectivity) to improve the substrate specificity, enantioselectivity, reaction rate).
	3. Find suitable replacement enzyme but unaffected by the whole system
		Evaluation
		Enzyme stability
		• enzyme yield (g product/g enzyme)
		
		Enzyme productivity
		• reaction yield (% mol product/ mol substrate)
		• yield on substrate (g product/g substrate)
		
		Volumetric productivity
		• space-time yield (g product/L reactor/hour)
		
		Efficiency of recovery of final product
		• product concentration (g product/ L reactor)
		• enantiomeric excess, ee %

5 Case Study I: Thermodynamics and Kinetics of ω-Transaminase-based Cascades for the Production of Chiral Amines from Alcohols

5.1 Introduction

Optically active amines are important building blocks for the synthesis of many chiral molecules, mainly for pharmaceutical compounds. The chiral molecules can be produced by enantioselective synthesis using chemical (Nugent and El-Shazly 2010) or enzymatic catalyst (Kohls et al. 2014) with aldehydes or ketones as starting raw materials. Recently, several interesting studies have been reported in using inexpensive and readily available substrates such as, alcohols, instead of carbonyl compounds, for the synthesis of many chiral amines. In chemical catalysis, one of the emerging methods is to convert an alcohol into an amine by ammonia using metal catalysts in the so-called 'hydrogen-borrowing' process (Bähn et al. 2011). In this process, the alcohol is first oxidised to an aldehyde or ketone which subsequently undergoes a nucleophilic addition to give an imine, and finally, the hydrogenation of imine with the generated hydrogen from the first step, yields the target amine product. Nevertheless, in many metal-catalysed reactions, obtaining high enantioselectivity is still a major challenge (Nugent and El-Shazly 2010).

Alternatively, several promising *in vitro* enzymatic cascades for the amination of alcohols have been developed recently since in general no enzyme is able to convert directly an alcohol into an amine. To date, such synthetic schemes consist of two to five redox enzymes in a way that allows the concept of redox self-sufficient cascades (Sattler et al. 2012; Tauber et al. 2013; Lerchner et al. 2013; Knaus et al. 2015; Chen et al. 2015; Palacio et al. 2016). This concept enables regeneration of nicotinamide cofactors *in situ* without any additional hydride source, particularly from glucose or formate. Recently, an artificial metabolism *in vitro* has been successfully constructed involving several redox self-sufficient cascades for the production of nylon-6 monomer 6-aminohexanoic acid (Sattler et al. 2014), giving 75% conversion at the expense of only ammonia and oxygen as the sole reagents and thus minimising waste products. Hence, the concept of self-sufficient processes is particularly attractive and many more examples will be forthcoming in the future due to their green credentials.

One of the most interesting redox self-sufficient cascades employs two primary enzymes (alcohol dehydrogenase; ADH, EC 1.1.1.1 and ω-transaminase; ω–TA, EC 2.6.1.18) that are directly involved

in the amination of alcohols. In this specific example, an alcohol is oxidized by an alcohol dehydrogenase to a ketone which is subsequently aminated to the corresponding chiral amine by ω-TA (**Figure 5.1**). Remarkably, in the final step, the introduction of alanine dehydrogenase (AlaDH; EC 1.4.1.1) in the cascade serves a dual purpose. Besides regenerating the NAD for the oxidation in the first step and regenerating L-alanine for the reduction in the transamination step *in situ*, the AlaDH reaction is energetically favourable that in principle could shift the unfavourable equilibrium of the oxidation and amination reactions towards the product and to achieve a favourable conversion. Although in principle, this is an attractive scheme, when tested experimentally it gave low conversions (25%) for the amination of *sec*-alcohol (Tauber et al. 2013).

A key challenge in this redox neutral cascade is to run the oxidation and amination steps simultaneously in a one-pot fashion in order for the recycle systems to work efficiently (Schrittwieser et al. 2011). Likewise it is difficult to set up efficiently, since the thermodynamics and the kinetics have to match. Thermodynamically, it is known that the ω-TA reaction is often hindered by an adverse equilibrium position, particularly using alanine as the amino donor (Tufvesson et al. 2011). In a single step transformation of acetophenone to (*S*)-phenylethylamine (PEA) using L-alanine (L-Ala) as an amino donor, an equilibrium constant of $4.03*10^{-5}$ was reported (Tufvesson et al. 2012). Several cascade reaction schemes have been proposed to couple with the ω-TA as a means of overcoming thermodynamic limitations (Simon et al. 2014). In such examples, alanine has frequently been chosen the amino donor for the ω-TA reaction due to the availability of several enzymes that are able to convert pyruvate back into alanine (e.g. AlaDH) or to convert pyruvate into a non-inhibitory by-product (e.g. lactate dehydrogenase, pyruvate decarboxylase, and amino acid dehydrogenase). Nevertheless, the extent to which such a reaction can drive the cascade is unknown (Abu and Woodley 2015).

Additionally, the enzymatic cascades typically involve a combination of several engineered enzymes which (may come from different hosts) *in vitro* for the conversion of non-natural substrates. Despite the fact that native enzymes are highly selective, they frequently suffer from low productivity when used on non-natural substrates. In a cascade, unbalanced kinetic rates between the interconnecting enzymes will limit the conversion of the target compounds. For example, a transketolase-catalysed conversion was found to be 25 times faster than the subsequent ω-TA conversions in a two-step reaction in the synthesis of chiral amino-alcohols (Rios-Solis et al. 2015), which therefore limits the yield. In their study, the relative rates were matched between the enzymes by fine-tuning the expression level and successfully increased up to 6-fold yield. Another issue the ω-TA enzyme frequently suffers from is substrate and production inhibition. For example, a study done by Truppo et al. (2010) for the amination of ACP, the ω-TA (ATA-113, purchased from Codexis Inc.

(Redwood City, United States)) activity was significantly inhibited by the product PEA and gives a low conversion. To date, process and kinetic modelling of enzymatic cascades has been less explored, due to the complexities of incorporating the kinetic models of the individual enzymes with the many kinetic parameters involved (Xue and Woodley 2012), particularly involving a redox neutral cascade. Studying the role of kinetics in this cascade is important in order to understand its full potential for industrial implementation.

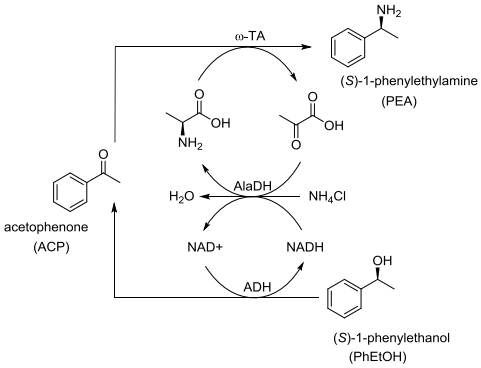

Figure 5.1: The asymmetric amination of (*S*)-1-phenylethylamine from 1-phenylethanol using ADH/ω-TA/AlaDH cascades reactions; 1-phenylethanol (PhEtOH), acetophenone (ACP), (*S*)-1-phenylethylamine (PEA), ADH: alcohol dehydrogenase, ω-TA: ω-transaminase and AlaDH: alanine dehydrogenase.

In order to evaluate the extent of such thermodynamic limitations, in this work, the synthesis of (*S*)-1-phenylethylamine (PEA), an interesting compound as an anti-emetic agent (Zhang 2000), was chosen. The enzymatic cascade is illustrated in **Figure 5.1**. In this scheme, (*S*)-1-phenylethanol (PhEtOH) was used as the starting material. It is oxidised to the ketone, acetophenone (ACP) by alcohol dehydrogenase, which is subsequently aminated by the ω-TA to produce the chiral amine, PEA. In this study, how the thermodynamically favoured reactions can drive the unproductive equilibrium reactions as well as how kinetics also plays an important role towards achieving a sufficiently favourable conversion were investigated.

5.2 Materials and Methods

5.2.1 Materials

(*S*)-1-phenylethylamine and (*S*)-1-phenylethanol were purchased from Merck (Darmstadt, Germany). L-alanine, ammonium chloride, nicotinamide adenine dinucleotide (NAD), reduced nicotinamide adenine dinucleotide (NADH), triethanolamine and sodium pyruvate were purchased from Sigma-Aldrich (St. Louis, MO, USA) respectively. Acetophenone was purchased from Fluka (St. Louis, MO, USA). All chemicals were >99.99% purity and they were used in this study without further alteration. Lyophilized enzyme ω-TA (ATA-256, a recombinant from *Escherichia coli*, EC 2.6.1.18) was purchased from Codexis Inc. (Redwood City, United States), while enzyme ADH (ADH030, a recombinant from *Escherichia coli*, EC 1.1.1.2) and AlaDH (ADH160, a *Bacillus subtilis*, EC 1.4.1.1) were purchased from Evocatal GmbH (Düsseldorf, Germany). In this study, the activity of enzymes was experimentally measured. The protein concentration was determined with Bradford reagent (Bio-Rad Protein Assay), using bovine serum albumin as a standard. Specific activity for enzyme AlaDH was 6.7 U/mg (1 unit oxidizes 1 μmoles of NADH per min at 30^{o}C, pH 7). Specific activity for enzyme ADH was 1.5 U/mg (1 unit reduces 1 μmoles of NAD per min at 30^{o}C). Specific activity for ω-TA was 2.6 mU/mg (1 unit is the amount that catalyzes the formation of 1 μmol of ACP per min at 30^{o}C, pH 7).

5.2.2 Equilibrium studies

ADH-catalysed reaction: 1 mM of each substrate concentration for both reaction direction (forward: NAD, PhEtOH; reverse: ACP, NADH), containing 0.05mg/ml ADH. AlaDH-catalysed reaction: 1 mM each substrate concentration for both reaction direction (forward: NADH, Pyr, NH_4Cl; reverse: L-Ala, NAD), containing 0.05 mg/ml AlaDH. All reactions were carried out at a 3 mL scale in 4 mL vial containing 100 mM triethylamine hydrochloride-HCl (TEA) buffer, pH 7. Reaction mixtures were continuously mixed in a thermoshaker (HCL, Bovenden, Germany) at constant temperature (30^{o}C) and agitation (450 rpm). Time-dependent concentrations of the reactants and products were measured until the equilibrium was reached from both directions of the reaction (Tewari et al. 2000). The ω-TA-catalysed reactions: The equilibrium data were determined by a method developed by Tufvesson and co-workers (Tufvesson et al., 2012). Briefly, different amounts of reactants were mixed in a reaction mixture, containing 10 mg/ml ATA256, 1 mM PLP in100 mM TEA-HCl buffer at pH 7 and 30^{o}C. The initial reactant concentrations were chosen in a range that allows the reactants to take place in both directions. In this case, the range of 1-10 mM (ACP) and 0.1-1 mM (PEA), while for the Pyr and Ala were used at 1 mM and 400 mM, respectively. The reactions were carried out at a 3 mL scale in 4 mL vial where the reaction mixtures were continuously mixed in a thermoshaker (HCL, Bovenden,

Germany) at constant temperature (30°C) and agitation (450 rpm). The reactants were allowed to react for 3 hr for the Q_t and the samples were taken to be analysed.

5.2.3 Kinetic studies

5.2.3.1 Initial reaction rate experiments

The kinetic data of the individual reaction were collected and summarised in **Table 5.1**. All reactions were carried out at a 3 mL total volume in 4 mL vial, containing 100 mM TEA buffer at pH 7. The reaction mixtures were continuously mixed in a thermoshaker (HCL, Bovenden, Germany) at constant temperature (30°C) and agitation (450 rpm). All reactions were performed in duplicate.

Table 5.1: Data collection for the initial reaction rate experiments

Enzymes	Variables	
	Forward reaction	**Reverse reaction**
ADH (0.1 mg/ml)	• 0.1 – 10 mM PhEtOH, 1 mM NAD • 0 – 10 mM NAD, 10 mM PhEtOH	• 1 – 30 mM ACP, 1 mM NADH • 0 – 1.5 mM NADH, 10 mM ACP
AlaDH (0.01 mg/ml)	• 10 - 1000 mM $NH4^+$, 10 mM Pyr, 1 mM NADH • 0.1 - 5 mM Pyr, 10 mM $NH4^+$, 1 mM NADH • 0 – 2 mM NADH, 10 mM $NH4^+$, 10 mM Pyr	• 1 – 100 mM Ala, 1 mM NAD • 0 – 5 mM NAD, 10 mM Ala
ω-TA (10 mg/ml)	• 10 – 400 mM Ala, 10 mM ACP • 10 – 5 mM Pyr, 10 mM PEA	• 0.5 – 10 mM PEA, 10 mM Pyr • 0 – 5 mM Pyr, 10 mM PEA

5.2.3.2 Nonlinear regression analysis

Using the initial rate reaction and the data collection from the experiments (**Table 5.1**), the kinetic parameters can be estimated. The objective function was formulated as Equation 5.1 and Equation 5.2, where both forward and reverse reactions which are calculated as the sum of the squares of the deviations between model prediction and experimental result (least squares) is minimized for both the forward and reverse reaction subject to the parameter values (θ).

$$J_1(\theta) = ½ \sum_{j=1}^{N} \left(r_{A_{exp}j} - r_{Aj}(\theta) \right)^2 \quad (5.1)$$

$$J_2(\theta) = ½ \sum_{j=1}^{N} \left(Q_{A_{exp}j} - Q_{Aj}(\theta) \right)^2 \quad (5.2)$$

The objective function was formulated within the range of 0–1,000 for different initial parameter values. The estimated parameters are shown in **Table 5.1**. The optimization was solved using the built-in least square function with a tolerance of 1.0E-06, in the Matlab® (The Mathworks, Natick, MA).

5.2.4 Analytical

The concentrations of PhEtOH, ACP and PEA were measured by gas chromatography (GC). Briefly, the sample was quenched by adding aqueous NaOH (5 M, 100 µL). For the extraction, 400 µL of ethyl acetate as well as 4-bromo-acetophenone (150 mM; 20 µL) as an internal standard was added. The organic phase was dried in magnesium sulphate and then the supernatant was transferred to a GC vial. For derivatization, 15 µL triethylamine and 10 µL acetic anhydride were also added into the GC vial. The concentration of reactants and products were analysed by Gas chromatography on a Clarus 500 (Perkin–Elmer) with a 25 m * 0.25 mm Agilent J&W CP-Chirasil-Dex CB column. 2 µL sample was injected, with a thermal gradient from 120 to 200 °C for 14 min, 1.4 mL/min Helium was used as a carrier gas. FID detection was carried out at 250 °C.

Activities of enzyme dehydrogenase were measured by Beckman DU-800 spectrophotometer (Beckman Coulter, Fullerton, CA, USA). The reduction and formation of NADH was monitored by measuring the absorbance at 340 nm. The concentration of compounds was calculated using the extinction coefficient (ε_{340} = 6.22 $mM^{-1}cm^{-1}$). The concentrations of the other compounds were calculated based on reaction stoichiometry where no side reactions were assumed.

5.3 Results and Discussion

5.3.1 Thermodynamic analysis

Here, a simple thermodynamic analysis was presented in order to predict the feasibility of the cascade reactions in **Figure 5.1**.

5.3.1.1 Experimentally-determined equilibrium constants

One potential method of improving the conversion of an otherwise thermodynamically limited reaction, is to couple the unfavourable reaction with an energetically favourable one (**Chapter 3).** In order to illustrate the effectiveness of this strategy the ADH/ωTA/AlaDH coupled system, presented in **Figure 5.1** was used. This cascade was described by multi-step chemical reactions (Equation 5.3 to 5.5).

$$\mathrm{PhEtOH} + \mathrm{NAD^+} \overset{\mathrm{ADH}}{\longleftrightarrow} \mathrm{ACP} + \mathrm{NADH} + \mathrm{H^+} \tag{5.3}$$

$$\mathrm{ACP} + \mathrm{Ala} \overset{\omega\mathrm{TA}}{\longleftrightarrow} \mathrm{PEA} + \mathrm{Pyr} \tag{5.4}$$

$$\mathrm{NH_4^+} + \mathrm{NADH} + \mathrm{H^+} + \mathrm{Pyr} \overset{\mathrm{AlaDH}}{\longleftrightarrow} \mathrm{NAD^+} + \mathrm{Ala} + \mathrm{H_2O} \tag{5.5}$$

Theoretically, the equilibrium constant of a chemical reaction is the value that determines the position of equilibrium in a reversible reaction at constant temperature and pressure. The equilibrium constant can be calculated by the ratio of the activities of products over the activities of reactants at equilibrium. In common practice, the activities in biologically-mediated reactions are assumed to be equal to the respective component concentration at equilibrium, giving the term 'apparent' equilibrium constant (*K'*) (Goldberg et al., 2004). The value of activity coefficient is assumed to be γ=1 in the *K'* calculation due to the biological systems frequently operate at dilute aqueous solutions, in which the components nearly shows ideal behaviour in a solution (Villadsen et al., 2011).

In this work, the *K'* of each enzyme-catalysed reaction in Equation 5.3 to 5.5 can be defined as the ratio of concentrations of products over reactants at equilibrium and can be calculated based on the Equation 5.6 to 5.8. The expressions for *K'* are written in terms of total species, rather than the individual ion species. Using a conventional approach, the equilibrium concentrations were determined by time-dependent concentration experiments catalysed by enzymes and were run in the forward and the reverse reactions (Tewari et al. 1998). At equal molar concentration of initial reactants, the equilibrium position at the forward reaction was reached at the same point in the reverse reaction. However this approach was only successful for the dehydrogenase-catalysed reactions due to the fast reaction rates as shown in **Figure 5.2**

$$K'_{\mathrm{ADH}} = \frac{[\mathrm{ACP}][\mathrm{NADH}][\mathrm{H^+}]}{[\mathrm{PhEtOH}][\mathrm{NAD^+}]} \tag{5.6}$$

$$K'_{\omega TA} = \frac{[PEA][Pyr]}{[ACP][Ala]} \tag{5.7}$$

$$K'_{AlaH} = \frac{[Ala][NAD^+][H_2O]}{[NH_4^+][Pyr][NADH][H^+]} \tag{5.8}$$

In the *K'* calculation, hydrogen ion concentration [H^+] is not included. The reason is that the [H^+] is an independent variable and the value is kept constant during the course of the reaction by a buffer. This buffer only allows a very small pH change as the system approaches equilibrium (Alberty et al. 2011). The, *K'* here is the values determined at the specified pH, which in this work is at pH 7. The same assumption for water activity in the aqueous solution, is that it does not change in the reaction mixture, and is therefore omitted in the *K'* calculation (Goldberg 2014). To keep the *K'* value dimensionless, the standard concentration c°=1 $molL^{-1}$ is included in the *K'* expression, giving the *K'* (30°C) = 9.86 $x10^{-2}$ and 5.11$x10^6$ for the ADH and AlaDH-catalysed reactions, respectively.

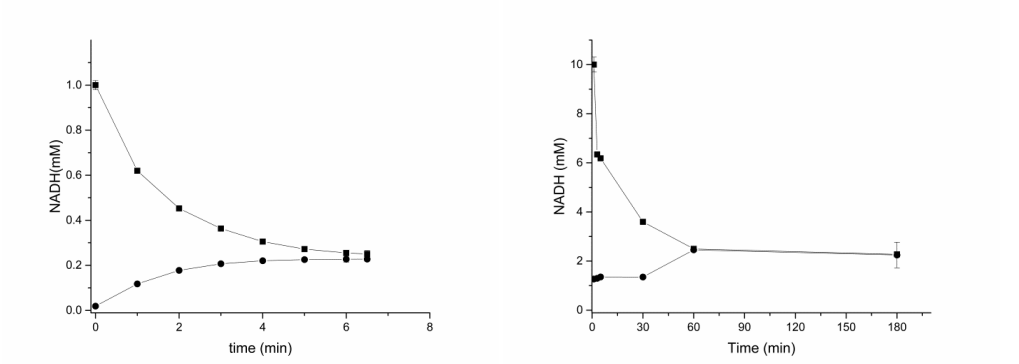

(a) (b)

Figure 5.2: Time-dependent concentrations of NADH in the forward reaction (square) and the reverse reaction (circle). (a) Alcohol dehydrogenase-catalysed reaction with the initial molal concentration of 1 mM of reactant and 0.05mg/ml ADH. (b) Alanine dehydrogenase-catalysed reaction with the initial molar concentration of 10 mM of reactant and 0.05 mg/ml AlaDH. All reactions were run at 30°C in 100 mM TEA-HCl buffer at pH 7.

Unlike the dehydrogenases, the ω-TA-catalysed reaction did not achieve equilibrium at both sides of reactions, although there are cases where the *K'* for some transaminase reactions were successfully determined by this method (Tewari et al. 1998; Gundersen et al. 2015). Only the reverse reaction

could be measured and this reaction suffers from low reaction rate and requires a high amount of ω-TA (10 mg/ml) to drive the reaction and give conversion of 74% (**Figure 5.3a**). It was also found that the enzyme continues to lose its activity after day 4, and therefore did not achieve a full conversion. Whereas in the forward reaction, the concentration of products could not be measured using an equal molar ratio of reactants (Ala and ACP). This constraint might be due to the fact that the equilibrium position lies far to the left direction and therefore any products were hardly formed from the reactants (Shin and Kim 1998).

Additionally, it may require a lot of ω-TA to increase the reaction rate to reach equilibrium, but using up to 20 mg/ml ω-TA was not successful in this study and the formation of precipitate was observed in the reaction solution. Alternatively, the method develop by Tufvesson and co-workers was used to determine the *K'* for ω-TA-catalysed reaction scheme it was probable to determine the forward and reverse reactions converge to the infinity (Tufvesson et al. 2012). This method is based on the measurements of the reaction rate using a various amount of substrate and product concentrations in a reaction mixture. Here, the *K'* for the amination of ACP was determined to be $1.14x10^{-4}$ as shown in **Figure 5.3b**, which is comparable to the previous study ($4.032x10^{-5}$), (Tufvesson et al. 2012).

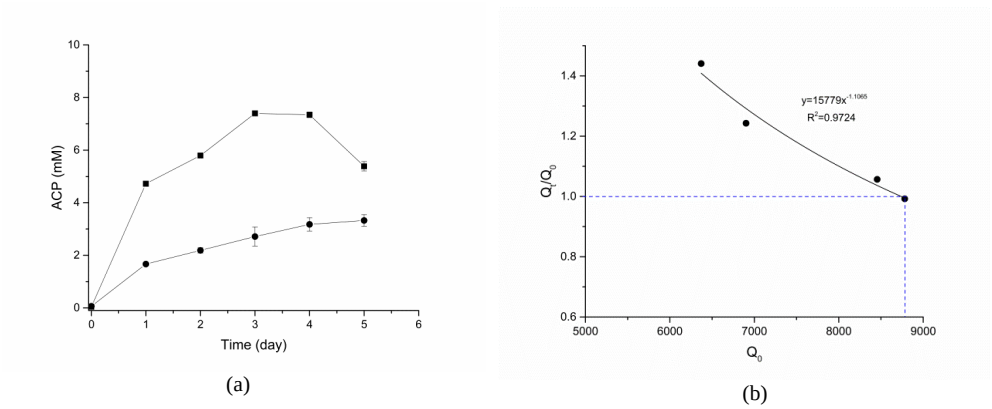

Figure 5.3: Experimentally determined *K'* for the ω-TA-catalysed reaction. (a) The reverse reaction could only be measured using the conventional method where 1 mg/ml (circle) and 10 mg/ml (square) were used in the reaction mixture ATA256. (b) Using a new method developed by Tufvesson that successfully determined the *K'*. In this experiment, the reactants were mixed in different amounts (Q_0), and the reaction mixture contained 10 mg/ml ATA256, 1 mM PLP in100 mM TEA-HCl buffer at pH 7 and 30°C. The reactants were allowed to react for 3 hr for the Q_t. From the Q_t/Q_0 versus Q_0 on the graph, the *K'* for the reaction can be determined at the point at where the Q_4/Q_0 equal 1 (dash line), giving the *K*' = 8780 for this reaction. The *K'* for the reverse direction is the reciprocal of the one for the forward reaction ($1.14x10^{-4}$).

5.3.1.2 Effect of Coupling

Interestingly, the key to maximise the equilibrium conversion of a cascade is determined by a single net reaction that controls the favourability of the cascade. Hence, the overall reaction can be simplified into a net reaction, as shown in (Equation 5.9). In this way, the overall *K'*, denoted as K'_{net} for the cascade, can be calculated by using Equation 5.10.

$$NH_4^+ + \text{PhEtOH} \overset{\text{Net}}{\leftrightarrow} \text{PEA} + H_2O \quad \text{(Eq. 5.9)}$$

$$K'_{\text{net}} = K'_{\text{ADH}} \times K'_{\omega\text{TA}} \times K'_{\text{AlaDH}} \quad \text{(Eq. 5.10)}$$

The K'_{net} can be calculated by multiplying the experimental *K'* values obtained from each reaction. While the corresponding $\Delta G_r'^o$ values for the net reaction, can be calculated by adding each of the corresponding $\Delta G_r'^o$ from each reaction. The experimental $\Delta G_r'^o$ values were then compared with the $\Delta G_r'^o$ values calculated using the group contribution method by Jankowski et al. (2008) as summarised in **Table 5.2**.

Table 5.2: The experimental *K'* values and the corresponding $\Delta G_r'^o$ for the synthesis of (*S*)-1-phenylethlamine at 30°C, pH 7. The experimental $\Delta G_r'^o$ values were also compared with the $\Delta G_r'^o$ values calculated from Jankowski Group Contribution method. Each reaction was carried out in triplicate, giving the *K'* experimental errors.

Enzyme reaction	*K'*	$\Delta G_r'^o$ (kJ/mol)[a]	Group contribution (kJ/mol)
ADH reaction	$9.86\text{x}10^{-2} \pm 2.71\text{x}10^{-4}$	+5.84	+9.25
ω-TA reaction	$1.14\text{x}10^{-4} \pm 1.11\text{x}10^{-4}$	+22.87	+16.78
AlaDH reaction	$5.11\text{x}10^{6} \pm 4.44\text{x}10^{-6}$	–38.91	–36.36
Net reaction	57.40 ± 1.31	–10.20	–10.33

[a] $\Delta G_r'^o = -RT\ln K'$, R=8.3145 J/mol·K , T=303K

To further improve the conversion, the ammonium concentration is the key compound that controls the favourability of the cascade and thus has an effect on the overall equilibrium as shown in Equation 5.11. The value of K'_{net} can be used to manipulate the amount of ammonia required in such as a way to push the overall equilibrium towards the production of PEA.

$$K'_{\text{net}} = \frac{[\text{PEA}]}{[\text{PhEtOH}][\text{NH}_4^+]} \tag{5.11}$$

For example, 10 molar equivalents of ammonia concentration theoretically could achieve approximately 84% conversion, assuming that the system is operated in an efficient *in-situ* re-generation system (**Figure 5.4**). Applying more than 60 molar equivalents of the ammonia to the system will push the overall equilibrium position to achieve maximum conversion of 97%. Nevertheless, supplying so much excess of ammonium to the cascade system, to some extent might damage to the enzymes. Besides, it was commonly found that many cascades have been operated experimentally with the use of an excess of alanine (5–10-equivalents) (Abu and Woodley 2015). However, according to the calculation in Equation 5.11, it would appear that such an excess is not required.

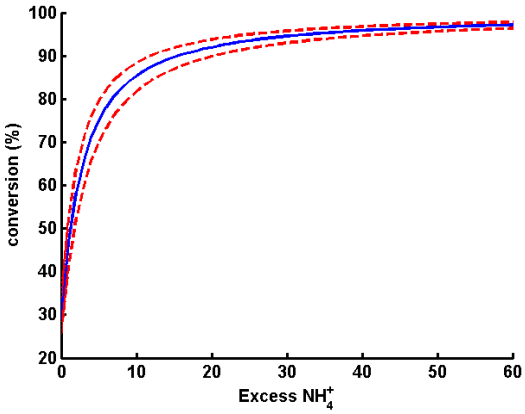

Figure 5.4: Estimation of equilibrium conversion of ADH/ω-TA/AlaDH cascade by varying the only amount of ammonium to push the overall equilibrium towards the production of PEA. Using the experimental *K'* = 57.40 (solid line) and experimental error (dashed line).

Therefore, the feasibility of such a cascade was explored in the dependency of conversion on the excess of alanine as well as the use of 10-equivalents of ammonia to obtain the predicted conversion of 84% (**Figure 5.4**) for the cascade. Here, the enzymatic cascade was performed at 10 mM PhEtOH with varying the concentration of alanine, 1 mM and 100 mM (in excess). This experiment further verifies that the alanine concentration in excess did not give an effect on the conversion (**Figure 5.5a**). In fact, in a recent study by Janssen's Group in the synthesis of amines using the similar cascade reactions, at a catalytic amount of alanine, 60% conversion was achieved (Palacio et al. 2016).

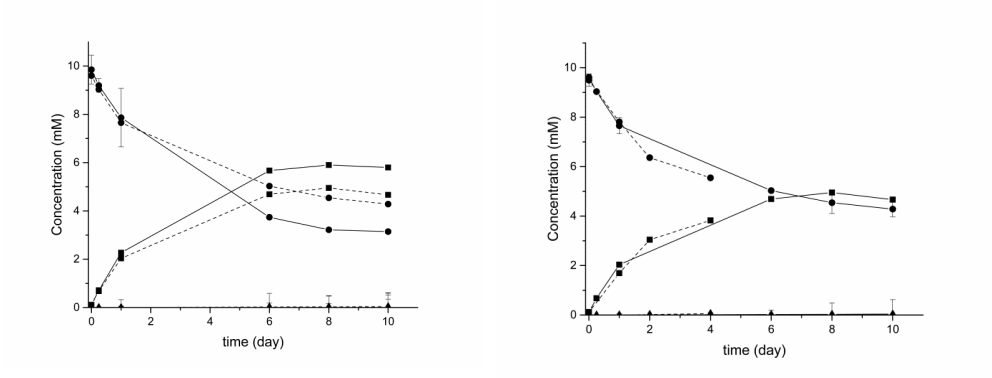

(a) (b)

Figure 5.5: (a) Effect of Ala in the redox neutral cascade, 1 mM Ala (solid lines) and 100 mM Ala (dash lines). Both cascades were carried out with 10 mM PhEtOH, 1 mM NAD, 100 mM NH4Cl, 1 mM PLP, 10 mg/ml ATA256, 1 μg/ml AlaDH and 1 μg/ml ADH. Symbols: PhEtOH (circle), ACP (square) and PEA (triangle).
(b) Cascade (solid lines) was carried out with 10 mM PhEtOH, 1 mM NAD, 100 mM NH_4Cl, 1 mM Ala, 1 mM PLP, 10 mg/ml ATA256, 1 μg/ml AlaDH and 1 μg/ml ADH while for the sequential cascade (dash lines) was carried out with 10 mM PhEtOH, 1 mM NAD, 100 mM Ala, 1 mM PLP, 10 mg/ml ATA256 and 1 μg/ml ADH. All experiments were run in 100 mM TEA buffer at pH 7 and 30^{o}C. Symbols: PhEtOH (circle), ACP (square) and PEA (triangle).

Unfortunately, in this study, the experimental results were not so positive when 10-equivalents of ammonia (100 mM) were used to obtain the 84% predicted conversion (**Figure 5.5**). Adding more ammonia to the cascade system to concentration up to 1000 mM also did not increase the target conversion. Moreover, precipitation of the enzymes was observed at 200 mM ammonia.

It was further identified that there was an uncoupling in the redox neutral cascades as accumulation of intermediate compounds (ACP) was observed in the system (**Figure 5.5a**). Further experiments were done to identify the uncoupling of reactions in the cascade. The AlaDH enzyme was removed from the cascade system where the oxidation of alcohol (in a catalytic amount of NAD^{+}) and the amination of ketone (in excess of alanine) were run sequentially towards the amine. Similar trends were observed for the sequential cascade (**Figure 5.5b**) and the redox neutral cascade (**Figure 5.5a**), confirming the uncoupling of AlaDH-catalysed reaction. The uncoupling effect causes the ineffective thermodynamic approach and thus limits the conversion of the target product. This might also the answer for why Tauber et al. only achieved 25% conversion. Hence, in the following subsections, the kinetic modelling was used as a tool to identify possible reasons of the uncoupling reactions, for examples, the presence of cross-reaction (e.g. NADH is oxidized to NAD by other enzyme) and unmatched enzyme activities and reaction conditions in the enzymatic network.

5.3.2 Development of kinetic models

5.3.2.1 ADH kinetic model

ADH-catalysed reaction follows an ordered bi bi mechanism where two substrates and two products of reaction are added to the enzyme in an ordered direction (Leskovac 2004). The substrate (NAD) is added first and the product (NADH) is released before the other substrate (in this study, PhEtOH) is added and the product (ACP) is released. The full kinetic model for the ADH-catalysed reaction is expressed in Equation 5.12.

$$r_{\mathrm{ADH}} = \frac{v_{\max}^{\mathrm{f}} v_{\max}^{\mathrm{r}} [\mathrm{NAD}][\mathrm{PhEtOH}] - \dfrac{[\mathrm{ACP}][\mathrm{NADH}]}{K_{\mathrm{eq}}}}{\begin{aligned} & v_{\max}^{\mathrm{r}} K_{\mathrm{m}}^{\mathrm{PhEtOH}} [\mathrm{NAD}] + v_{\max}^{\mathrm{r}} K_{\mathrm{m}}^{\mathrm{NAD}} [\mathrm{PhEtOH}] + v_{\max}^{\mathrm{r}} [\mathrm{NAD}][\mathrm{PhEtOH}] \\ & + \frac{v_{\max}^{\mathrm{f}} K_{\mathrm{m}}^{\mathrm{NADH}}}{K_{\mathrm{eq}}} [\mathrm{ACP}] + \frac{v_{\max}^{\mathrm{f}} K_{\mathrm{m}}^{\mathrm{ACP}}}{K_{\mathrm{eq}}} [\mathrm{NADH}] + \frac{v_{\max}^{\mathrm{f}}}{K_{\mathrm{eq}}} [\mathrm{ACP}][\mathrm{NADH}] \end{aligned}} \qquad (5.12)$$

Equation 5.12 consists of Michaelis-Menten kinetic parameters (K_m and V_{max}), inhibition constants (K_i) and equilibrium constant (K_{eq}). **Figure 5.6** and **Figure 5.7** illustrate the plots for the initial rate experiments for the forward and the reverse reactions, respectively. The estimated parameters were summarised in **Table 5.3**. The value of K_{eq}, which was obtained from the equilibrium study, was used for the estimation of the full model. The reaction is heavily influenced by uncompetitive substrate inhibitions as well as unfavorable reaction equilibrium.

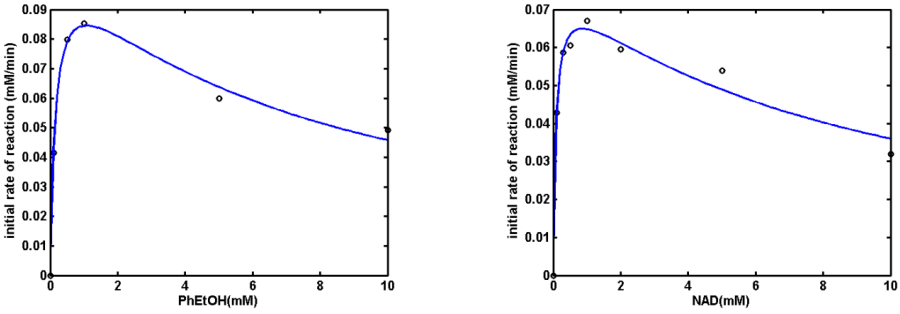

(a) (b)

Figure 5.6: Initial rate experiments for the ADH kinetics in the oxidation of PhEtOH (forward reaction). The experiments were carried out with 0.1 mg/ml at pH 7 and 30°C in 100 mM TEA-HCl buffer. (a) Varying the PhEtOH concentration at fixed 1mM NAD and (b) varying the NAD concentration at fixed 10 mM PhEtOH. Experimental data (symbol) and prediction (solid line).

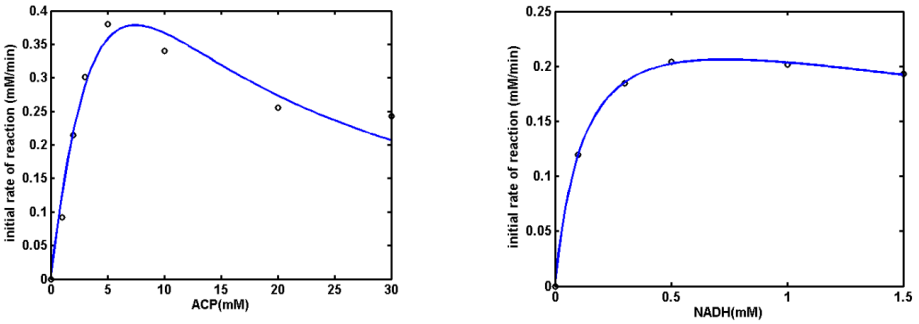

(a) (b)

Figure 5.7: Initial rate experiments for the ADH kinetics in the reduction of acetophenone (reverse reaction). The experiments were carried out with 0.1 mg/ml at pH 7 and 30°C in 100 mM TEA-HCl buffer. (a) Varying the ACP concentration at fixed 1 mM NADH and (b) varying the NADH concentration at fixed 10 mM ACP. Experimental data (symbol) and prediction (solid line).

Table 5.3: Estimated parameters for ADH-catalysed reaction.

Kinetic Parameter	Estimated values
$V_{\max}^{f}$	0.110 mM/min
$V_{\max}^{r}$	1.393 mM/min
$K_{\mathrm{m}}^{\mathrm{PhEtOH}}$	0.159 mM
$K_{\mathrm{m}}^{\mathrm{NAD}}$	0.0848 mM
$K_{\mathrm{m}}^{\mathrm{ACP}}$	9.988 mM
$K_{\mathrm{m}}^{\mathrm{NADH}}$	0.1334 mM
$K_{\mathrm{si}}^{\mathrm{PhEtOH}}$	7.259 mM
$K_{\mathrm{si}}^{\mathrm{NAD}}$	8.696 mM
$K_{\mathrm{si}}^{\mathrm{ACP}}$	5.560 mM
$K_{\mathrm{si}}^{\mathrm{NADH}}$	3.978 mM

5.3.2.2 AlaDH kinetic model

AlaDH catalyses a reversible reaction by an ordered kinetic mechanism in which NADH, pyruvate, NH_4^+ is added and Ala and NAD are released in an ordered fashion (Grimshaw and Cleland 1981).

The full kinetic model for the AlaDH-catalysed reaction can be written as Equation 5.13 (Leskovac 2004).

$$r_{\mathrm{AlaDH}} = \frac{v_{\max}^{\mathrm{f}} v_{\max}^{\mathrm{r}} [\mathrm{NADH}][\mathrm{Pyr}][\mathrm{NH_4^+}] - \frac{[\mathrm{Ala}][\mathrm{NAD}]}{K_{\mathrm{eq}}}}{\begin{aligned} &v_{\max}^{\mathrm{r}} K_{\mathrm{m}}^{\mathrm{NH_4^+}} [\mathrm{NADH}][\mathrm{Pyr}] + v_{\max}^{\mathrm{r}} K_{\mathrm{m}}^{\mathrm{Pyr}} [\mathrm{NADH}][\mathrm{NH_4^+}] + v_{\max}^{\mathrm{r}} K_{\mathrm{m}}^{\mathrm{NADH}} [\mathrm{Pyr}][\mathrm{NH_4^+}] \\ &+ v_{\max}^{\mathrm{r}} [\mathrm{NADH}][\mathrm{Pyr}][\mathrm{NH_4^+}] + \frac{v_{\max}^{\mathrm{f}} K_{\mathrm{m}}^{\mathrm{NAD}}}{K_{\mathrm{eq}}} [\mathrm{Ala}] + \frac{v_{\max}^{\mathrm{f}} K_{\mathrm{m}}^{\mathrm{Ala}}}{K_{\mathrm{eq}}} [\mathrm{NAD}] + \frac{v_{\max}^{\mathrm{f}} K_{\mathrm{m}}^{\mathrm{Ala}}}{K_{\mathrm{eq}}} [\mathrm{Ala}][\mathrm{NAD}] \end{aligned}} \quad (5.13)$$

Figure 5.8 and **Figure 5.9** illustrates the experimental initial rate plots determined for the forward reaction and the estimated parameters are summarised in **Table 5.4**. Usually the K_m values for NH_4^+ were reported in the range between 20 to 300 mM with the pH optimum between 8.5 to 9.0 (Yoshida and Freese 1964; Grimshaw and Cleland 1981). While in this study, the K_m for NH_4^+ was calculated to be 757.14 mM at pH 7, which was 2 times higher than the optimum pH. It was also found that NH_4^+ bind directly to a residue on AlaDH, indicating that NH_4^+ rather than NH_3 was the true substrate for this enzyme (Smith et al. 1993).

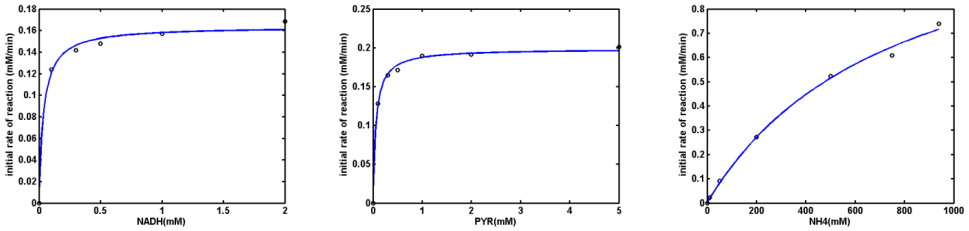

(a) (b) (c)

Figure 5.8: Initial velocity experiments for the AlaDH kinetics in the amination reaction (forward reaction). The experiments were carried out with 10 µg/ml AlaDH at pH 7 and 30oC in 100 mM TEA-HCl buffer. Varying (a) NADH concentration (b) Pyr concentration and (c) NH4+ concentration, at fixed concentration for other substrates. Experimental data (symbol) and fitted (solid line).

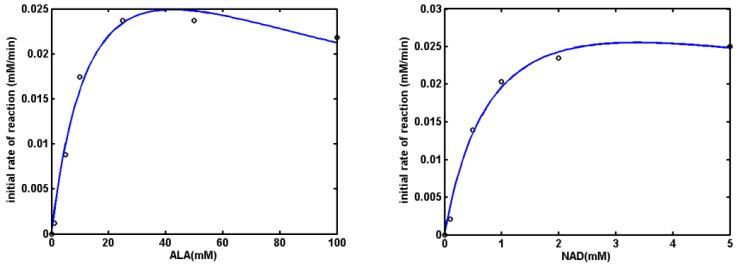

(a) (b)

Figure 5.9 : Initial velocity experiments for the AlaDH kinetics in reverse reaction. The experiments were carried out with 10 µg/ml AlaDH at pH 7 and 30°C in 100 mM TEA-HCl buffer. Varying (a) Ala and (b) NAD at fixed concentration for NAD (1 mM) and Ala (10 mM), respectively. Experimental data (symbol) and fitted (solid line).

Table 5.4: Estimated parameters for AlaDH-catalysed reactions

Kinetics Parameters	**Estimated values**
$V_{\max}^{f}$	1.29 mM/min
$V_{\max}^{r}$	0.045 mM/min
$K_{\mathrm{m}}^{\mathrm{NH_4^+}}$	757.14 mM
$K_{\mathrm{m}}^{\mathrm{Pyr}}$	0.20 mM
$K_{\mathrm{m}}^{\mathrm{NADH}}$	0.036 mM
$K_{\mathrm{m}}^{\mathrm{Ala}}$	17.29 mM
$K_{\mathrm{m}}^{\mathrm{NAD}}$	0.97 mM

5.3.2.3 ω-TA kinetic model

The enzyme ω-TA catalyses the transfer of an amino group from a donor molecule to a pro-chiral acceptor ketone, yielding a chiral amine by a ping-pong bi-bi mechanism (Leskovac 2004). In this study, the mechanism can be expressed by the mathematical model as shown in Equation 5.14. The enzyme requires pyridoxal phosphate (PLP) as a cofactor to catalyse this reaction.

$$r_{\omega TA} = \frac{V_{max}^{f} V_{max}^{r} \left([Ala][ACP] - \frac{[PEA][Pyr]}{K_{eq}} \right)}{V_{max}^{r} K_m^{ACP} [Ala] + V_{max}^{r} K_m^{Ala} [ACP] + \frac{V_{max}^{f} K_m^{Pyr}}{K_{eq}} [PEA] + \frac{V_{max}^{f} K_m^{PEA}}{K_{eq}} [Pyr] + V_{max}^{r} [Ala][ACP] + \frac{V_{max}^{f} K_m^{Pyr}}{K_i^{Ala} K_{eq}} [Ala][PEA] + \frac{V_{max}^{f}}{K_{eq}} [PEA][Pyr] + \frac{V_{max}^{r} K_m^{Ala}}{K_i^{Pyr}} [ACP][Pyr] + \frac{V_{max}^{f} K_m^{PEA}}{K_i^{Ala} K_{eq}} [Ala][Pyr] + \frac{V_{max}^{r} K_m^{Ala}}{K_i^{PEA}} [ACP][PEA]} \quad (5.14)$$

In this model, the Ala is bound first, while the coproduct Pyr is released before the second substrate ACP is added and the final product PEA leaves the enzyme last. Equation 5.14 consists of Michaelis-Menten kinetic parameters (K_m and V_{max}), inhibition constants (K_i) and equilibrium constant (K_{eq}). Unfortunately, in this study, the initial rate of ACP formation could only be measured in the reverse reaction as shown in **Figure 5.10**.

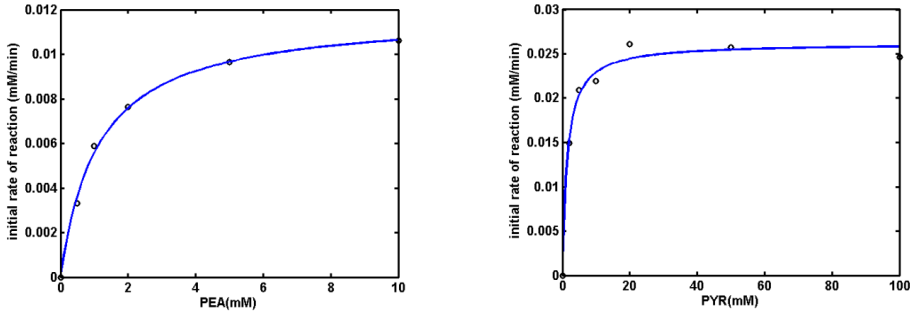

(a) (b)

Figure 5.10: Initial velocity experiments for the ω-TA kinetic in the amination of pyruvate (reverse reaction) with 10 mg/ml ATA256, 1 mM PLP at pH 7 and 30°C in 100 mM TEA-HCl buffer. (a) Varying the PEA concentration while maintaining the Pyr concentration at 10 mM and (b) varying the Pyr concentration, while maintaining the PEA concentration at 10 mM. Experimental data (symbol) and fitted (solid line).

The kinetics of ω-TA for the amination of ACP could not be measured by the initial rate experiments due to the slow reaction in this direction. Only a small amount of PEA was obtained in an excess of 10-equivalents Ala and a conversion of 3.50% was reached after 24 hr of reaction. The result consistent with the previous reports where the use of excess amine donor Ala does not indicate much success (**Table 2.1**, previously discussed in Section 3). In order to investigate the full potential of the cascade, the ω-TA kinetic parameters from the literature were used for further analysis in the next section (Shin and Kim 1998) and the values were summarised in **Table 5.5**.

Table 5.5: Kinetic parameters for the ω-TA-catalysed reaction.

Kinetics Parameters	**Estimated values, 95% CI**	**Literature data** (Shin and Kim 1998)
$V_{\max}^{f}$	x	5.18×10^{-4} mM/min
$V_{\max}^{r}$	0.0118 mM/min	0.42 mM/min
$K_{\mathrm{m}}^{\mathrm{Ala}}$	x	1.07 mM
$K_{\mathrm{m}}^{\mathrm{ACP}}$	x	0.54 mM
$K_{\mathrm{m}}^{\mathrm{PEA}}$	1.121 mM	35.03 mM
$K_{\mathrm{m}}^{\mathrm{Pyr}}$	1.437 mM	9.58 mM
$K_{\mathrm{I}}^{\mathrm{Ala}}$	x	2.85 mM
$K_{\mathrm{I}}^{\mathrm{PEA}}$	x	1.02 x 10^{-2} mM

5.3.2.4 Kinetic models for the cascade

By integrating the kinetic model of the individual reactions (Equation 5.12, 5.13 and 5.14), the kinetic models describing the redox neutral cascade for the amination of PEA from PhEtOH in **Figure 5.1** can be developed. The objectives of the kinetic modelling are to identify the kinetic parameters that are significant in the cascade and to determine the relative rates between the interconnecting enzymes in the cascade. Using the estimated parameters in the initial rate experiments in the previous section, the effect of the reaction equilibrium as well as the effect in the presence of products can be investigated. The interaction matrix is used to define the type of interactions exists between compounds and enzymes in the cascade example (**Table 5.6**).

Table 5.6: Interaction matrix for the redox neutral cascade in the production of PEA. Substrate (S), product (P), non-interacting compound (X) and inhibitor (I).

compounds	**Enzymes**		
	ADH	**ω-TA**	**AlaDH**
PhEtOH	S-I	x	x
ACP	P-I	S-I	x
Ala	x	S	P
Pyr	x	P	S
PEA	x	P-I	x
NH_4^+	x	x	S
Co-factors			
NADH	P-I	x	S
NAD+	S-I	x	P

Based on the interaction matrix, eight (8) differential equations were derived for the mass balance of the redox neutral cascade in one-pot fashion **Table 5.7**. The following assumptions were made for the mathematical models.

- Reaction volume is constant
- Perfect mixing in the reactor
- pH and temperature are constant
- Kinetic parameters for the ADH and AlaDH were experimentally determined
- Kinetic parameters for ω-TA were taken from Shin and Kim (1998) and were assumed correct

Table 5.7: Mass balances for all variables for the redox neutral cascade

$\frac{dC_{\mathrm{PhEtOH}}}{dt} = -r_{\mathrm{ADH}}$
$\frac{dC_{\mathrm{NAD}}}{dt} = -r_{\mathrm{ADH}} + r_{\mathrm{AlaDH}}$
$\frac{dC_{\mathrm{ACP}}}{dt} = r_{\mathrm{ADH}} - r_{\omega\mathrm{TA}}$
$\frac{dC_{\mathrm{Ala}}}{dt} = -r_{\omega\mathrm{TA}} + r_{\mathrm{AlaDH}}$
$\frac{dC_{\mathrm{NH_4^+}}}{dt} = -r_{\mathrm{AlaDH}}$
$\frac{dC_{\mathrm{Pyr}}}{dt} = r_{\omega\mathrm{TA}} - r_{\mathrm{AlaDH}}$
$\frac{dC_{\mathrm{NADH}}}{dt} = r_{\mathrm{ADH}} - r_{\mathrm{AlaDH}}$
$\frac{dC_{\mathrm{PEA}}}{dt} = r_{\omega\mathrm{TA}}$

The results from simulation show that no conversion was obtained for the redox neutral cascade (**Figure 5.11**), due to the adverse equilibrium position in the amination of ketone as well as due to the unmatched relative rate between the dehydrogenases and ω-TA. This was confirmed by separating the cascade into two parallel cascades as shown in **Figure 5.12**.

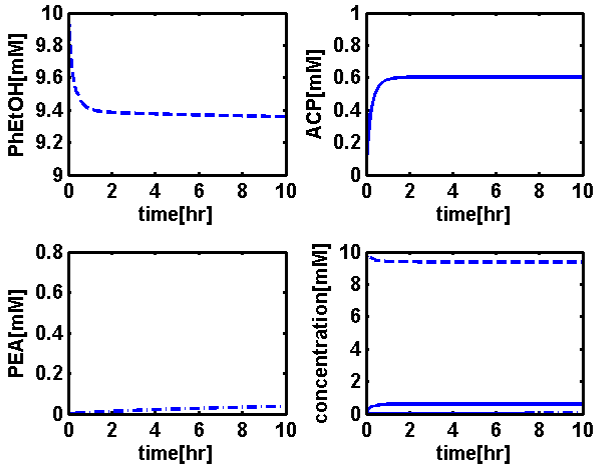

Figure 5.11: Simulation of the redox neutral cascade.

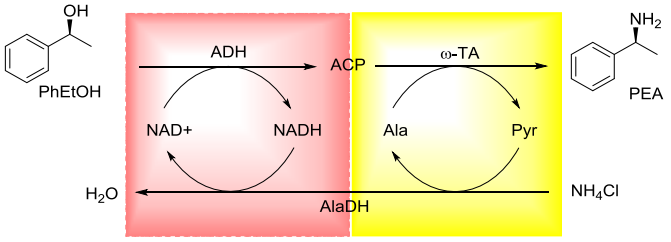

Figure 5.12: Simulation of ADH/AlaDH and ω-TA/AlaDH of parallel cascades.

Simulations showed that the ADH/AlaDH parallel cascade achieves a full conversion of ketone after 10 hr in the absence of ω-TA in the cascades (**Figure 5.13**). In contrast, a very low conversion is given by the ω-TA/AlaDH parallel cascade, showing that the ω-TA reaction is the underlying bottleneck in the ADH/ω-TA/AlaDH system. Similar findings were reported in a study where the reductive amination of 2-oxoglutarate was 420 times faster than the reductive amination by the aspartate aminotransferase, showing that the transaminase reaction was the rate limiting step given the high catalytic efficiency of glutamate dehydrogenase (Salerno et al. 1982). In this simulation, the rate for AlaDH-catalysed reaction was 13 times faster than the rate in ADH-catalysed reaction, whereas 2500 time faster than the rate in ω-TA-catalysed reaction different. The unbalanced reaction rates render the

redox neutral cascades efficiency and thus limit the overall conversion. Experiments were also carried out using a lower amount of dehydrogenases and a higher amount of ω-TA in a reaction mixture, but because of the large different reaction rates, such experiments did not give a significant difference.

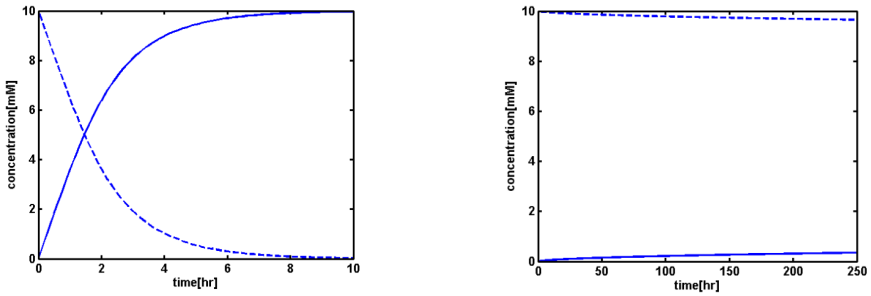

(a) (b)

Figure 5.13: Simulation of ADH/AlaDH parallel cascade; 10 mM PhEtOH (dash line), 10 mM Pyr, 1mM NAD, achieves full conversion of ACP (solid line) after 10 hr, in absence of ω-TA in the cascades. (b) Simulation of ω-TA/AlaDH parallel cascade; 10 mM ACP (dash line), 10 mM NADH, 1mM Ala, did not achieve full conversion of PEA (solid line).

Using a different type of ω-TAs (ATA50 and ATA81 provided by c-LEcta GmbH (Leipzig, Germany), also did not give any significant results (**Figure 5.14**). The results also suggest that that the amination of ACP with Ala is strongly kinetically limited. It has also been shown by a study where the ω-TAs have much lower reactivity towards ACP compared to that reactive acceptor, Pyr (Shin and Kim 2002). The amination of ACP could be kinetically limited even at low enzyme concentrations due to the products, PEA and Pyr, are much more reactive than the reactants. Therefore, the conversion of PEA would be far from reaching equilibrium, which might be the main reason why the use of the thermodynamic approach has failed. Besides, the product inhibition by PEA is too severe and may not allow considerable reaction progress, thereby greatly decreasing the reverse reaction rate. This is particularly true if the reactivities of the products are higher than those of the substrates (Truppo et al. 2010). While compared with the dehydrogenases, these enzymes have fast reaction rates (were not kinetically limited) from both forward and reverse direction, allowing the system to reach equilibrium faster.

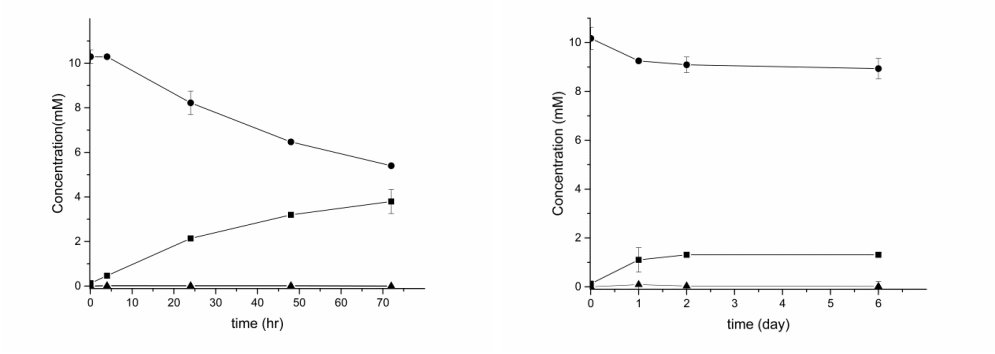

(a) (b)

Figure 5.14: The use of different types of ω-TA in the redox neutral cascade; (a) ATA50 (5 mg/ml) and (b) ATA81 (10 mg/ml). Both cascades were run at pH 7 and 30°C in 100 mM TEA buffer, containing 10 mM PhEtOH, 1 mM PLP, 1 µg/ml AlaDH, 1 µg/ml ADH, 1 mM NAD, 1 mM Ala and 100 mM NH4Cl. Symbols: PhEtOH (circle), ACP (square) and PEA (triangle).

5.3.2.5 Incompatible reaction conditions between dehydrogenases and transaminase

While increasing the pH 7 to pH 8.5, also did not increase the conversion as shown in **Figure 5.15**. While for the pH effect, the optimal pH for the (*S*)-specific ω-TA was found at pH 7.5, and thus increasing the pH leads to lower conversions and enantioselectivity (Fesko et al. 2013).

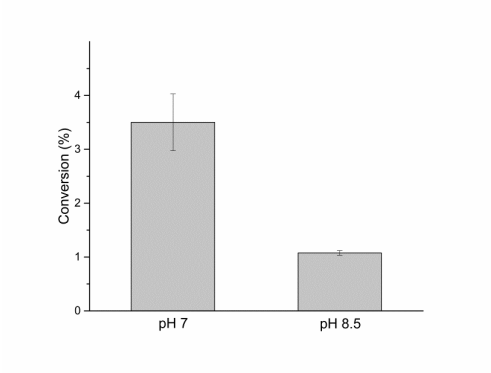

Figure 5.15: The initial rate could not be measured due to the slow reaction rate in the amination of ACP and only a small amount of PEA was obtained after 24 hr by the use of Ala in excess (10-equivalents). Both experiments were run with 10 mg/ml ATA256 and 1 mM PLP at 30°C in 100 mM TEA-HCl buffer.

In contrast to the dehydrogenases where the ADH activities were increased up to 3-fold (4.22 U/mg) at pH 8.5 from the pH 7 (1.5 U/mg) and for the AlaDH activities were increased up to 7-fold (44.86 U/mg) at pH 8.5 from the pH 7 (6.7 U/mg). This is true for the reductive amination of pyruvate where frequently has a pH optimum of 8.5, giving the K_m value for NH_4^+ and PhEtOH to be 22.60 mM and 0.298 mM, respectively **Figure 5.16**. These results show that the unmatched reaction conditions between the dehydrogenases and ω-TA at different pH. The interconnected enzymes have to fit in compatible reaction conditions in order to have efficient processes. Besides, proper selection of enzymes that has a specific stereopreference is required to avoid any cross-reactions in this redox neutral cascade.

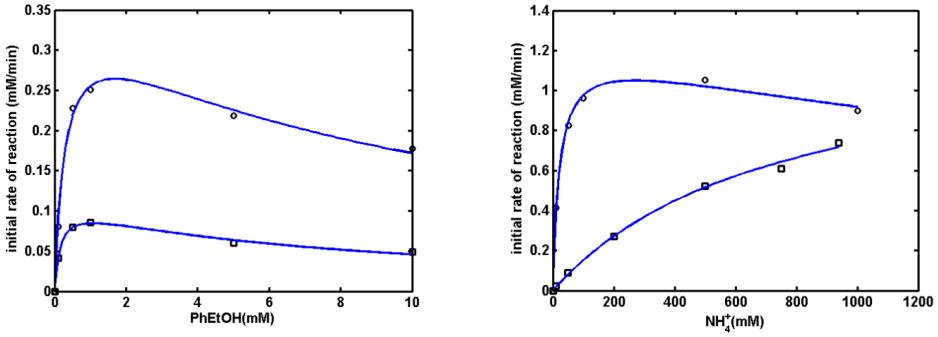

(a) (b)

Figure 5.16: Dehydrogenase kinetics (a, ADH) and (b, AlaDH) at different pH, showing a higher reaction rate at pH 8.5 (circle) than pH 7 (square). Fitted (solid line). The experiments were carried out at 30°C in 100 mM TEA-HCl buffer, with 100 µg/ml and 10 µg/ml for ADH and AlaDH, respectively.

5.3.2.6 Cross-reaction in the redox neutral cascade

Previous experiments showed that the AlaDH reaction step was uncoupled from the cascade redox due to the presence of cross-reaction during the process. It was observed a significant increase (5-fold) in the intermediate (ACP) compared to the amount NAD added in the cascade system (**Figure 5.5b** and **Figure 5.14a**). It was known that NADH is not the most stable compound that easily oxidized to NAD by other enzymes or spontaneously, particularly by NOX. Due to the purity level of enzyme, the use a crude cell extract that is more relevant for industrial applications, rather than a highly purified enzyme, has a possibility to get a cross-reaction in a reaction system, especially for the redox neutral cascades that are connected via the transfer of the redox equivalents.

Table 5.8: Estimated parameters for NOX-catalysed reaction (Presečki and Vasić-Rački 2009)

Kinetics Parameters	Estimated values
$V_{\max}^{f}$	63.299 ± 1.024 (U/mg)
$K_{\mathrm{m}}^{\mathrm{NADH}}$	0.047 ± 0.002 mM
$K_{\mathrm{m}}^{\mathrm{NAD}}$	0.417 ± 0.022 mM

To further identify the cross-reaction, using the kinetic parameters of NOX in **Table 5.8**, the data were taken from the literature (Presečki and Vasić-Rački 2009) and simulated for the ADH/NOX system as shown in **Figure 5.17**.

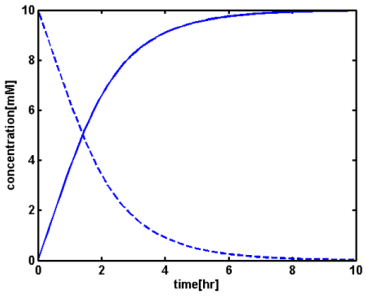

Figure 5.17: The simulation of the ADH/NOX cascade was carried out using the kinetic parameter available from literature (Presečki and Vasić-Rački 2009). The initial reaction condition with 10 mM NAD, assuming the temperature and pH to be constant in the process. PhETOH (dash line) and ACP (solid line).

From the simulation results it was found that the slow reaction rate of ω-TA in the cascade compared to the fast reaction by NOX, resulting in the uncoupling of the reactions since there is no additional source of electrons which generates enough reduced NADH necessary to drive the amination of pyruvate and thus limit the conversion of the target product (**Figure 5.18**).

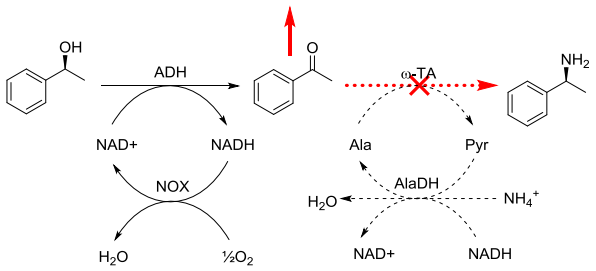

Figure 5.18: NADH-oxidase (NOX) oxidised NADH to NAD before its hydride was consumed in the reductive amination, resulting in a significant increase of ACP (arrow red). NADH-oxidase might presence in the lyophilized enzyme derived from the *E. coli*.

Further, I performed some experiments in order to determine the presence of NOX in the lyophilized enzyme ω-TA (ATA-256). After 6 hours, 1 mM of NADH was completely oxidised to NAD in the reaction buffer (Tris-HCl at pH 7 and 30^{o}C), containing only 10 mg/ml of ω-TA. Indeed, this is what the simulation results (**Figure 5.17**) demonstrate that the NOX can oxidise the NADH within hours to complete the conversion of the intermediate (ACP). Refer to Appendix B.

5.4 Conclusions

In this study, a simple approach was presented using basic thermodynamic data (equilibrium constant, *K'*) to determine thermodynamic feasibility of a single reaction as well as a redox neutral cascade. Unfortunately, in this study, the redox neutral cascade did not successfully convert the substrate to the target chiral amine from alcohol by the thermodynamic approach. It was due to the fact that the ω-TA reaction was too slow for the side reaction to take place by NADH-oxidase (NOX presence in lyophilized ω-TA (ATA-256)). This cross-reaction causes the uncoupling reactions in the desirable cascade and therefore thermodynamic approach would not be effective in this case.

It was also found that the ω-TA reaction is the underlying bottleneck in the ADH/ω-TA/AlaDH system and thus the activity of this enzyme needs to be improved to match with the interconnecting dehydrogenases, which is essential for the thermodynamics. Hence, the activity of the ω-TA needs to be improved several fold (e.g. 100 fold) by protein engineering (e.g. by changing the enzyme structure in order to enhance the substrate-binding of alanine and acetophenone) in order to balance its rate with

the fast reactions catalysed by dehydrogenases. Thus the recycling systems (co-substrate Ala and co-factor NAD) can be run efficiently and the redox neutral cascade can fulfil its objective, enabling high conversion.

In conclusion, the findings indicate that quantitatively the possibilities for improving conversion of thermodynamically limited reactions not only require application of enzyme coupling reactions (coupling the unfavourable reaction with an energetically favourable reaction) but also used matching of the relative kinetic rates between the interconnecting enzymes. Besides, the modelling and simulation enabled to quantitatively understand the behavior in the redox neutral cascade as well as suggested the direction for improving the properties of ω-TA.

6 Case Study II: One-pot Cascade Synthesis of 2-Ketoglutarate from Glucuronate

6.1 Introduction

The formation of 2-ketoglutarate from glucuronate can be carried out using novel enzyme reactions shown in **Figure 6.1a**. Here, the first NAD-dependent uronate dehydrogenase (UDH, EC 1.1.1.203) oxidizes the D-glucuronate (GU) to D-glucarate (GA) and is then converted into a linear keto-deoxy-glucarate (KDG) by glucarate dehydratase (GlucD, EC 4.2.1.40). Subsequently, the KDG dehydratase (KdgD, EC 4.2.1.41) catalyzed the KDG into α-ketoglutaric semialdehyde (KGSA). Finally, the KGSA is oxidized to α-ketoglutarate (KG) by an α-ketoglutaric semialdehyde dehydrogenase (KGSAIDH, EC 1.2.1.26). Interestingly, the NADH oxidase (Nox, EC 1.6.3.4) is introduced to complete the cascade with the aim for NAD regeneration **Figure 6.1b**.

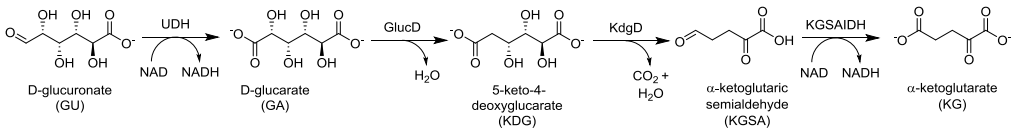

(a)

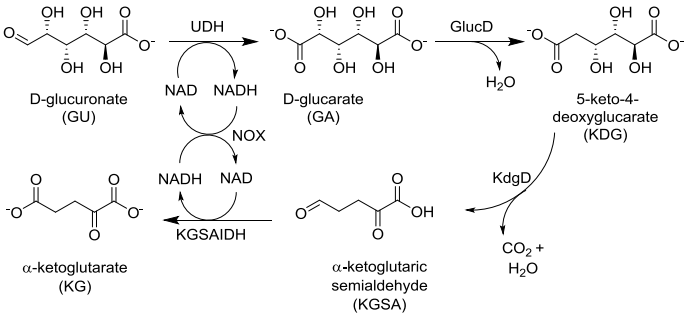

(b)

Figure 6.1: The overall reaction mechanism for the formation of 2-ketoglutarate from glucuronate. (a) A linear cascade and (b) a closed-loop cascade with the NAD regeneration *in situ* by NADH-oxidase (Nox).

6.2 Kinetic modelling

In this example, the kinetic modelling was developed to describe and understand the dynamic behavior of the enzymatic cascade. The kinetic parameters for each enzyme were available in the scientific literature (Watanabe et al. 2006; Aghaie et al. 2008), although there are no kinetic models that have been reported so far for the complete synthetic cascade. For the NOX-catalysed reaction, the kinetics were described by the Michaelis-Menten equation with product (NAD) inhibition (Findrik et al. 2007). In this study, the kinetic parameters of each enzyme (**Table 6.1**) and the progress curves of the overall process were kindly provided by Prof. Dr. Volker Sieber and Barbara Beer (Technical University of Munich).

Table 6.1: Kinetic parameters of each enzyme

Enzyme	**K_m [mM]**	**V_{max} [u/mg]**	**k_{cat} [s^{-1}]**	**k_{cat}/K_m [mM^{-1} s^{-1}]**
UDH	GU: 0.50	GU: 194	GU: 100.9	GU: 201.8
	NAD: 0.09			
GlucD	0.30	8.70	7.40	24.70
KdgD	0.04	0.85	0.49	12.25
KGSAlDH	KGSA: 0.1	KGSA: 33	KGSA: 31.7	KGSA: 317
	NAD: 0.46	NAD: 37.9	NAD: 36.5	NAD: 79.0
Nox	0.048	5.67	4.91	102

In this modelling work, eight (8) differential equations were derived for the mass balances (**Table 6.2**). The assumptions for the developed models as follows:

- pH and temperature are maintained constant during the operation
- perfect mixing
- No issue in stability or enzyme deactivation

Table 6.2: Mass balances for variables in the system (if in batch system)

Mass balance	Reaction kinetic
$\frac{dC_{GU}}{dt}$	$-r_{UDH}$
$\frac{dC_{GA}}{dt}$	$r_{UDH} - r_{GluD}$
$\frac{dC_{KDG}}{dt}$	$r_{GluD} - r_{KdgD}$
$\frac{dC_{KGSAI}}{dt}$	$r_{KdgD} - r_{KGSAIDH}$
$\frac{dC_{KG}}{dt}$	$r_{KGSAIDH}$
$\frac{dC_{NAD+}}{dt}$	$r_{Nox} + r_{Nox} - r_{UDH} - r_{KGSAIDH}$
$\frac{dC_{NADH}}{dt}$	$r_{UDH} + r_{KGSAIDH} - r_{Nox} - r_{Nox}$

5 constitutive equations based on each enzyme presents in the cascade as shown in **Table 6.3**. The GlucD, KdgD, and Nox follows the irreversible the Michaelis-Menten mechanism while for the UDH and KGSAIDH follows the Michaelis-Menten with two substrates (substituted-enzyme mechanism). The kinetic parameters for all enzymes are simplified to the initial reaction rate expressions. The effects of inhibition are introduced in the UDH-, GlucD- and Nox-catalysed reactions, although the inhibition parameters were not determined experimentally. This is because without such effects, the overall cascade trend and conversion were not well predicted. It was found that, the three reactions exhibit uncompetitive product inhibitions. The parameters were taken from the scientific literature, $K_i^{\mathrm{GA}} = 0.2$ mM, $K_i^{\mathrm{KDG}} = 0.005$ mM and $K_i^{\mathrm{NAD}} = 0.417$ mM (Findrik et al. 2007).

Table 6.3: Constitutive equations

Enzyme	Constitutive equations (Initial rate expression)
r_{UDH}	$\frac{V_{UDH}\,[\mathrm{GU}][\mathrm{NAD}]}{\left(K_{\mathrm{m}}^{\mathrm{GU}} + [\mathrm{GU}]\left(1 + \frac{[\mathrm{GA}]}{K_i^{\mathrm{GA}}}\right)\right)\left(K_{\mathrm{m}}^{\mathrm{NAD}} + [\mathrm{NAD}]\right)}$
r_{GlucD}	$\frac{V_{GlucD}\,[\mathrm{GA}]}{K_m^{GA} + [\mathrm{GA}]\left(1 + \frac{[\mathrm{KDG}]}{K_i^{\mathrm{KDG}}}\right)}$
r_{KdgD}	$\frac{V_{\mathrm{KdgD}}\,[\mathrm{KDG}]}{K_{\mathrm{m}}^{\mathrm{KDG}} + [\mathrm{KDG}]}$
$r_{KGSAIDH}$	$\frac{V_{KGSAIDH}\,[\mathrm{KGSA}][\mathrm{NAD}]}{\left(K_m^{\mathrm{KGSA}} + [\mathrm{KGSA}]\right)\left(K_{\mathrm{m}}^{\mathrm{NAD+}} + [\mathrm{NAD}]\right)}$
r_{Nox}	$\frac{V_{Nox}\,[NADH]}{K_{\mathrm{m}}^{\mathrm{NADH}} + [\mathrm{NADH}]\left(1 + \frac{[\mathrm{NAD}]}{K_i^{\mathrm{NAD}}}\right)}$

6.3 Dynamic simulation results

The mathematical models were developed to predict the dynamic process behaviour of the cascade as in **Figure 6.1**. From the simulation results, there is good agreement between the experimental data and the prediction (**Figure 6.2**). The kinetic investigations showed that in such enzymatic cascade, the complex interaction occur between all reaction components and enzymes, particularly when the NOX was involved in the cascade reactions. This enzyme frequently suffers from low operational stability since the activity greatly depends on the oxygen concentration. Besides, the NAD was found to inhibit the NADH oxidation by the Nox (Findrik et al. 2007). Therefore, neglected the inhibition effects will result in inaccurate prediction. To improve the suggested models, further experiments are required in order to determine the effects (K_i^{GA}, $K_i^{\mathrm{KDG}}$and K_i^{NAD}) and their physical meaning on the cascade.

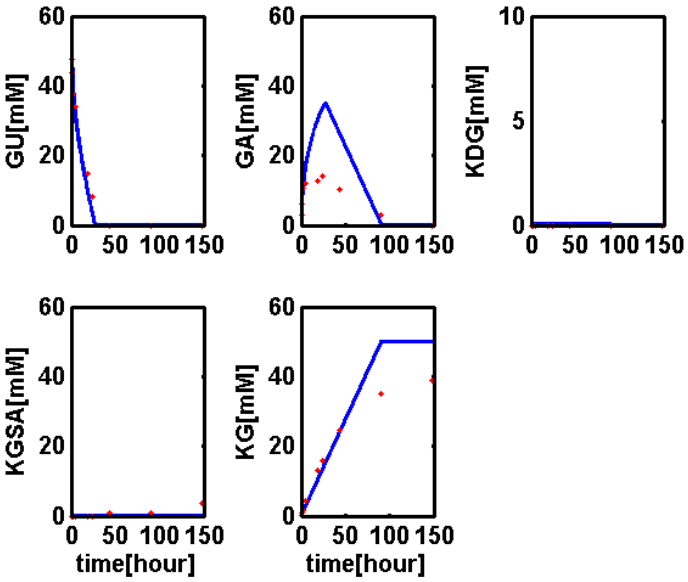

Figure 6.2: The dynamic simulation of the overall cascade. Experimental data (red, circle), simulation (solid line).

6.4 Conclusions

In this study, the mathematical models for the one-pot cascade synthesis of 2-ketoglutarate from Glucuronate, were developed. This cascade consists of 4 enzymes (uronate dehydrogenase, glucarate dehydratase, keto-deoxy-d-galactarate dehydratase and α-ketoglutaric semialdehyde dehydrogenase) that run in that order (sequentially) was successfully achieved a high conversion, with NOX as the regeneration system for NAD. The findings show that the kinetics can be controlled in a highly efficient way (by balancing the rates between interconnecting enzymes) to achieve a sufficiently favourable conversion of 78% for a given target product.

7 Case Study III: The Use of Activity Coefficients in Determining the Equilibrium Constant in the ω-Transamination of (*S*)-Phenylethylamine

7.1 Introduction

Biocatalysis is today established as a useful complement to synthetic methods for the production of many interesting chemical compounds (Liese et al., 2006). Many of the syntheses benefit from the excellent characteristics of enzyme catalysed reactions, such as high selectivity under mild reaction conditions, particularly for the synthesis of optically pure chiral pharmaceutical intermediates (Pollard and Woodley, 2007). The number of biocatalytic applications continues to grow in many industry sectors, as new enzymes and pathways become available, thanks in large part to the further development of protein engineering technologies (Turner, 2009; Bornscheuer et al., 2012).

Despite this, the applicability of a surprisingly large number of potentially interesting enzymes is still limited to laboratory scale. There are several reasons for this, but one of the most critical is that many of the most interesting biologically-mediated reactions from a synthetic perspective turn out to be thermodynamically limited processes. In nature such reactions may run in the reverse direction, but from a synthetic perspective this may not be useful. For example with many enzymatic reactions is important to synthesize a new chiral center, rather than resolve an existing one (no matter how good the selectivity). In this way such reactions are therefore hampered by low reaction yields (Tewari, 1990). Remarkably, the area of equilibrium thermodynamics of biological systems has gained relatively little attention and until now, and surprisingly little thermodynamic information has been available in the scientific literature (von Stockar and van der Wielen, 1997; von Stockar, 2013). Although there are a number of reports of thermodynamic properties (e.g. enthalpy changes, equilibrium constant and Gibbs free energy), unfortunately these data are limited to *in-vivo* biochemical reactions and scattered across a range of conditions such as, temperature, pH, ionic strength, buffer and co-factor types (Goldberg et al., 2004). These problems pose many challenges for the implementation and optimization of *in-vitro* enzymatic processes.

Such problems are exacerbated by the fact that the terminology used to describe the thermodynamics of biological systems is not always consistent with that used to describe the thermodynamics of chemical systems (Alberty et al., 2011). For example, the term ‘apparent’

equilibrium constant has usually been reported for biological systems instead of the more usual activity-based equilibrium constant, where the reactant activity (the effective concentration of reactant) is equal to the respective reactant molal or molar concentration at equilibrium (Goldberg, 2014). The activity coefficient, which reflects deviations from a hypothetical ideal solution, is often neglected since enzymes are known to operate at dilute aqueous solutions (Alberty et al., 2011). Accordingly, many of the available equilibrium data are the apparent values of equilibrium constants, and it is these that frequently have been used to describe the metabolic pathways (Mavrovouniotis, 1996; Maskow and von Stockar, 2005; Efe et al., 2008). For metabolic pathways, the very low concentrations may justify such an approach, but for *in-vitro* reactions this may not always be the case. The problem is made worst by the fact that activities are difficult to measure experimentally due to the complex environment in biological systems (e.g. pH, ionic strength (Vojinović and von Stockar, 2009).

For all these reasons the prediction of the activity coefficient from calculated values would be attractive, and recently the thermodynamic model e-PC-SAFT (Held et al., 2010) was used for such a purpose, with the intent of focussing on biologically mediated reactions. Although this is not the only approach possible, the ePC-SAFT method is able to calculate the activity coefficient by considering the specific interactions caused by hydrogen bonding and charges that occur in a biological solutions, giving more accurate and reliable data. Interestingly, Hoffman and co-workers found that the value of the activity coefficient significantly deviates from unity by 3- to 6-fold even at dilute reactant concentrations (2 to 10 $mmolkg^{-1}$) in a feruloyl esterase-catalysed reaction (Hoffmann et al., 2013). A similar finding was also reported for the isomerization of glucose-6-phosphate at low reactant concentrations, 1 to 50 $mmolkg^{-1}$ (Hoffmann et al., 2014). Since the activity coefficients deviate from unity, this infers non-ideal behaviour in such systems even at low reactant concentrations. Hence, neglecting non-ideality in a biological reaction could contribute to the erroneous assumptions in calculating the equilibrium data.

In order to contribute to further progress in this area, the asymmetric synthesis of optically-pure chiral amines with ω-transaminase (EC 2.6.1.18) was used in this study. This enzyme is able to catalyze the transfer of an amine group between a donor molecule and an acceptor ketone with superb enantioselectivity (Fuchs et al., 2015). This makes it an attractive reaction compared to the alternative chemically-catalysed route, which frequently suffers from poor enantioselectivity (Nugent and El-Shazly, 2010). However, a key challenge of running this enzyme in the synthetic direction is that the products are frequently less energetically stable than the reactants, resulting in a thermodynamically unfavourable equilibrium (Tufvesson et al., 2011). Most studies have, to some extent, successfully overcome the thermodynamic constraints in such reactions by the application of equilibrium shifting

strategies such as use of an excess of a co-substrate or coupling cascades (Abu and Woodley, 2015). Remarkably, very little information on thermodynamics was quantified in many of these studies. In order to address this paucity of data, recently, we reported on experimentally-determined equilibrium constants for ω-transaminase reactions in order to better understand the dependence of the thermodynamics on the types of molecules used, and in particular the amine donor. Nonetheless, the effect of the thermodynamic activity of the components in aqueous solution was neglected (Gundersen et al., 2015; Tufvesson et al., 2012), and motivated us subsequently to consider the impact of this.

Hence, the objective of this work was to determine the activity-based equilibrium constants for such reactions, and compare it with the simpler concentration based constants. In this work we have used the cyclohexanone amination with (*S*)-1-phenylethylamine (PEA) catalysed by the ω-transaminase as a model reaction (**Figure 7.1**). The synthetic direction towards the PEA is economically more attractive (a chiral (center) molecule is synthesized), while the equilibrium position of the reaction favours the backward direction.

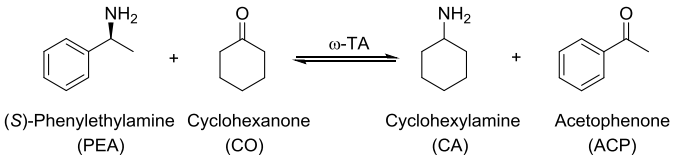

Figure 7.1: The cyclohexanone (CO) amination with (S)-1-Phenylethylamine (PEA) catalysed by the ω-transaminase (ω-TA) enzyme.

7.2 Theoretical background

Theoretically, the equilibrium constant (K_a) of a chemical reaction is the value that determines the position of equilibrium in a reversible reaction at constant temperature and pressure. In this model reaction (**Figure 7.1**), the value of K_a for the reaction model is the ratio of the activities of products (CA and ACP) over the activities of reactants (PEA and CO) at equilibrium in the forward reaction (Equation 7.1).

$$K_a = \frac{a_{\mathrm{CA}} a_{\mathrm{ACP}}}{a_{\mathrm{PEA}} a_{\mathrm{CO}}} \tag{7.1}$$

In Equation 7.1, a is the activity of the component and refers to the effective concentration of the component in an ideal solution. By definition, an ideal solution is one in which the molecular interaction in solution is similar to the molecular interaction in the pure compounds at standard state conditions (1 atm, 298 K, 1 M of component activities). The activity, a, of components can be also written as the product of the molal concentration e.g. mol/kg (denoted as m) and the activity coefficient (denoted as γ) as shown in Equation 7.2. The activity coefficient, γ, reflects the deviation of components from ideal behaviour (an ideal solution gives γ=1).

$$K_a = \frac{(\gamma m)_{\mathrm{CA}}(\gamma m)_{\mathrm{ACP}}}{(\gamma m)_{\mathrm{PEA}}(\gamma m)_{\mathrm{CO}}} \tag{7.2}$$

Likewise, the term K_a is a function of product of the concentration (K_m) and the activity coefficient (K_γ) of all components in the reaction as shown in Equation 7.3.

$$K_a = K_m K_\gamma \tag{7.3}$$

In common practice, the activities in biologically-mediated reactions are assumed to be equal to the respective component concentration at equilibrium, giving the term 'apparent' equilibrium constant (K'). For example in the NIST database (Goldberg et al., 2004), typically, the concentration-based molarities (K_c) or molalities (K_m) have been reported for the K' values. In this way, in the K_m calculation, the value of K_γ=1 is assumed, due to the fact that biological systems often operate at dilute aqueous solutions (Villadsen et al., 2011). Thus, the standard state conditions for these reactions are 1 atm, 298 K, and concentration of hydrogen ions, $[H^+]$, at pH 7 (Villadsen et al., 2011).

$$K_m = \frac{m^{\mathrm{eq}}_{\mathrm{ACP}} m^{\mathrm{eq}}_{\mathrm{CA}}}{m^{\mathrm{eq}}_{\mathrm{PEA}} m^{\mathrm{eq}}_{\mathrm{CO}}} \tag{7.4}$$

In this work, the K_m values were measured experimentally at varying reaction conditions (initial concentration of component, pH, and temperature) in both directions of the reaction and the activities and the values of K_γ were modelled and predicted using ePC-SAFT.

7.3 Materials and Methods

7.3.1 Materials

(*S*)-1-Phenylethylamine and cyclohexanone was purchased from Merck (Darmstadt, Germany) and Sigma-Aldrich (St. Louis, MO, USA), respectively. Cyclohexylamine and 1-phenylethanone were purchased from Fluka (St. Louis, MO, USA). All chemicals were >99.99% purity and they were used in this study without further alteration. Lyophilized ω-transaminase (ATA-81) was provided from c-LEcta GmbH (Leipzig, Germany).

7.3.2 Reaction Equilibria

All reactions were carried out in duplicate with different reaction conditions. In the study of different initial reactant concentration, the respective acceptor substrate and amine donor were used between 5 to 50 mM. The reactions were carried out at a 3 mL scale in 4 mL vial containing 1 mg/ml ATA-81, 1 mM pyridoxal-5'-phosphate, 5 % (v/v) Dimethyl sulfoxide in 100 mM Tris-HCl buffer, pH 7. The reaction mixtures were continuously mixed in a thermoshaker (HCL, Bovenden, Germany) at constant temperature (30^{o}C) and agitation (450 rpm). All reactions were run in both directions (forward and reverse) in the time-dependent manners until the equilibrium was reached at the same position on both sides. The same procedure was used for the K_m as a function of pH (7, 8 and 9) and temperature (30^{o}C and 37^{o}C).

7.3.3 Analytical

The sample was quenched by adding the aqueous NaOH (5 M, 100 µL). For the extraction, 400 µL of ethyl acetate as well as 4-bromo-acetophenone (150 mM; 20 µL) as internal standard was added. The organic phase was dried with magnesium sulphate and then the supernatant was transferred to a GC vial. For derivatization, 15 µL triethylamine and 10 µL acetic anhydride were also added into the GC vial. The concentration of reactants and products were analyzed by Gas chromatography on a Clarus 500 (Perkin–Elmer) with a 25 m * 0.25 mm CP-Chirasil-Dex CB column (Agilent J&W GC scientific). 2 µL samples were injected, with a thermal gradient from 120 to 200 °C for 14 min, 1.4 ml/min Helium was used as a carrier gas. FID detection was carried out at 250 °C.

7.4 ePC-SAFT modelling

The ePC-SAFT modelling was used to calculate the activity coefficient γ of the reactants and products of the ω-TA reaction. The ePC-SAFT determines the residual Helmholtz energy of a system a^{res} which is expressed as the sum of the contributions as shown in Equation 7.5. Each of contributions is independent from each other and thus can be added according to the requirement.

$$a^{\mathrm{res}} = a^{\mathrm{hc}} + a^{\mathrm{disp}} + a^{\mathrm{assoc}} + a^{\mathrm{ion}} \tag{7.5}$$

ePC-SAFT characterises a molecule as a chain composed of spheres that interact with other molecules by repulsive forces (a^{hc}), attractive van-der-Waals forces (a^{disp}), and formation of hydrogen bonds (a^{assoc}). These energy contributions were used as in the original PC-SAFT model. While for the energy contribution of charged species (a^{ion}) was calculated according to a Debye-Hückel equation as described in Cameretti et al. (2005). The value of a^{res} is then can be used to determine the thermodynamic properties such as, activity coefficients (Held et al. 2010).

7.5 Results and Discussion

7.5.1 Experimentally determined concentration-based equilibrium constants (K_m)

For the equilibrium measurement, the K_m values were calculated based on Equation 7.4 which was determined from the time dependent concentration measurements. In the experiments, the reactants were allowed to reach equilibrium from both directions of the reaction. At equal molal (25 mM) concentration of reactants (ACP, PEA) in the forward (synthetic) and reverse directions, the same equilibrium point was reached (at a constant temperature of 30^{o}C and pH 7). Equilibrium was reached after 48 hours of reactions (**Figure 7.2**).

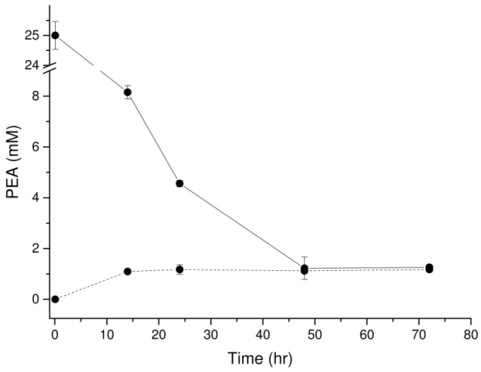

Figure 7.2: Time-dependent concentrations of (*S*)-phenylethylamine (PEA) in the forward reaction (solid line) and the reverse reaction (dashed line) with the initial molal concentration of 25 mM of reactant. The reactions were run at 30^{o}C in 100 mM Tris-Hcl buffer at pH 7.

Similar equilibrium trends were also observed using different initial molalities of reactants (5, 10 and 50 mM) as presented in **Table 7.1.** The values of K_m as well as the extent of reaction were calculated from the molality of reactants and products at equilibrium. In these experiments, it was seen that the K_m decreased with an increase in initial reactant molality. It was also found that the rate of reaction decreased toward the equilibrium at an initial reactant concentration of 50 molal. The slow reaction rate is probably due to the inhibition at high concentrations and thus gave the low conversion. Aside from thermodynamic limitations, ω-transaminase-catalysed reactions frequently suffer from the substrate and product inhibition by the ketones, particularly in the transamination of PEA from ACP (Truppo et al., 2009).

Table 7.1: The equilibrium values of Km and conversion at different initial molalities. The reactions were run at 30^{o}C in 100 mM Tris-HCl, pH 7

$[CO]_{t=0}$ (mM)	$[PEA]_{t=0}$ (mM)	$[ACP]_{eq}$ (mM)	K_m	Conversion (%)
5	5	4.82±0.01	763± 108	96.51
10	10	9.59±0.01	551± 8	95.91
25	25	23.8±0.03	467± 15	95.58
50	50	47.34±0.21	321± 52	94.71

The kinetics of the ω-transaminase reaction strongly depend on pH, whereas the substrate selectivity is controlled by the p*Ka* of the charged amino acid residues located in the substrate binding pocket (Park and Shin, 2011). To investigate further the effect of pH on the equilibrium position, experiments were run at different pH values (7, 8 and 9) at an initial reactant concentration of 10 molal (constant temperature). The K_m of the ω-transaminase reaction was found to be pH-dependent, where K_m decreased with an increase in pH (**Table 7.2**), probably because of proton dissociation of the amine at pH 9. The pKa of PEA and CA is 9.0 and 10.6, respectively.

In the temperature-dependent study, K_m is decreases with increasing temperature. For the reaction at constant pH, the K_m at 30^{o}C is 557± 46 compared to the K_m at 37^{o}C (K_m = 448± 25).

Table 7.2: Experimental K_m values as a function of pH (7, 8 and 9) with 10 mM initial reactant molalities in 100 mM Tris-HCl, 30^{o}C.

pH	$[CO]_{t=0}$ (mM)	$[PEA]_{t=0}$ (mM)	$[ACP]_{eq}$ (mM)	K_m	Conversion (%)
7	10	10	9.59±0.02	557± 46	95.93
8	10	10	9.58±0.02	521±50	95.80
9	10	10	9.48±0.06	347± 89	94.91

7.5.2 Prediction of equilibrium data with e-PC-SAFT modelling

7.5.2.1 Estimation of activity-based equilibrium constant (K_a) at 30^{o}C and pH 7

The K_a of the reaction is estimated at infinite dilution of reactants and products where the activity coefficient for each component approach unity, γ^{∞}. The K_a (30^{o}C) is found to be 600 at pH 7 as shown in **Figure 7.3** at infinite dilution of the products at equilibrium. On the same graph, the predicted K_m from the modelling qualitatively agrees approximately with the experimental data. At lower concentration the different is noticeable but currently theory cannot explain these results. Interestingly, the K_m decreases with an increasing concentration of products at equilibrium.

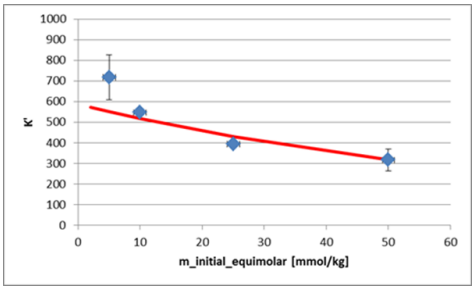

Figure 7.3: The K_m values versus the equilibrium molality of acetophenone at different initial molal concentrations in 100 mM Tris-HCl buffer, pH 7 and 30°C. Experimental data (symbols) and modelled PC-SAFT (solid line).

Subsequently, the activity coefficient can be determined by the K_a based on the Equation 7.3. Since the value of K_a is constant, the K_γ values should be varied according to the values of K_m. In this reaction example, the K_m decreases while the K_γ increases. Accordingly, the γ increases above the infinite value γ^{∞}.

Interestingly, in a recent study using the same class of enzyme, the influence of activity coefficient, modelled by ePC-SAFT, was low in the reactant concentration between 2.5 to 10 mmolkg^{-1}. This effect probably due to the similar structure of reactants and products involved in the alanine aminotransferase (EC 2.6.1.2) reaction (Voges et al., 2016).

7.5.2.2 Estimation of concentration-based equilibrium constant (K_m) at different pH and temperature

To further validate the dependency of K_m on pH, the p*Ka* values of CA and PEA were used to predict K_m, accounting for the protonation of the amines due to the pH changes in the reaction. The predicted values of K_m are in a good agreement with the experimental data as illustrated in **Figure 7.4**

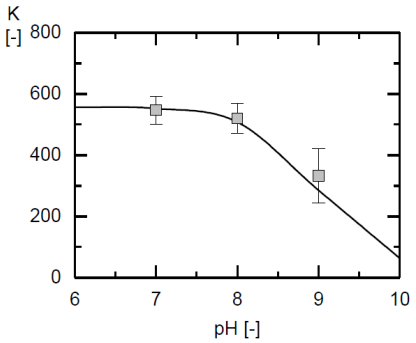

Figure 7.4: K_m values versus the equilibrium molality of cyclohexanone of the reaction at different pH values (7, 8 and 9) in 100 mM Tris-HCl buffer, 10 mM initial molality and 30°C. Experimental data (symbols) and modelled PC-SAFT (solid line).

7.5.3 Validation of predicted equilibrium data

Subsequently, the assumption used to predict the value of K_m at different initial molalities was validated. The dispersion-energy parameters between the products were neglected in the prediction. To validate this assumption, the experiments at different ratios of initial molalities were used (1:5 and 5:1) at 10 mM reactant. As illustrated in **Figure 7.5**, the experimental data qualitatively agree with the prediction, validating the assumption.

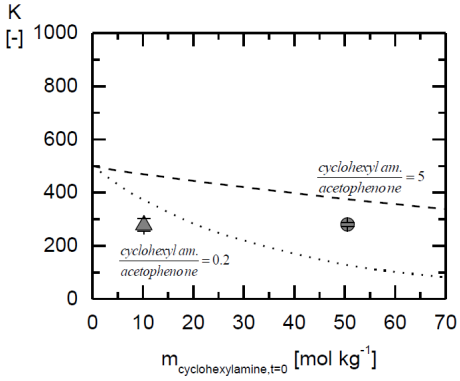

Figure 7.5: K_m values versus the equilibrium molality of cyclohexylamine of the reaction.

7.6 Conclusions

An equilibrium study was carried out to understand the role of activity coefficients to determine the equilibrium constant in enzymatic reactions. In this work, the concentration-based equilibrium constant (K_m) was found to be varied with its reaction conditions (initial reactant concentrations, pH, and temperature). The results show that the activity coefficient of components deviate from unity, showing its non-ideal behaviour in the reaction medium. The activity-based equilibrium constant K_a at a constant temperature (30^{o}C) and pH 7 was calculated to be 600 in the transamination reaction of PEA from ACP.

It can be concluded that accounting for the activity coefficients in the calculation of equilibrium constant will be more reliable due to the non-ideality of the systems. Such valuable data would be potentially useful for further analysis, for example, the equilibrium constant enables the estimation of a maximum theoretical reaction as well as determination of thermodynamic feasibility of a reaction based on economic constraints.

8 Discussion

To date, several promising enzymatic cascades have been reported in the scientific literature and it can be expected that many more examples will be forthcoming in the future (Riva and Fessner, 2014). Despite great interest in the application of enzymatic cascades, the feasibility of many enzymatic cascades has rarely been explored and thus difficult for process evaluation and improvement of such cascades. This thesis has suggested the implementation of enzymatic cascades is dependent of fundamental knowledge of thermodynamics and kinetics. The main objective of this thesis is to evaluate the process concepts in enzymatic cascades using tools such, thermodynamic and kinetic analysis. The tools are not only useful for understanding existing cascade processes but can also stimulate insight into the new concept of enzymatic cascades as well as can search ideas for process improvement.

8.1 Effect of equilibrium on the cascade conversion

In order to develop a highly efficient process for the enzymatic cascades, thermodynamic data such as, the Gibbs free energy and equilibrium constant are required to quantify the favourability and the maximum theoretical yield of the enzymatic cascades. In the asymmetric amination of alcohol using a redox neutral cascade (Chapter 5), the apparent equilibrium constants (K') of each enzyme reaction (ADH, ω-TA and AlaDH) were experimentally determined. The favourability of the overall cascade is thermodynamically favoured. However, when running the cascade in one-pot fashion in an excess of ammonium concentration (where the AlaDH-catalysed reaction was placed in the last reaction step as a way to drive the overall equilibrium), the redox cascade was not able to convert the alcohol into the target amine. It was found that ω-TA was not only thermodynamically limited but also kinetically limited in the synthetic direction. This means that balanced rates in the redox neutral cascade are essential for the thermodynamics to work (will be discussed in the next section). This might also explain why some of the asymmetric amination of sec-alcohols using the same cascade scheme did not achieve high conversion (<50%) due to kinetic and thermodynamic constraints (Tauber et al. 2013). However, in the production of ether amines, the equilibria of the redox neutral cascades (K' values were determined between 12 and 14) was driven by the high concentration of ammonia (28-molar

equivalents), giving >60% conversion (Palacio et al. 2016). However, no kinetic studies are reported from both studies.

Although this strategy was not successful in my hand, there are several other examples that have been successfully used the enzyme coupling reactions as a tool to alleviate thermodynamic constraints. The driving force of such strategies is placed at the end of the cascade reaction steps. One of the strategies is by coupling several reversible enzymatic reactions with an irreversible reaction at the end of the reaction steps in order to have energetically downhill equilibria. This example is exemplified in the synthesis of D-xylulose 5-phosphate from hydroxypyruvate and D-fructose 1,6-biphosphate (Zimmermann et al. 1999). Here, the first two steps are reversible reactions (D-fructose1,6-bisphosphate aldolase (EC 4.1.2.13) and triosephosphate isomerase (EC 5.3.1.1)), followed by an irreversible reaction in the final step by transketolase-catalysed reaction (EC 2.2.1.1) which successfully drive the overall equilibria (82 % overall yield).

Another strategy is by coupling with high energy substrate (e.g. molecule oxygen) in the cascade reactions. This strategy was successfully presented by Oberleitner and co-workers in the production of biorenewable polyesters using a redox cascade (Oberleitner et al. 2014). The cascade composed of three reaction steps; alcohol dehydrogenase (ADH, EC 1.1.1), enoate reductase (ERED, EC 1.3.1.31) and Baeyer-Villiger monooxygenase (BVMO, EC 1.14.13) reactions. The main problem is that the ADH-catalysed reaction greatly suffers from unfavourable equilibrium towards ketone formation. However, the last oxygenation step was able to shift the equilibrium position, resulting in high conversion (>99%).

8.2 Effect of reaction rate on the cascade route

Despite enzyme is highly selective, the rate of an enzyme reaction is frequently low when converting non-natural substrates. In the perspective of enzymatic cascades, the imbalanced coupling rates in synthetic routes may lead to an accumulation of intermediates (Kurumbang et al. 2014). For example, it could build-up the intermediate concentration (I_1), if the second enzyme reaction (E_2) in the linear cascade is the rate-limiting step (**Figure 8.1a**). This can result in low intermediate concentration (I_2) and thus limits the product formation. On the other hand, the high concentration of intermediates may also inhibit the reaction rate and reduce the enzyme stability. In this case, the first step of reactions (E_1) may need to be separated in order to improve the reaction rates (**Figure 8.2a**.). This is because the kinetics can be controlled in a highly efficient way when the reaction steps are independents in a cascade. By separating the enzymes, the optimal reaction conditions (e.g., pH and temperature) can also be considered. A different approach can be used by running the first reaction step until

completion followed by the second and third steps where each reaction step is separated by time in a one-pot system (**Figure 8.2b**). This approach still requires additional reagents for each reaction step. In this way, the kinetics can also be controlled independently.

If the relative rates are matched, the enzymes can be put together in one pot so that the amount of reagents for each reaction can be reduced and the cost of the down-stream processing can be decreased **Figure 8.2c**. This example was shown in the kinetic modelling of the formation of 2-ketoglutarate from glucoronate (Chapter 6) where the cascade reactions successfully achieved high conversion. In other cases where toxic or unstable intermediates are involved, the concentrations must be kept low, so that these do not accumulate.

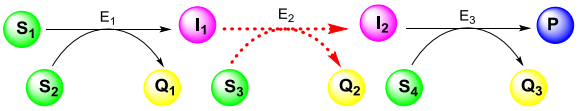

(a)

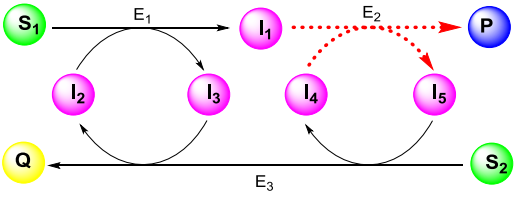

(b)

Figure 8.1: Examples of cascade schemes. (a) Linear cascade and (b) redox cascade.

In the case of a closed-loop cascade shown in **Figure 8.1b**, if the second enzyme reaction (E_2) is the rate-limiting step, both recycling systems may not able to work as they should be. This is because each reaction steps are interconnected. This example was shown in the first case study (Chapter 5). In the redox neutral cascade, the oxidation and reduction steps must run simultaneously in one pot and thus required balanced reaction rates (**Figure 8.2c**). This means that the reaction conditions are the same. Similarly, a parallel cascade (e.g. regenerating cofactors or co-substrates *in situ* are involved), which the reaction steps are connected for the redox equivalents (electron transfer).

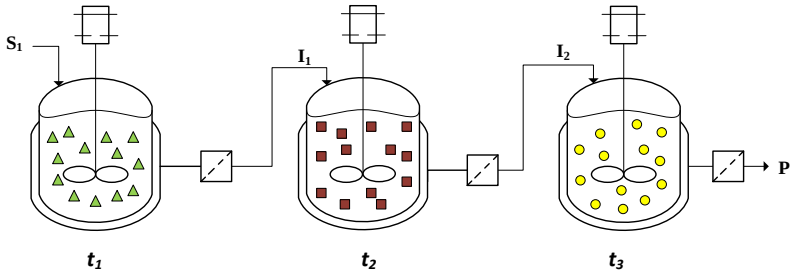

(a) multiple pots

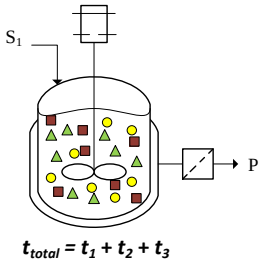

(b) 3-step one pot separated by time

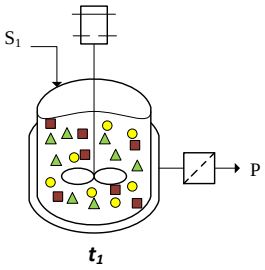

(c) 3-step one pot simultaneous cascade

Figure 8.2: Reactor configurations for cascade reactions. S (substrate), I (intermediate), P (product), symbols (enzymes) and *t* (time).

8.3 Flow chemistry as a key enabling technology

Enzymatic cascades can be conducted in flow which completely different process compared to one pot fashion. By employing excellent immobilization protocols, several enzymes in a linear arrangement can be designed for a continuous process (**Figure 8.3**). Reagents can be introduced anywhere in the flow system at time according to the enzyme requirements. Besides, the purification steps may not be required for the flow system. Recently, Suljic and Pietruszka (2014) conducted a chemo-enzymatic continuous flow approach in the synthesis of arylated dihydrocoumarins, resulting in high yield (82 %). Immobilization of enzymes using chitosan beads (Rehn et al. 2013) and methacrylate beads (Andrade et al. 2014) will give perfect catalytic activities and increase product throughput. In future, flow chemistry will continue to grow as one of enabling technologies for organic chemistry in improving synthetic efficiency of enzymatic cascades (Wegner et al. 2012).

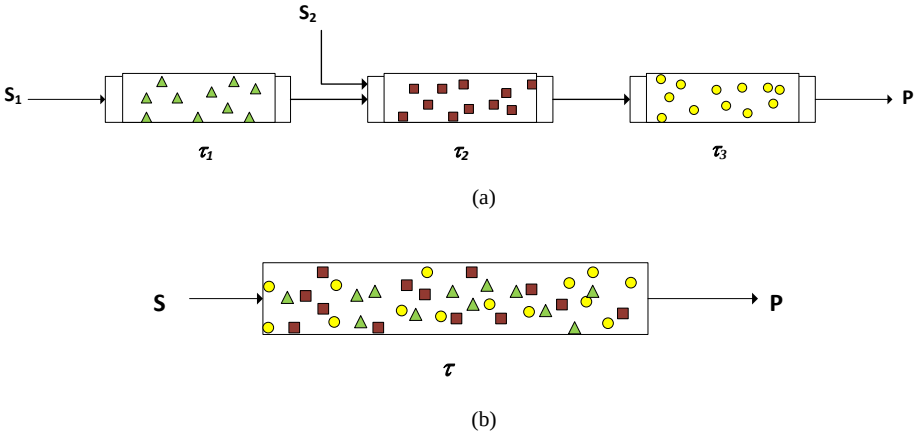

Figure 8.3: Examples of continuous flow cascade system. (a) Separation of enzymes and (b) combination of enzymes. S (substrate), P (product), symbols (enzymes) and τ (residence time).

8.4 Is the activity coefficient required in calculating the equilibrium constant in enzyme-catalysed reactions?

Collecting thermodynamically useful equilibrium data for the enzyme-catalysed reactions (e.g. equilibrium constant, Gibbs free energy of reaction) is always difficult due to the complexity interaction in the reaction media (e.g. pH, temperature, and buffer) as well as interaction among enzymes, substrate(s), co-factors and reagents and product(s). Due to this complexity, the terminology used for thermodynamic biological systems is different from the conventional chemical reaction (Alberty et al. 2011). Frequently in equilibrium study, the term 'apparent' equilibrium constants have been reported instead of activity-based, in which the reactant activities are assumed to be equal to the respective reactant molal or molar concentrations at equilibrium (Goldberg 2014). The activity coefficient, deviation from its hypothetical ideal solution, is often neglected due to the enzymes operate at dilute aqueous solutions (Alberty et al. 2011).

In the case study 3, the role of activity coefficients in determining the equilibrium constant in the ω-transamination of PEA was investigated. In this study, the activities were measured in forward and reverse directions of the reaction and the activity coefficient of the reactants and products were predicted by the ePC-SAFT modelling. Finding shows that the concentration-based equilibrium constant was found to be varied with the change in reaction conditions (initial reactant concentrations,

pH, and temperature). The activity coefficients of components significantly deviate from unity, showing its non-ideal behaviour in the reaction medium. While the activity-based equilibrium constant was determined to be constant (K_a=600) at 30^{o}C and pH 7 in the transamination reaction of PEA from ACP. Thus, accounting the activity coefficients in the calculation of equilibrium constant will be more reliable due to the non-ideality of the systems.

Therefore, understanding the fundamental knowledge of thermodynamics (e.g. thermodynamic equations) and their properties (e.g. equilibrium constant) are basic aspects that are important in the field of biocatalysis. The non-ideality behaviour might also be a reason why the equilibrium shifting strategy in the amination of alcohol in the first case study was unsuccessful. More accurate and reliable experimental data as well as reliable and robust predictive tools are urgently needed.

9 Conclusions

The main conclusions can be summarised from this thesis as follows:

- The apparent equilibrium constants (K') were determined experimentally for individual reactions in a redox neutral cascade for the asymmetric amination of (*S*)-phenylethanol (PhEtOH) to the corresponding chiral amine, (*S*)-phenylethylamine (PEA). The K' of ADH- and ω-TA-catalysed reaction was $9.86 \times 10^{-2} \pm 2.71 \times 10^{-4}$ and $1.14 \times 10^{-4} \pm 1.11 \times 10^{-4}$, respectively. Both show the thermodynamically unfavourable reactions, (ADH (+5.84 kJ/mol) and ω-TA (+22.87 kJ/mol)). While the AlaDH-catalysed reaction is energetically favourable that has a large and negative energy (−38.91 kJ/mol) with the K' of $5.11 \times 10^{6} \pm 4.44 \times 10^{-6}$ kJ/mol. The overall reaction was feasible (K'_{net} = 57.40 ± 1.31) with the energy-releasing reaction (−10.20 kJ/mol) where AlaDH reaction has been identified as a driving force that control the feasibility of the ADH/ω-TA/AlaDH coupled system where the ammonium concentration is the key compound that has an effect on the overall equilibrium.
- The extent to which the ammonium concentration can drive the redox neutral cascade was investigated. It was observed a significant increase by 5-fold in the intermediate (ACP) compared to the amount of co-factor NAD added in the cascade system, due to an uncoupling of the cascades. The NADH was oxidized to NAD by NOX presence in the enzyme ω-TA (ATA256) as there might be no additional source of electrons that generates enough reduced NADH necessary to drive the amination of pyruvate. This problem might interfere with the thermodynamic analysis and finally limits the overall conversion.
- The K_{a} (the activity-based equilibrium constant) in the transamination reaction of PEA from ACP using cyclohexylamine as an amino donor was determined to be constant (K_{a} =600) at 30°C and pH 7. Whereas the K_{m} (the concentration-based equilibrium constant) decreased with the increase in initial reactant molarity (5 to 50 mM) at constant pH (pH 7) and temperature (30°C).
- The activity coefficients of components significantly deviate from unity shows the thermodynamically non-ideal system, instead of being ideal behaviour, for the transamination reaction.

- With respect to the methodology, enzyme coupling reactions must have energetically downhill equilibria in order for the cascade reactions to work towards the synthetic direction. Following the thermodynamics, balancing the activities of interconnected enzymes will determine the efficiency of the cascade reactions.

10 Future work

To further continuing this work in future, several recommendations are outlines here.

- Finding the optimal operating conditions (pH, temperature, reaction medium and concentration of substrates) that enable all reactions to catalyse efficiently with one another while retaining the selectivity obtained from individual reactions.
- Comparing the efficiency of the redox neutral cascade with different types of enzymatic cascades as shown in **Figure 3.9** and **Figure 3.10**.
- Analysing different types of process configurations to maximise performance of the enzymatic cascades such as, by removing the product PEA *in situ* and supplying sufficient PhEtOH due to the product and substrate inhibition.
- Using the activity-based equilibrium constant (K_a) and compared to the apparent data in the transamination reaction of PEA using cyclohexylamine as an amino donor to find suitable operating strategies (e.g. the application of *in situ* product removal or two phase systems) to achieve a sufficiently high conversion.
- Calculating the economic value of the cascade in term of cost of enzymes and co-factors that would need to be considered.
- Assessing the environmental impact of the enzymatic cascades processes.
- Using the concept of flow chemistry would be attractive to improve the reaction rates in enzymatic cascades.

References

Abrahamson MJ, Vázquez-Figueroa E, Woodall NB, Moore JC and Bommarius AS. (2012). Development of an amine dehydrogenase for synthesis of chiral amines. *Angew Chem Int Ed Engl* 51:3969–72.

Abrahamson MJ, Wong JW and Bommarius AS. (2013). The evolution of an amine dehydrogenase biocatalyst for the asymmetric production of chiral amines. *Adv Synth Catal* 355:1780–1786.

Abu R, Woodley JM. (2015). Application of enzyme coupling reactions to shift thermodynamically limited biocatalytic reactions. *ChemCatChem*, 7:3094–3105.

Adrio J and Demain A. (2014). Microbial enzymes: Tools for biotechnological processes. *Biomolecules*, 4:117–139.

Aghaie A, Lechaplais C, Sirven P, Tricot S, Besnard-Gonnet M, Muselet D, de Berardinis V, Kreimeyer A, Gyapay G, Salanoubat M and Perret A. (2008). New insights into the alternative D-glucarate degradation pathway. *J Biol Chem* 283:15638–46.

Alberty RA, Cornish-Bowden A, Goldberg RN, Hammes GG, Tipton K and Westerhoff H V. (2011). Recommendations for terminology and databases for biochemical thermodynamics. *Biophys Chem*, 155:89–103.

Alberty RA. (2003). *Biochemical reactions.* John Wiley & Sons, Inc., New Jersey.

Alberty RA. (2006). *Biochemical thermodynamics: Applications of Mathmatica*. John Wiley & Sons, Inc., New Jersey.

Andrade LH, Kroutil W and Jamison TF. (2014). Continuous flow synthesis of chiral amines in organic solvents: immobilization of E.*coli* cells containing both ω-transaminase and PLP. *Org Lett*, 16:6092–6095.

Bähn S, Imm S, Neubert L, Zhang M, Neumann H and Beller M. (2011). The catalytic amination of alcohols. *ChemCatChem*, 3:1853–1864.

Bommarius AS, Blum JK and Abrahamson MJ. (2011). Status of protein engineering for biocatalysts:

How to design an industrially useful biocatalyst. *Curr Opin Chem Biol,* 15:194–200.

Bommarius BR, Schürmann M and Bommarius AS. (2014). A novel chimeric amine dehydrogenase shows altered substrate specificity compared to its parent enzymes. *Chem Commun,* 50:14953–14955.

Bornadel A, Hatti-Kaul R, Hollmann F and Kara S. (2015). A Bi-enzymatic convergent cascade for ε-caprolactone synthesis employing 1,6-hexanediol as a "Double-smart co-substrate." *ChemCatChem*, 7:2442–2445.

Bornscheuer UT, Huisman GW, Kazlauskas RJ, Lutz S, Moore JC and Robins K. (2012). Engineering the third wave of biocatalysis. *Nature*, 485:185–194.

Brink NG, Miettinen JK, Olsen J, Virtanen AI and Sörensen NA. (1953). Beef Liver Glucose Dehydrogenase. I. Purification and Properties. *Acta Chem Scand,* 7:1081–1089.

Bruggink A, Schoevaart R and Kieboom T. (2003). Concepts of nature in organic synthesis: Cascade catalysis and multistep conversions in concert. *Org Process Res Dev*, 7:622–640.

Cameretti LF, Sadowski G and Mollerup JM. (2005). Modeling of aqueous electrolyte solutions with perturbed-chain statistical associated fluid theory. *Ind Eng Chem Res*, 44:3355–3362.

Cassimjee KE, Branneby C, Abedi V, Wells A and Berglund P. (2010). Transaminations with isopropyl amine: equilibrium displacement with yeast alcohol dehydrogenase coupled to in situ cofactor regeneration. *Chem Commun,* 46:5569–71.

Chen F-F, Liu Y-Y, Zheng G-W and Xu J-H. (2015). Asymmetric amination of secondary alcohols by using a redox-neutral two-enzyme cascade. *ChemCatChem.* 7:3838–3841.

Eckstein MF, Lembrecht J, Schumacher J, Eberhard W, Spiess AC, Peters M, Roosen C, Greiner L, Leitner W and Kragl U. (2006). Maximise equilibrium conversion in biphasic catalysed reactions: How to obtain reliable data for equilibrium constants? *Adv Synth Catal*, 348:1597–1604.

Efe C, Straathof AJJ and van der Wielen LAM. (2008). Options for biochemical production of 4-hydroxybutyrate and its lactone as a substitute for petrochemical production. *Biotechnol Bioeng*, 99:1392–406.

Fesko K, Steiner K, Breinbauer R, Schwab H, Schürmann M and Strohmeier GA. (2013). Investigation of one-enzyme systems in the ω-transaminase-catalyzed synthesis of chiral amines.

J Mol Catal B Enzym, 96:103–110.

Findrik Z and Vasic-Racki D. (2009). Overview on reactions with multi-enzyme systems. *Chem Biochem Eng Q*, 23:545–553.

Findrik Z, Vrsalović Presecki A and Vasić-Racki D. (2007). Mathematical modelling of NADH oxidation catalyzed by new NADH oxidase from *Lactobacillus brevis* in continuously operated enzyme membrane reactor. *J Biosci Bioeng*, 104:275–80.

Flickinger MC. (2009). *Encyclopedia of Industrial Biotechnology*. John Wiley & Sons, Inc., New Jersey.

Freeman A, Woodley JM and Lilly MD. (1993). *In situ* product removal as a tool for bioprocessing. *Biotechnology* 11:1007–1012.

Fuchs M, Farnberger JE and Kroutil W. (2015). The industrial age of biocatalytic transamination. *European J Org Chem*, 2015:6965–6982.

García García MI, Sola Carvajal A, García Carmona F and Sánchez Ferrer Á. (2012). Characterization of a novel N-*Acetylneuraminate lyase* from *Staphylococcus carnosus* TM300 and its application to N-acetylneuraminic acid production. *J Agric Food Chem*, 60:7450–7456.

Gargiulo S, Opperman DJ, Hanefeld U, Arends IWCE and Hollmann F. (2012). A biocatalytic redox isomerisation. *Chem Commun*, 48:6630.

Goldberg K, Edegger K, Kroutil W and Liese A. (2006). Overcoming the thermodynamic limitation in asymmetric hydrogen transfer reactions catalyzed by whole cells. *Biotechnol Bioeng*, 95:192–8.

Goldberg RN. (2014). Standards in biothermodynamics. *Perspect Sci* 1:1–8.

Goldberg RN, Tewari YB and Bhat TN. (2004). Thermodynamics of enzyme-catalyzed reactions - A database for quantitative biochemistry. *Bioinformatic*s 20:2874–2877.

Goldberg RN, Tewari YB and Bhat TN. (2007). Thermodynamics of enzyme-catalyzed reactions: Part 7—2007 update. *J Phys Chem Ref Data*, 36:1347–1397.

Green AP, Turner NJ and O'Reilly E. (2014). Chiral amine synthesis using ω-transaminases: An amine donor that displaces equilibria and enables high-throughput screening. *Angew Chemie*, 126:10890–10893.

Grimshaw CE and Cleland WW. (1981). Kinetic mechanism of *Bacillus subtilis* L-alanine

dehydrogenase. *Biochemistry*, 20:5650–5655.

Gundersen MT, Abu R, Schürmann M and Woodley JM. (2015). Amine donor and acceptor influence on the thermodynamics of ω-transaminase reactions. *Tetrahedron: Asymmetry*, 26:567–570.

Hall M and Bommarius AS. (2011). Enantioenriched compounds via enzyme-catalyzed redox reactions. Chem Rev 111:4088–4110.

Hall M, Stueckler C, Hauer B, Stuermer R, Friedrich T, Breuer M, Kroutil W and Faber K. (2008). Asymmetric bioreduction of activated C=C bonds using *Zymomonas mobilis* NCR enoate reductase and old yellow enzymes OYE 1–3 from yeasts. *European J Org Chem*, 2008:1511–1516.

Halling PJ. (1990). Solvent selection for biocatalysis in mainly organic systems: Predictions of effects on equilibrium position. *Biotechnol Bioeng*, 35:691–701.

Hehre WJ. (2003). *A Guide to Molecular Mechanics and Quantum Chemical Calculations*. Wavefunction, Inc., Irvine, California

Held C, Cameretti LF and Sadowski G. (2011). Measuring and modeling activity coefficients in aqueous amino-acid solutions. *Ind Eng Chem Res*, 50:131–141.

Held C, Neuhaus T and Sadowski G. (2010). Compatible solutes: Thermodynamic properties and biological impact of ectoines and prolines. *Biophys Chem*, 152:28–39.

Henry CS, Broadbelt LJ and Hatzimanikatis V. (2007). Thermodynamics-based metabolic flux analysis. *Biophys J*, 92:1792–805.

Herter S, Mckenna SM, Frazer AR, Leimkühler S, Carnell AJ and Turner NJ. (2015). Galactose oxidase variants for the oxidation of amino alcohols in enzyme cascade synthesis. *ChemCatChem*, 7:2313–2317.

Hoffmann P, Held C, Maskow T and Sadowski G. (2014). A thermodynamic investigation of the glucose-6-phosphate isomerization. *Biophys Chem*, 195:22–31.

Hoffmann P, Voges M, Held C and Sadowski G. (2013). The role of activity coefficients in bioreaction equilibria: thermodynamics of methyl ferulate hydrolysis. *Biophys Chem*, 173-174:21–30.

Höhne M, Kühl S, Robins K and Bornscheuer UT. (2008). Efficient asymmetric synthesis of chiral amines by combining transaminase and pyruvate decarboxylase. *ChemBioChem*, 9:363–365.

Höllrigl V, Hollmann F, Kleeb AC, Buehler K and Schmid A. (2008). TADH, the thermostable alcohol dehydrogenase from *Thermus sp.* ATN1: A versatile new biocatalyst for organic synthesis. *Appl Microbiol Biotechnol*, 81:263–273.

Holzer AK, Hiebler K, Mutti FG, Simon RC, Lauterbach L, Lenz O and Kroutil W. (2015). Asymmetric biocatalytic amination of ketones at the expense of NH_3 and molecular hydrogen. *Org Lett*, 17: 2431–2433.

Hukkerikar AS, Sarup B, Ten Kate A, Abildskov J, Sin G and Gani R. (2012). Group-contribution+ (GC+) based estimation of properties of pure components: Improved property estimation and uncertainty analysis. *Fluid Phase Equilib*, 321:25–43.

Hummel W and Gröger H. (2014). Strategies for regeneration of nicotinamide coenzymes emphasizing self-sufficient closed-loop recycling systems. *J Biotechnol*, 191:22–31.

Hussain S, Leipold F, Man H, Wells E, France SP, Mulholland KR, Grogan G and Turner NJ. (2015) .An (R)-imine reductase biocatalyst for the asymmetric reduction of cyclic imines. *ChemCatChem*, 7:579–583.

Illanes A, Cauerhff A, Wilson L and Castro GR. (2012). Recent trends in biocatalysis engineering. *Bioresour Technol*, 115:48–57.

Jankowski MD, Henry CS, Broadbelt LJ and Hatzimanikatis V. (2008). Group contribution method for thermodynamic analysis of complex metabolic networks. *Biophys J*, 95:1487–1499.

Jemli S, Ayadi-Zouari D, Hlima H Ben and Bejar S. (2016). Biocatalysts: Application and engineering for industrial purposes. *Crit Rev Biotechnol*, 36:246–258.

Knaus T, Mutti FG, Humphreys LD, Turner NJ and Scrutton NS. (2015). Systematic methodology for the development of biocatalytic hydrogen-borrowing cascades: Application to the synthesis of chiral α-substituted carboxylic acids from α-substituted α,β-unsaturated aldehydes. *Org Biomol Chem*, 13:223–233.

Köhler V and Turner NJ. (2014). Artificial concurrent catalytic processes involving enzymes. *Chem Commun*, 51:450–464.

Kohls H, Steffen-Munsberg F and Höhne M. (2014). Recent achievements in developing the biocatalytic toolbox for chiral amine synthesis. *Curr Opin Chem Biol*, 19:180–192.

Koszelewski D, Clay D, Rozzell D and Kroutil W. (2009). Deracemisation of α-chiral primary amines

by a one-pot, two-step cascade reaction catalysed by ω-transaminases. *European J Org Chem*, 2009:2289–2292.

Koszelewski D, Lavandera I, Clay D, Rozzell D and Kroutil W. (2008). Asymmetric synthesis of optically pure pharmacologically relevant amines employing ω-transaminases. *Adv Synth Catal*, 350:2761–2766.

Kotik M, Archelas A, Faměrová V, Oubrechtová P and Křen V. (2011). Laboratory evolution of an epoxide hydrolase - towards an enantioconvergent biocatalyst. *J Biotechnol*, 156:1–10.

Kratzer R, Woodley JM and Nidetzky B. (2015). Rules for biocatalyst and reaction engineering to implement effective, NAD(P)H-dependent, whole cell bioreductions. *Biotechnol Adv*, 33:1641–1652.

Kroutil W, Mang H, Edegger K and Faber K. (2004). Biocatalytic oxidation of primary and secondary alcohols. *Adv Synth Catal*, 346:125–142.

Kurumbang NP, Dvorak P, Bendl J, Brezovsky J, Prokop Z and Damborsky J. (2014). Computer-assisted engineering of the synthetic pathway for biodegradation of a toxic persistent pollutant. *ACS Synth Biol*, 3:172–181.

Lalonde J. (2016). Highly engineered biocatalysts for efficient small molecule pharmaceutical synthesis. *Curr Opin Biotechnol*, 42:152–158.

Lerchner A, Achatz S, Rausch C, Haas T and Skerra A. (2013). Coupled enzymatic alcohol-to-amine conversion of isosorbide using engineered transaminases and dehydrogenases. *ChemCatChem*, 5:3374–3383.

Leskovac V. (2004). *Comprehensive Enzyme Kinetics*. Kluwer Academic Publishers, New York

Letcher TM. (2007). *Thermodynamics, solubility, and environmental issues*. Elsevier Science.

Leuchs S and Greiner L. (2011). Alcohol dehydrogenase from *Lactobacillus brevis*: A versatile robust catalyst for enantioselective transformations. *Chem Biochem Eng Q*, 25:267–281.

Leuchs S, Na'amnieh S and Greiner L. (2012). Enantioselective reduction of sparingly water-soluble ketones: Continuous process and recycle of the aqueous buffer system. *Green Chem.* 15:167–176.

Li H, Luan Z-J, Zheng G-W and Xu J-H. (2015). Efficient synthesis of chiral indolines using an imine reductase from *Paenibacillus lactis*. *Adv Synth Catal*, 357:1692–1696.

Liese A, Seelbach K and Wandrey C. (2006). *Industrial Biotransformations*, Second Edition. Wiley-VCH Verlag GmbH & Co. KGaA

Lima-Ramos J, Tufvesson P and Woodley JM. (2014). Application of environmental and economic metrics to guide the development of biocatalytic processes. *Green Process Synth*, 3:195–213.

Lye GJ and Woodley JM. (1999). Application of *in situ* product-removal techniques to biocatalytic processes. *Trends Biotechnol*, 17:395–402. doi:

Ma SK, Gruber J, Davis C, Newman L, Gray D, Wang A, Grate J, Huisman GW and Sheldon RA. (2010). A green-by-design biocatalytic process for atorvastatin intermediate. *Green Chem*, 12:81–86.

Mallin H, Wulf H and Bornscheuer UT. (2013). A self-sufficient Baeyer-villiger biocatalysis system for the synthesis of ε-caprolactone from cyclohexanol. *Enzyme Microb Technol*, 53:283–7.

Marrero J and Gani R. (2001). Group-contribution based estimation of pure component properties. *Fluid Phase Equilib*, 183-184:183–208.

Maskow T and von Stockar U. (2005). How reliable are thermodynamic feasibility statements of biochemical pathways? *Biotechnol Bioeng*, 92:223–30.

Mavrovouniotis ML. (1990). Group contributions for estimating standard Gibbs energies of formation of biochemical compounds in aqueous solution. *Biotechnol Bioeng*, 36:1070–1082.

Mavrovouniotis ML. (1991). Estimation of standard Gibbs energy changes of biotransformations. *J Biol Chem*, 266:14440–14445.

Mavrovouniotis ML. (1996). Duality theory for thermodynamic bottlenecks in bioreaction pathways. *Chem Eng Sci*, 5:1495–1507.

Mavrovouniotis ML, Stephanopoulos G and Stephanopoulos G. (1992). Synthesis of biochemical production routes. *Comput Chem Eng*, 16:605–619.

Meier RJ, Gundersen MT, Woodley JM and Schürmann M. (2015). A practical and fast method to predict the thermodynamic preference of ω-transaminase-based transformations. *ChemCatChem*, 7:2594–2597.

Muschiol J, Peters C, Oberleitner N, Mihovilovic MD, Bornscheuer UT and Rudroff F. (2015). Cascade catalysis – Strategies and challenges en route to preparative synthetic biology. *Chem Commun*, 51:5798–5811.

Mutti FG, Fuchs CS, Pressnitz D, Turrini NG, Sattler JH, Lerchner A, Skerra A and Kroutil W. (2012). Amination of ketones by employing two new (S)-Selective ω-transaminases and the His-Tagged ω-TA from *Vibrio fluvialis*. *European J Org Chem*, 2012:1003–1007.

Mutti FG, Knaus T, Scrutton NS, Breuer M and Turner NJ. (2015). Conversion of alcohols to enantiopure amines through dual-enzyme hydrogen-borrowing cascades. *Science*, 349:1525–1529.

Nestl BM, Hammer SC, Nebel BA and Hauer B. (2014). New generation of biocatalysts for organic synthesis. *Angew Chem Int Ed Engl*, 53:3070–3095.

Ni Y, Holtmann D and Hollmann F. (2014). How green is biocatalysis? To calculate is to know. *ChemCatChem*, 6:930–943.

Noor E, Bar-Even A, Flamholz A, Lubling Y, Davidi D and Milo R. (2012). An integrated open framework for thermodynamics of reactions that combines accuracy and coverage. *Bioinformatics*, 28:2037–2044.

Noor E, Bar-Even A, Flamholz A, Reznik E, Liebermeister W and Milo R. (2014). Pathway thermodynamics highlights kinetic obstacles in central metabolism. *PLoS Comput Biol*, 10:e1003483.

Nugent TCC and El-Shazly M. (2010). Chiral amine synthesis - Recent developments and trends for enamide reduction, reductive amination, and imine reduction. *Adv Synth Catal*, 352:753–819.

O'Reilly E, Iglesias C and Turner NJ. (2014). Monoamine oxidase-ω-transaminase cascade for the deracemisation and dealkylation of amines. *ChemCatChem*, 6:992–995.

Oberleitner N, Peters C, Rudroff F, Bornscheuer UT and Mihovilovic MD. (2014). *In vitro* characterization of an enzymatic redox cascade composed of an alcohol dehydrogenase, an enoate reductases and a Baeyer-Villiger monooxygenase. *J. Biotechno,*. 192:393–399.

Palacio CM, Crismaru CG, Bartsch S, Navickas V, Ditrich K, Breuer M, Abu R, Woodley JM, Baldenius K, Wu B and Janssen DB. (2016). Enzymatic network for production of ether amines from alcohols. *Biotechnol Bioeng*, 113:1853–1861.

Park E-S, Dong J-Y and Shin J-S. (2013a). ω-Transaminase-catalyzed asymmetric synthesis of unnatural amino acids using isopropylamine as an amino donor. *Org Biomol Chem*, 11:6929–33.

Park E-S, Malik MS, Dong J-Y and Shin J-S. (2013b). One-pot production of enantiopure alkylamines

and arylalkylamines of opposite chirality catalyzed by ω-transaminase. *ChemCatChem*, 5:1734–1738.

Parmeggiani F, Lovelock SL, Weise NJ, Ahmed ST and Turner NJ. (2015). Synthesis of D- and L-phenylalanine derivatives by phenylalanine ammonia lyases: A multienzymatic cascade process. *Angew Chemie*, 127:4691–4694.

Paul CE, Arends IWCE and Hollmann F. (2014). Is simpler better? Synthetic nicotinamide cofactor analogues for redox chemistry. *ACS Catal*, 4:788–797.

Peters M, Eckstein MF, Hartjen G, Spiess AC, Leitner W and Greiner L. (2007). Exploring conversion of biphasic catalytic reactions: Analytical solution and parameter study. *Ind Eng Chem Res*, 46:7073–7078.

Pickl M, Fuchs M, Glueck SM and Faber K. (2015). Amination of ω-functionalized aliphatic primary alcohols by a biocatalytic oxidation-transamination cascade. *ChemCatChem*, 7:3121–3124.

Piérard A and Wiame JM. (1960). Properties of Alanine dehydrogenase. *Biochim Biophys Acta*, 37:490–502.

Pissarra PDN and Nielsen J. (1997). Thermodynamics of metabolic pathways for penicillin production: Analysis of thermodynamic feasibility and free energy changes during fed-batch cultivation. *Biotechnol Prog*, 13:156–165.

Polizzi KM, Bommarius AS, Broering JM and Chaparro-Riggers JF. (2007). Stability of biocatalysts. Curr *Opin Chem Biol*, 11:220–225.

Pollard DJ and Woodley JM. (2007). Biocatalysis for pharmaceutical intermediates: the future is now. *Trends Biotechnol*, 25:66–73.

Presečki AV and Vasić-Rački Đ. (2009). Mathematical modelling of the dehydrogenase catalyzed hexanol oxidation with coenzyme regeneration by NADH oxidase. *Process Biochem*, 44:54–61.

Raj H, Szymański W, de Villiers J, Rozeboom HJ, Veetil VP, Reis CR, de Villiers M, Dekker FJ, de Wildeman S, Quax WJ, Thunnissen A-MWH, Feringa BL, Janssen DB and Poelarends GJ. (2012). Engineering methylaspartate ammonia lyase for the asymmetric synthesis of unnatural amino acids. *Nat Chem*, 4:478–484.

Reetz MT. (2013). Biocatalysis in organic chemistry and biotechnology: Past, present, and future. *J Am Chem Soc*, 135:12480–12496.

Rehn G, Adlercreutz P and Grey C. (2014). Supported liquid membrane as a novel tool for driving the equilibrium of ω-transaminase-catalyzed asymmetric synthesis. *J Biotechnol*, 179:50–55.

Rehn G, Grey C, Branneby C and Adlercreutz P. (2013). Chitosan flocculation: An effective method for immobilization of E.*coli* for biocatalytic processes. *J Biotechnol*, 165:138–144.

Ricca E, Brucher B, Schrittwieser JH. (2011). Multi-enzymatic cascade reactions: Overview and perspectives. *Adv Synth Catal*, 353:2239–2262.

Richter N, Simon RC, Kroutil W, Ward JM and Hailes HC. (2014). Synthesis of pharmaceutically relevant 17-α-amino steroids using an ω-transaminase. *Chem Commun*, 50:6098–100.

Ringborg RH and Woodley JM. (2016). The application of reaction engineering to biocatalysis. *React Chem Eng*, 1:10–22.

Rios-Solis L, Morris P, Grant C, Odeleye AOO, Hailes HC, Ward JM, Dalby PA, Baganz F and Lye GJ. (2015). Modelling and optimisation of the one-pot, multi-enzymatic synthesis of chiral amino-alcohols based on microscale kinetic parameter determination. *Chem Eng Sci*, 122:360–372.

Riva S and Fessner W. (2014). *Cascade Biocatalysis*. Wiley-VCH Verlag GmbH & Co. KGaA, Weinheim, Germany.

Ruschig U, Müller U, Willnow P and Höpner T. (1976). CO_2 Reduction to formate by NADH catalysed by formate dehydrogenase from *Pseudomonas oxalaticus*. *Eur J Biochem*, 70:325–330.

Salerno C, Ovadi J, Keleti T and Fasella P. (1982). Kinetics of coupled reactions catalyzed by aspartate aminotransferase and glutamate dehydrogenase. *Eur J Biochem*, 121:511–517.

Santacoloma PA, Sin G, Gernaey K V. and Woodley JM. (2011). Multienzyme-catalyzed processes: Next-generation biocatalysis. *Org Process Res Dev*, 15:203–212.

Sattler JH, Fuchs M, Mutti FG, Grischek B, Engel P, Pfeffer J, Woodley JM and Kroutil W. (2014). Introducing an in situ capping strategy in systems biocatalysis to access 6-aminohexanoic acid. *Angew Chemie*, 126:14377–14381.

Sattler JH, Fuchs M, Tauber K, Mutti FG, Faber K, Pfeffer J, Haas T and Kroutil W. (2012). Redox self-sufficient biocatalyst network for the amination of primary alcohols. *Angew Chem Int Ed Engl*, 51:9156–9159.

Savile CK, Janey JM, Mundorff EC, Moore JC, Tam S, Jarvis WR, Colbeck JC, Krebber A, Fleitz FJ,

Brands J, Devine PN, Huisman GW and Hughes GJ. (2010). Biocatalytic asymmetric synthesis of chiral amines from ketones applied to sitagliptin manufacture. *Science*, 329:305–309.

Schrittwieser JH, Sattler J, Resch V, Mutti FG and Kroutil W. (2011). Recent biocatalytic oxidation-reduction cascades. *Curr Opin Chem Biol*, 15:249–256.

Sehl T, Kulig J, Westphal R and Rother D. (2014). Synthetic enzyme cascades for valuable diols and amino alcohols : smart composition and optimization strategies. *Industrial Biocatalysis*, 1:887-930.

Seo J-H, Kyung D, Joo K, Lee J and Kim B-G. (2011). Necessary and sufficient conditions for the asymmetric synthesis of chiral amines using ω-aminotransferases. *Biotechnol Bioeng*, 108:253–63.

Shin JS and Kim BG. (1998). Kinetic modeling of omega-transamination for enzymatic kinetic resolution of alpha-methylbenzylamine. *Biotechnol Bioeng*, 60:534–540.

Shin JS and Kim BG. (2002). Exploring the active site of amine:pyruvate aminotransferase on the basis of the substrate structure-reactivity relationship: How the enzyme controls substrate specificity and stereoselectivity. *J Org Chem*, 67:2848–2853.

Simon RC, Richter N, Busto Eand Kroutil W (2014) Recent developments of cascade reactions involving ω-transaminases. *ACS Catal*, 4:129–143.

Singh RK, Tiwari MK, Singh R and Lee J-K. (2013). From protein engineering to immobilization: Promising strategies for the upgrade of industrial enzymes. *Int J Mol Sci*, 14:1232–77.

Smith MT, Emerich DW and Emerichs W. (1993). Alanine dehydrogenase from soybean nodule bacteroids. *J Biol Chem*, 268:10746–10753.

Suljić S and Pietruszka J. (2014). Synthesis of 3-arylated 3,4-dihydrocoumarins: Combining continuous flow hydrogenation with laccase-catalysed oxidation. *Adv Synth Catal*, 356:1007–1020.

Tauber K, Fuchs M, Sattler JH, Pitzer J, Pressnitz D, Koszelewski D, Faber K, Pfeffer J, Haas T and Kroutil W. (2013). Artificial multi-enzyme networks for the asymmetric amination of sec-alcohols. *Chemistry*, 19:4030–4035.

Tauber K, Hall M, Kroutil W, Fabian WMFF, Faber K and Glueck SM. (2011). A highly efficient ADH-coupled NADH-recycling system for the asymmetric bioreduction of carbon-carbon

double bonds using enoate reductases. *Biotechnol Bioeng*, 108:1462–1467.

Tewari YB. (1990). Thermodynamics of industrialy-lmportant, enzyme-catalyzed reactions. *Appl Biochem Biotechnol*, 23:187–204.

Tewari YB, Goldberg RN and Rozzell JD. (2000). Thermodynamics of reactions catalysed by branched-chain-amino-acid transaminase. *J Chem Thermodyn*, 32:1381–1398.

Tewari YB, Kishore N, Goldberg RN and Luong TN. (1998). An equilibrium and calorimetric study of some transamination reactions. *J Chem Thermodyn*, 30:777–793.

Toftgaard Pedersen A, Birmingham WR, Rehn G, Charnock SJ, Turner NJ and Woodley JM. (2015). Process requirements of galactose oxidase catalyzed oxidation of alcohols. *Org Process Res Dev*, 19:1580–1589.

Torres Pazmiño DE, Snajdrova R, Baas B-J, Ghobrial M, Mihovilovic MD and Fraaije MW. (2008). Self-sufficient baeyer–villiger monooxygenases: Effective coenzyme regeneration for biooxygenation by fusion engineering. *Angew Chemie*, 120:2307–2310.

Truppo MD, Rozzell JD, Moore JC and Turner NJ. (2009). Rapid screening and scale-up of transaminase catalysed reactions. *Org Biomol Chem*. 7:395–398.

Truppo MD, Rozzell JD and Turner NJ. (2010). Efficient production of enantiomerically pure chiral amines at concentrations of 50 g/L using transaminases. *Org Process Res Dev*, 14:234–237.

Tufvesson P, Bach C and Woodley JM. (2013). A model to assess the feasibility of shifting reaction equilibrium by acetone removal in the transamination of ketones using 2-propylamine. *Biotechnol Bioeng*, 111:309–319.

Tufvesson P, Jensen JS, Kroutil W and Woodley JM. (2012). Experimental determination of thermodynamic equilibrium in biocatalytic transamination. *Biotechnol Bioeng*, 109:2159–2162.

Tufvesson P, Lima-ramos J, Jensen JS, Al-Haque N, Neto W snd Woodley JM. (2011). Process considerations for the asymmetric synthesis of chiral amines using transaminases. *Biotechnol Bioeng*, 108:1479–1493.

Turner NJ. (2009). Directed evolution drives the next generation of biocatalysts. *Nat Chem Biol* 5:567–573.

Turner NJ. (2011). Ammonia lyases and aminomutases as biocatalysts for the synthesis of α-amino and β-amino acids. *Curr Opin Chem Biol*, 15:234–240.

Turner NJ and O'Reilly E. (2013). Biocatalytic retrosynthesis. *Nat Chem Biol*, 9:285–288.

Villadsen J, Nielsen J and Lidén G. (2011). *Bioreaction Engineering Principles*, 3rd Ed. Springer US, Boston, MA.

von Stockar U. (2013). *Biothermodynamics: The role of thermodynamics in biochemical engineering*, EPFL Press, Lausanne, Switzerland.

von Stockar U and van der Wielen LAM. (2003). Back to basics: Thermodynamics in biochemical engineering. *Adv Biochem Eng Biotechnol*, 80:1–17.

von Stockar U and van der Wielen LAM. (1997). Thermodynamics in biochemical engineering. *J Biotechnol*, 59:25–37.

Vojinović V and Von Stockar U. (2009). Influence of uncertainties in pH, pMg, activity coefficients, metabolite concentrations, and other factors on the analysis of the thermodynamic feasibility of metabolic pathways. *Biotechnol Bioeng*, 103:780–795.

Voss CV, Gruber CC, Faber K, Knaus T, Macheroux P and Kroutil W. (2008). Orchestration of concurrent oxidation and reduction cycles for stereoinversion and deracemisation of sec-alcohols. *J Am Chem Soc*, 130:13969–13972.

Wang B, Land H and Berglund P. (2013). An efficient single-enzymatic cascade for asymmetric synthesis of chiral amines catalyzed by ω-transaminase. *Chem Commun (Camb)*, 49:161–163.

Watanabe S, Kodaki T and Makino K. (2006). A novel alpha-ketoglutaric semialdehyde dehydrogenase: evolutionary insight into an alternative pathway of bacterial L-arabinose metabolism. *J Biol Chem*, 281:28876–28888.

Weckbecker A, Gröger H, Hummel W. (2010). Regeneration of nicotinamide coenzymes: principles and applications for the synthesis of chiral compounds. *Adv Biochem Eng Biotechnol*, 120:195–242.

Wegner J, Ceylan S and Kirschning A. (2012). Flow chemistry - A key enabling technology for (multistep) organic synthesis. *Adv Synth Catal*, 354:17–57.

Wenda S, Illner S, Mell A and Kragl U. (2011). Industrial biotechnology—the future of green chemistry? *Green Chem*, 13:3007–3047.

Wichmann R, Vasic-Racki D. (2005). *Technology Transfer in Biotechnology*. Springer Berlin Heidelberg, Berlin, Heidelberg.

Woodley JM. (2013). Protein engineering of enzymes for process applications. *Curr Opin Chem Biol*, 17:310–6.

Woodley JM. (2012). *Reaction and Process Engineering*. In: Karlheinz Drauz, Harald Gröger OM (ed) Enzyme Catalysis in Organic Synthesis, 3rd Ed. Wiley-VCH, pp 217–247.

Woodley JM, Bisschops M, Straathof AJJ and Ottens M. (2008). Future directions for in-situ product removal (ISPR). *J Chem Technol Biotechnol*, 83:121–123.

Xue R and Woodley JM. (2012). Process technology for multi-enzymatic reaction systems. *Bioresour Technol*, 115:183–195.

Yoshida A and Freese E. (1964). Enzymatic properties of alanine dehydrogenase of Bacillus subtilis. *Biochim Biophys Acta*, 96:248–262.

Yun H and Kim B-G. (2008). Asymmetric synthesis of (*S*)-alpha-methylbenzylamine by recombinant Escherichia coli co-expressing omega-transaminase and acetolactate synthase. *Biosci Biotechnol Biochem*, 72:3030–3033.

Zhang Y. (2000). Synthesis of 14C-labeled *S*-(-)-1-phenylethylamine and its application to the synthesis of a potential antiemetic agent. *J Label Compd Radiopharm*, 43:1087–1093.

Zimmermann V, Hennemann H-G, Daussmann T and Kragl U. (2007). Modelling the reaction course of N-acetylneuraminic acid synthesis from N-acetyl-D-glucosamine-new strategies for the optimisation of neuraminic acid synthesis. *Appl Microbiol Biotechnol*, 76:597–605.

Zimmermann FT, Schneider A, Schörken U, Sprenger GA and Fessner WD. (1999). Efficient multi-enzymatic synthesis of D-xylulose 5-phosphate. *Tetrahedron Asymmetry*, 10:1643–1646.

Appendices

Appendix A: GC analytical methods

A.1 GC Chromatograms

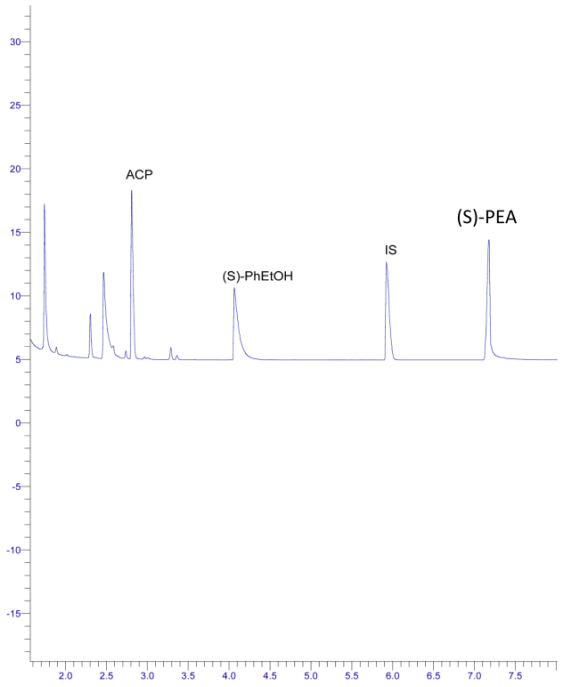

Figure A.1: GC Chromatogram of acetophenone (ACP), (*S*)-phenylethylamine (PhEtOH), internal standard (IS) and (*S*)-phenylethylamine (PEA).

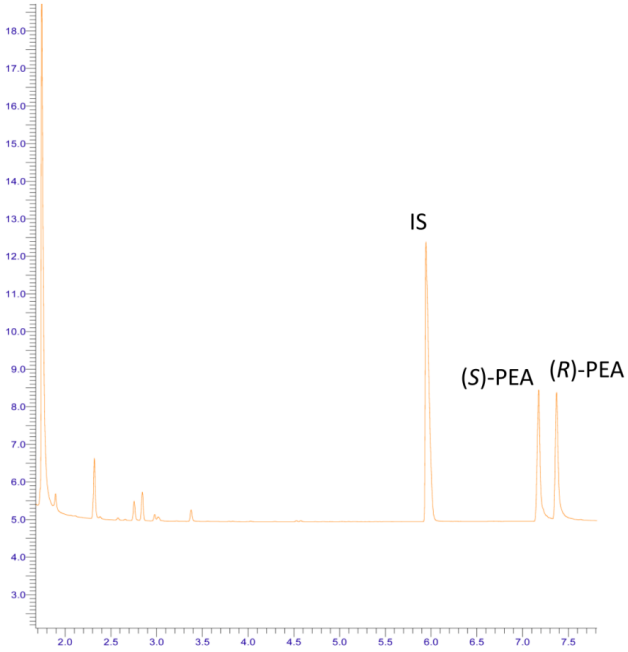

Figure A.2: GC Chromatogram of (*S*) and (*R*)-phenylethylamine (PEA) configurations

A.2 Standard curve of compounds

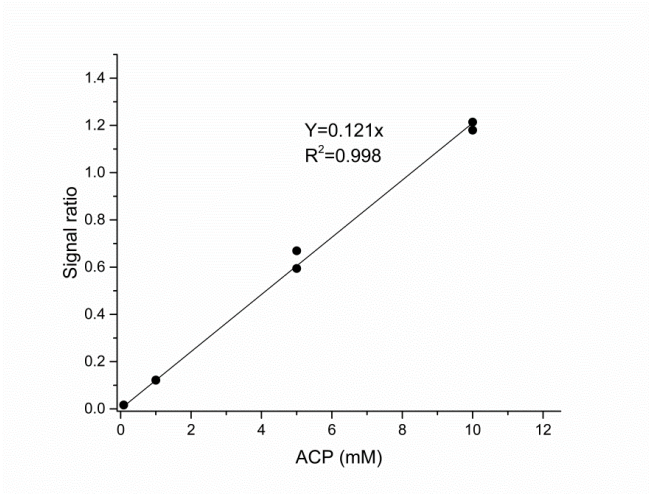

Figure A.3: Standard curve for acetophenone (ACP)

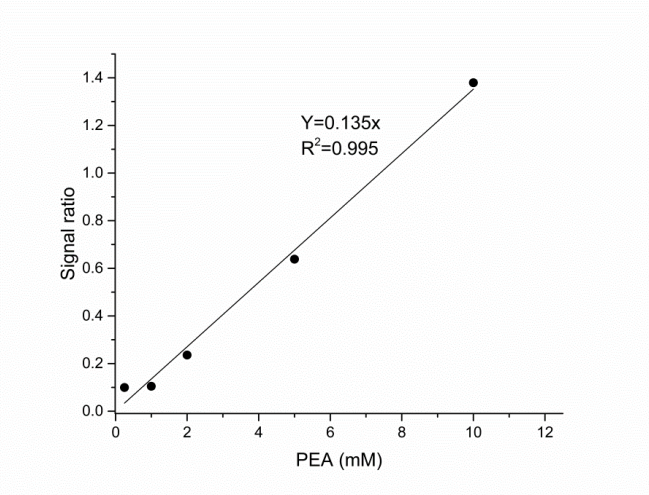

Figure A.4: Standard curve for (*S*)-phenylethylamine (PEA)

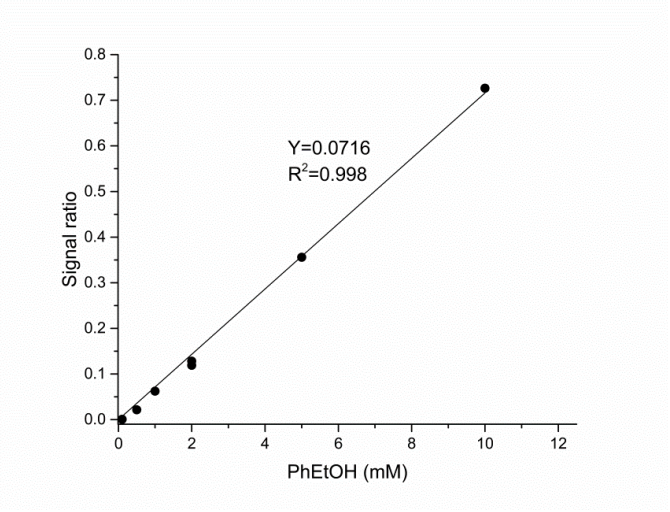

Figure A.5: Standard curve for (*S*)-phenylethanol (PhEtOH)

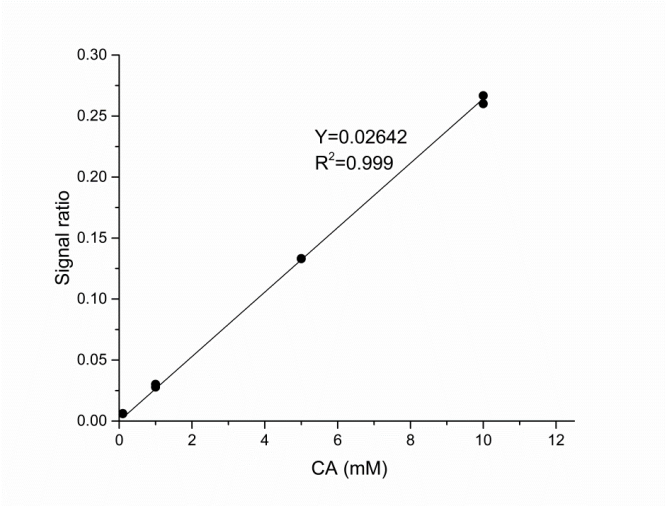

Figure A.6: Standard curve for cyclohexylamine (CA)

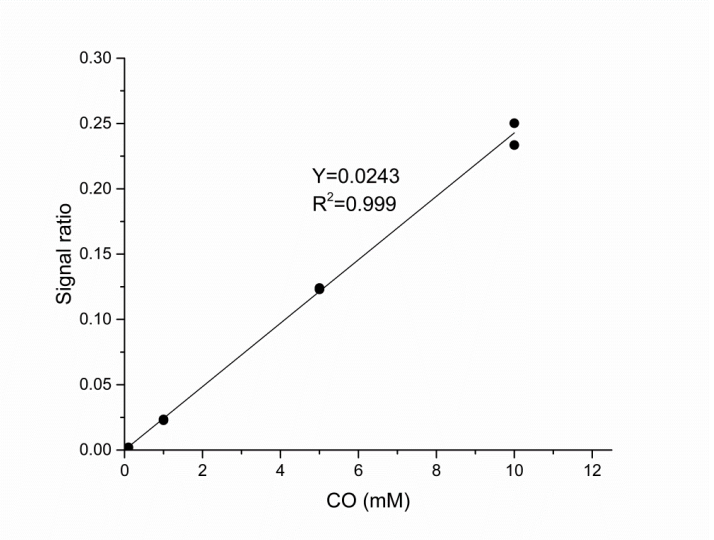

Figure A.7: Standard curve for cyclohexanone (CO)

Appendix B: The presence of NOX in ω-TA (ATA256)

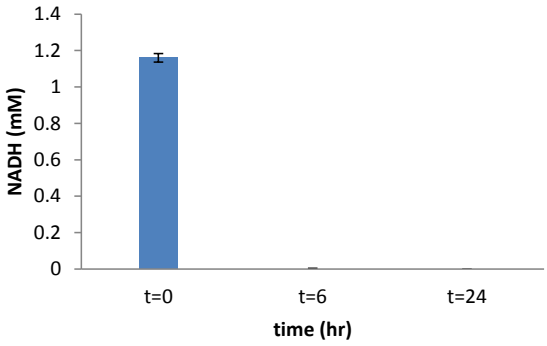

Figure B: The presence of NOX in lyophilized enzyme ω-TA (ATA256). 1 mM NADH was oxidized to NAD after 6 and 24 hours, containing 10 mg/ml ω-TA in the reaction buffer (Tris-HCl at pH 7 and 30°C).

Appendix C: Publications

1. **Abu R** and Woodley, JM. 2015. Application of Enzyme Coupling Reactions to Shift Thermodynamically Limited Biocatalytic Reactions. *ChemCatChem*, 7, 3094–3105.

2. Gundersen MT, **Abu R**, Schürmann M. and Woodley, JM. 2015. Amine donor and acceptor influence on the thermodynamics of ω-transaminase reactions. *Tetrahedron: Asymmetry*, 26, 567–570.

3. **Abu R**, Gundersen MT and Woodley JM. 2015. Thermodynamic Calculations for Systems Biocatalysis. *In 12th International Symposium on Process Systems Engineering and 25th European Symposium on Computer Aided Process Engineering* Elsevier, 37, 233–238.

4. Palacio CM, Crismaru CG, Bartsch S, Navickas V, Ditrich K, Breuer M, **Abu R**, Woodley JM, Baldenius K, Wu B and Janssen DB. 2016. Enzymatic network for production of ether amines from alcohols. *Biotechnology and Bioengineering*, 113, 1853–1861.

ChemPubSoc Europe

DOI: 10.1002/cctc.201500603

CHEMCATCHEM Minireviews

Application of Enzyme Coupling Reactions to Shift Thermodynamically Limited Biocatalytic Reactions

Rohana Abu[a, b] and John M. Woodley*[a]

This manuscript is dedicated to Wolf-Dieter "Woody" Fessner on the occasion of his 60th birthday.

In recent years, much interest has been shown in the use of multi-enzyme cascades as a tool in organic synthesis. Such enzymatic cascades can provide added value to a synthetic scheme by starting from cheaper raw materials or making more valuable products. Additionally, they can be used to help shift the equilibrium of otherwise thermodynamically unfavourable reactions to give a higher conversion of the target product. By coupling an energetically unfavourable reaction with a more favourable one, the multi-enzyme cascade mimics the approach taken in nature in metabolic pathways. Nevertheless, it can be challenging to combine several engineered enzymes in vitro for the conversion of non-natural substrates. In this mini-review we focus on enzyme coupling reactions as a tool to alleviate thermodynamic constraints in synthetically useful biocatalytic reactions. The implications of thermodynamic parameters such as the equilibrium constant on the multi-enzyme cascades and the conventional methods of equilibrium shifting are also discussed in addition to methods used to estimate such values.

1. Introduction

Today, biocatalysis is established as a valuable tool in organic synthesis, especially for the synthesis of optically pure chiral molecules, both at the preparative and industrial scale.[1] Although several hundred industrial examples have now been reported, many more have failed to make the transition from the laboratory to the process plant. One reason for this is that the most interesting syntheses do not usually already exist in nature, which means that it is necessary to engineer enzymes to perform such conversions at a sufficient rate. Likewise, the investment required in protein engineering means that the expansion of the substrate repertoire is important to justify the implementation of a given biocatalyst. A second reason for the failure of reactions to make the transition from the laboratory to the process plant is the limitation often imposed by enzymes that operate at low concentrations of substrate and product. Indeed, it is this very feature that has been evolved in enzymes over millions of years. Here too, protein engineering can provide part of the solution if screens can be adequately designed. The use of substrate feeding and continuous product removal technologies can also be beneficial. A final challenge to overcome is that in some cases the thermodynamics of a reaction means that running the synthesis in the desired direction is not energetically favourable. This problem arises surprisingly frequently and, although the use of an excess of substrate or alternatively continuous product removal technologies can be used, this remains a major challenge. Recently, it was argued that the use of so-called "coupling enzymes" to assist thermodynamically limited reactions could also be employed to overcome this problem.

To date, several promising multi-enzyme cascade reaction schemes have been reported in the scientific literature for the synthesis of interesting chemical products.[2] Unlike chemical catalysts, most enzymes operate under relatively similar reaction conditions (e.g., mild pressure (atmospheric) and temperature (20–50 °C), pH 5.0–8.0, aqueous solution), which facilitate the sequential combination of enzymes into a synthetic scheme and thereby allows effective reaction engineering strategies to shift the equilibrium in an analogous way to that in nature.

In this brief mini-review, we discuss the advantages and disadvantages of such a methodology and its implications for process implementation. We have divided the paper into several sections that include an overview of the relevant thermodynamic properties and suitable strategies for shifting equilibria (which includes the addition of excess co-substrates, the application of in situ product removal and in situ co-product removal, the use of smart substrate/co-substrate and enzyme coupling reactions (the main focus)). We exemplify these principles with a case study and conclude with practical methods to obtain thermodynamic data. These topics are summarised in Figure 1.

[a] R. Abu, Prof. Dr. J. M. Woodley
Department of Chemical and Biochemical Engineering
Technical University of Denmark
2800, Kgs. Lyngby (Denmark)
Fax: (+45) 4525-2885
E-mail: jw@kt.dtu.dk

[b] R. Abu
Department of Chemical and Biochemical Engineering
Universiti Malaysia Pahang
Faculty of Chemical&Natural Resources Engineering
Lebuhraya Tun Razak, 26300 Gambang, Kuantan (Malaysia)

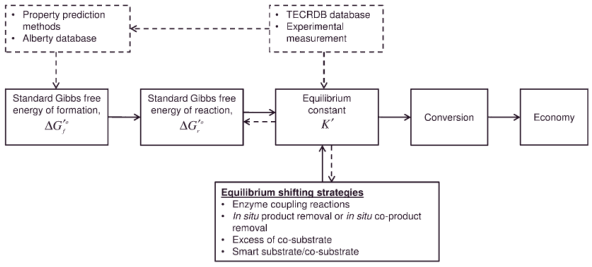

Figure 1. Summary of potential process solutions to improve the productivity of thermodynamically challenged biocatalytic reactions. Knowledge of the equilibrium constant determines the suitable operating strategies to achieve the maximum conversion of thermodynamically challenged biocatalytic reactions.

2. Theoretical Background

The thermodynamic favourability of a chemical reaction can be calculated from the standard Gibbs free energy change of reaction (usually denoted as $\triangle G^0_r$) using Equation (1):

$$\Delta G^0_r = \sum_j^p n_j \Delta G^0_{f,j} - \sum_i^r n_i \Delta G^0_{f,i} \quad (1)$$

In Equation (1), $\triangle G^0_r$ is measured under standard conditions (1 atm, 298 K, 1 M substrate (reactant) thermodynamic activity; $[H^+]$ is defined as 1 M, i.e., pH 0) and is the standard Gibbs free energy of the formation of substrate(s) *r* and product(s) *p*. The subscript *i* denotes species of substrate(s), and *j* species of product(s), and *n* is the stoichiometric coefficient of a given species. $\triangle G^0_f$ is the change in free energy that occurs if a compound is formed from its elements in their most thermodynamically stable state under standard-state conditions. Usually, for biologically mediated reactions, the standard Gibbs free energy of reaction is denoted as $\triangle G'^0_r$ to indicate that it is defined under slightly different standard-state conditions (1 atm, 298 K, 1 M substrate activity, and $[H^+]$ is defined as 10^{-7} M, i.e., pH 7). To calculate the Gibbs free energy in Equation (1), the $\triangle G'^0_f$ value is needed, which can be obtained from the Alberty database[3] if the compound is listed. For many metabolites this is very useful, but in the case of a de novo pathway (synthetic network), many of the compounds are not listed. As a second approach, such values could also be predicted using computational property prediction tools, such as the group contribution method (see Section 5). To complicate matters further, in practice, biocatalytic reactions rarely operate under the standard-state conditions, and therefore, Equation (2) may be used to calculate the Gibbs free energy change of the reaction under non-standard-state conditions (ΔG_r). This allows deviations from the standard state both in temperature and, importantly, concentration.

$$\Delta G_r = \Delta G'^0_r + RT\ln\frac{\prod_j^p c_j^{n_j}}{\prod_i^r c_i^{n_i}} \quad (2)$$

In Equation (2), *R* is the gas constant, *T* is the temperature, c_i and c_j are the concentrations of substrate and product species, respectively, and *n* is the stoichiometric coefficient of a given species. As indicated in Equation (2), usually in a biologically mediated reaction, the substrate thermodynamic activities are assumed to be equal to the respective substrate molar concentrations[4] as the solutions are generally dilute, although the precise influence of such assumptions remains the subject of ongoing research.[5]

The favourability of a given reaction can be determined by the sign of ΔG_r, for which a negative ΔG_r means that the reaction will be driven spontaneously towards the products and a positive ΔG_r means that the reaction is unfavourable. If the system is at equilibrium $\Delta G_r = 0$, which in turn, by rearrangement of Equation (2), gives the (concentration-based) equilibrium constant K' [Eq. (3)].

$$\Delta G'^0_r = -RT\ln K' \quad (3)$$

To complement and validate predictions, experimental values can also be obtained. For metabolic reactions, many experimental values of K' determined previously can be obtained from the Thermodynamics of Enzyme-Catalyzed Reactions Database (TECRDB)[6] and in other cases experimental measurements need to be performed using a suitable approach[7] to obtain such data (see Section 5).

3. Strategies to Shift Equilibria

3.1. Conventional strategies to shift equilibria

Thermodynamic data such as the equilibrium constant K' (either obtained by prediction or experiments) can be used to find suitable operating strategies to achieve a sufficiently high conversion of an energetically unfavourable reaction.[8]

The achievement of a sufficiently high conversion is essential so that the value added by the reaction (difference in economic value between products and substrates) can be exploited fully (Figure 1). Examples of strategies to shift equilibria include the addition of a co-substrate in excess to "push" the equilibrium position or the application of in situ product removal (ISPR) or in situ co-product removal (IScPR) to "pull" the equilibrium position towards the target product (Figure 2).

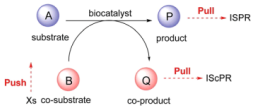

Figure 2. Conventional strategies to shift equilibria based on Le Châtelier's Principal: a) pushing the equilibrium position by addition of excess of co-substrate (X_s) and b) pulling the equilibrium position by either ISPR or IScPR towards the target product.

3.1.1. Addition of excess co-substrate

A technique employed frequently to shift the equilibrium position for reactions with more than one substrate is to use one of the substrates in stoichiometric excess. The extent to which this excess is required to achieve a given conversion can be determined by the equilibrium constant K' of the reaction. For example, for a reversible reaction with K' less than 1, a 50% conversion is the best achievable (Figure 3a).

In principle, by "pushing" the reaction using an excess of co-substrate, the equilibrium position of such an unfavourable reaction can be driven up to 100% conversion. However, if K' is too low, for instance <0.01, more than 100 molar equivalents of excess co-substrate would be required (Figure 3b). Clearly, too high a concentration of the co-substrate could exceed the solubility of the substance in solution.[9] Therefore, it is essential to know the solubility limit of a substance if this technique is chosen or other reaction engineering strategies, such as substrate feeding techniques,[10] should be considered. Likewise, too high an amount of co-substrate can cause inhibition and/or instability of the enzyme,[11] although this can be solved partially (at least) by protein engineering[12] or enzyme immobilisation.[13]

3.1.2. Application of ISPR or IScPR

ISPR and IScPR are technologies that in principle can "pull" products from the reaction mixture to shift the equilibrium.[14] The products are removed during the reaction using technologies such as evaporation under reduced pressure (for volatile products) or extraction into an organic solvent phase (for hydrophobic products).[15] With the use of thermodynamic properties, such as equilibrium constant K' for a given target conversion, the maximum allowable concentration of product (or co-product) in the solution to achieve a given conversion can be determined. For example, if IScPR is used, if the value of K' for a reaction is 0.01 and one of the substrates is the limiting substrate at a concentration of 50 mM, then the maximum concentration of co-product in the solution would be 0.001 mM to achieve 95% conversion (Figure 4a), which is clearly very low. However, if the value of K' is manipulated simultaneously by using an excess of co-substrate, for instance, 100 molar equivalents of the limiting reagent, the maximum co-product allowable in the solution would be 0.1 mM, 100-fold higher (Figure 4b). Thus, information on K' is very useful to predict the feasibility of such strategies. Clearly, there are other physicochemical properties of substrate and product that also need to be considered on selecting IScPR or ISPR that depend on the separation principle, such as the volatility, solubility, molecular weight or size, charge and hydrophobicity.[16]

The use of extraction technologies is of particular interest as a common problem on using enzymes as biocatalysts is the poor water solubility of many of the compounds of interest.

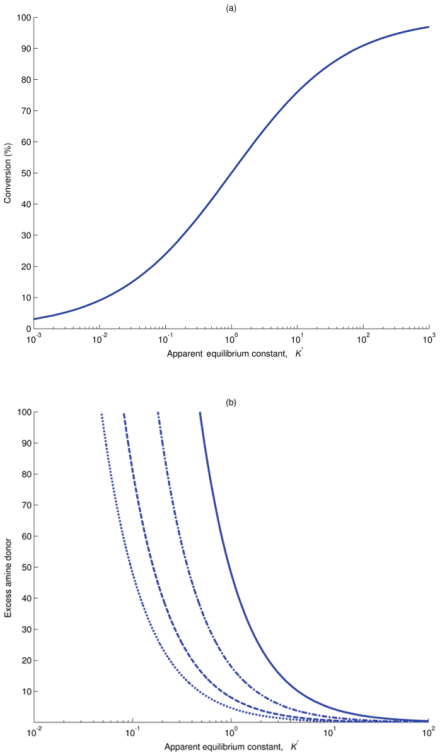

Figure 3. a) Maximum conversion of a reversible reaction with two substrates and b) the use of excess co-substrate as a function of equilibrium constant at 85% (••••), 90% (– – –), 95% (–•–•) and 98% (——) conversion.

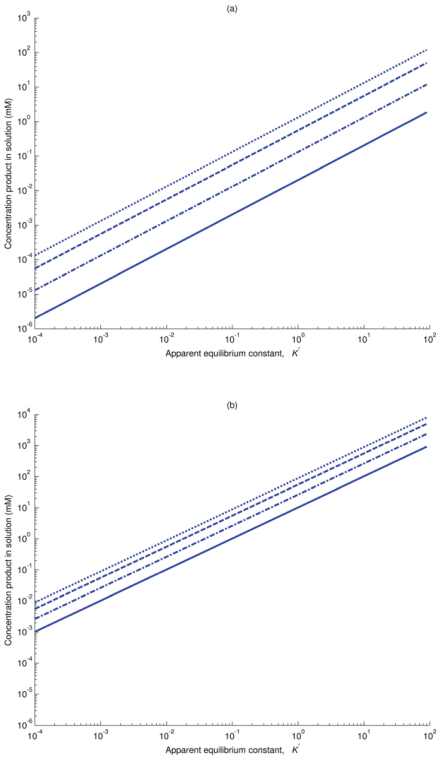

Figure 4. IScPR or ISPR a) without excess co-substrate and b) with excess co-substrate at 85% (••••), 90% (– – –), 95% (–•–•) and 98% (——) conversion.

For that reason, the use of a biphasic system is particularly useful for some hydrophobic substrates to increase the solubility of such substrates and to improve the reaction conversion by also extracting the product or co-product. Co-solvents used frequently include DMSO, *tert*-butyl methyl ether (MTBE), DMF and 1,2-dimethoxyethane (DME).[17]

In all cases the selectivity of the ISPR or IScPR method (of product or co-product over substrate and co-substrate) is essential to shift the equilibrium effectively.

3.2. Smart substrate or co-substrate – Spontaneous equilibrium shift

An alternative approach could be to shift the thermodynamically unfavourable reaction by using a so-called "smart" substrate or co-substrate.[18] A smart co-substrate is one that is converted into a thermodynamically stable co-product,[19] and a smart substrate[20] is one that is converted to a thermodynamically stable product, which both drive the reaction to completion simultaneously. Helpfully, these techniques avoid the use of a co-substrate in excess, which minimises waste products.

Recently, "a double co-substrate" was introduced by Bornadel and co-workers through a redox-neutral convergent cascade.[21] The first co-substrate allows the formation of a thermodynamically stable co-product that shifts the overall equilibrium towards the desired product, whereas the presence of a "double-smart co-substrate" allows the coupling to a secondary enzyme to converge to the same target product and give a higher conversion. This new strategy also improves the atom efficiency of the synthesis route.

3.3. Enzyme coupling reactions

An alternative to these conventional approaches is to use a coupling enzyme to shift the equilibrium position of unfavourable reactions. This approach can be applied to improve the conversion of otherwise thermodynamically limited reactions by coupling an unfavourable reaction with an energetically favourable one. This mimics the approach taken in nature in metabolic pathways. In nature, an individual enzyme usually works as part of a larger enzymatic network.[22] For example, in microbial cells complete metabolic pathways convert simple (sugar) starting molecules to complex products in multiple steps. One feature of such pathways is that they are thermodynamically favourable, in part because of the coupling of reactions that are unfavourable (positive Gibbs free energy) with those that are favourable (negative Gibbs free energy). Such a coupling can be performed either orthogonally (Figure 5a) or in parallel (Figure 5b).

However, not all in vitro reactions in a scheme will be thermodynamically favourable. For example, some unfavourable reactions in vitro may not be automatically coupled in an initial proposal for a synthetic scheme. Likewise, some reactions that can be very useful synthetically will need to be run in the opposite direction to that found in vivo. Such inconsistencies mean that in many cases the preliminary synthetic scheme is not thermodynamically favourable. Although protein engineering offers the opportunity to improve the kinetic profile of a network of enzymes, unfavourable thermodynamics requires a different approach. In principle, by coupling an unfavourable reaction with a more favourable one, as in nature, a given syn-

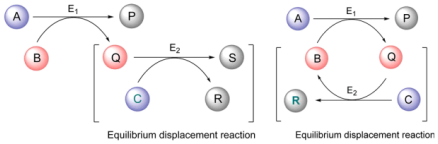

Figure 5. Possible strategies to shift the equilibrium position of an unfavourable reaction (E_1). The energetically favourable reaction (E_2) can be arranged either a) orthogonally or b) in parallel to drive the overall reaction towards the product. Substrate (A), co-substrates (B, C), product (P) and co-products (Q, S, R).

thetic scheme can be made to work. Although these principles are already established, the actual values of Gibbs free energy for individual reactions are reported rarely. Hence understanding the precise role of coupling reactions in the network is often not possible.

Although several methodologies have been proposed to analyse the thermodynamic favourability of existing natural pathways in microbial cells,[4b,23] these analyses are usually only helpful to understand metabolic networks of in vivo systems,[24] as in vitro compartmentalisation can be controlled at will and the concentration of components is frequently very different. Although there are several academic examples of enzymatic cascade reactions in vitro to shift equilibria, to the best of our knowledge, few detail the thermodynamics with which to support such claims.

4. Case Study

The concept of using alternative strategies to shift an unfavourable equilibrium is very well exemplified by the well-studied aminotransferase reaction.[18] There are many other enzymatic reactions of current (and potential) industrial interest in which equilibrium considerations also play an important role, such as alcohol dehydrogenases, ammonia lyases, amine dehydrogenases and aldolase-catalysed reactions (Table 1).

The ω-transaminase (ω-TA; EC 2.6.1.18) class of aminotransferase enzymes is of particular value for the synthesis of chiral amines, especially secondary and more complex amines. As a result of the superb selectivity of these enzymes, the chiral amine is rendered optically pure. Such molecules have great interest for the pharmaceutical industry and, although this is not the only way to make such molecules, there have been several interesting industrial examples reported in the literature (e.g., the synthesis of sitagliptin[34]). The enzyme catalyses the transfer of an amine group from a donor molecule to a carbonyl acceptor. One feature of running the enzyme in the synthetic direction to create a chiral centre is that the products are often less energetically stable than the substrates, which results in a thermodynamically unfavourable equilibrium and gives a poor conversion.

For example, in the synthesis of (*S*)-1-phenylethylamine (PEA), a pharmaceutical compound used as an antiemetic agent,[35] the ω-TA catalyses the transfer of an amine group from L-alanine (L-Ala) to 1-phenylethanone (ACP) to yield the target amine and the co-product pyruvate (Scheme 1). In this synthetic direction, the equilibrium constant for this transamination has been reported to be rather low.[7b,36] The products

Table 1. Thermodynamically limited enzymatic reactions of current (and potential) industrial interest.

Reaction scheme	Comments	Example of equilibrium shifting strategies
 *N*-acetylneuraminic acid aldolase (EC 4.1.3.3)	*N*-acetylneuraminic acid aldolase catalyses the aldol condensation of *N*-acetyl-D-mannosamine with pyruvate in the synthesis of *N*-acetylneuraminic acid (Neu5Ac) and suffers from unfavourable equilibrium thermodynamics	· excess of pyruvate[25] · enzyme coupling reaction–removing pyruvate via LDH[26]
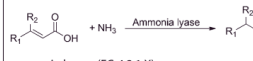 ammonia lyases (EC 4.3.1.X)	phenylalanine (PAL, EC 4.3.1.5),[27] aspartate (AspA, EC 4.3.1.1)[28] and 3-methylaspartate (MAL, EC 4.3.1.2)[29] ammonia lyase catalyses the unfavourable thermodynamic reaction in the amination of α,β-unsaturated carboxylic acid.	· excess of ammonia
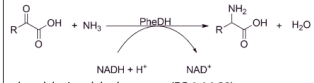 phenylalanine dehydrogenase (EC 1.4.1.20)	PheDH-based amine dehydrogenase catalyses *para*-fluorophenylacetone to (*R*)-1-(4-fluorophenyl)-propyl-2-amine.[30]	· excess of ammonia and co-factor re-generation by an enzyme-coupled approach (coupled with GDH)[30]
 alcohol dehydrogenases (EC 1.1.1.1, NAD-dependent) and (EC 1.1.1.2, NADP-dependent)	alcohol dehydrogenase catalyses the oxidation of alcohol to ketone (more unfavourable towards ketone).	· co-factor re-generation by either substrate-coupled approach (often a high excess of alcohol (e.g., 2-propanol)[31]) or enzyme-coupled approach (e.g. enoate reductase,[32] GDH[31]) · ISPR[33]

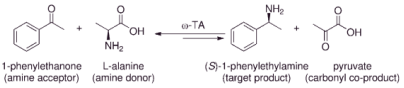

Scheme 1. Example of a thermodynamically limited reaction. ω-TA catalyses the transfer of an amine group from L-Ala to an amine acceptor, 1-phenylethanone (ACP), to yield the target amine PEA and the co-product pyruvate (Pyr).

Table 2. Addition of excess co-substrate (X_s) in the synthesis of 1-phenylethylamine from 1-phenylethanone.

Process conditions	Substrate [mM]	X_s	Kinetic conversion [%]	Expected equivalent conversion [%]	Ref.
ATA-113, pH 7.5, 30 °C, 24 h	416	L-Ala (2.4 equiv.)	<1 (*S*)	5	[20]
Vibrio fluvialis, pH 7, 30 °C, 24 h, 15% v/v DMSO	20	L-Ala (10 equiv.)	<1 (*S*)	9	[37]
ATA-103, pH 7.5, 30 °C, 10 h	50	L-Ala (10 equiv.)	3 (*S*)	9	[38]
ATA-117 (ArRmut11-ω-TA), pH 7, 30 °C, 20% v/v DMSO	50	IPA (20 equiv.)	25 (*R*)	55	[39]

are less energetically stable than the reactants, and thus a low conversion is expected. Indeed, this is supported by calculations based on the available experimental data of the equilibrium constant ($K' = 4.03 \times 10^{-5}$),[7b] which predict that a maximum of 10% conversion would be expected. A technique employed frequently to increase the conversion of reactions of this type is to use L-Ala in stoichiometric excess. However, reports of the use of an excess of the amine donor L-Ala do not indicate much success (Table 2). Based on our calculations, this technique is not feasible as, in principle, it requires an excess of 10000 molar equivalents of L-Ala to achieve a 90% conversion, which is clearly impractical. Additionally, the solubility of L-Ala will also become an issue as it is limited to 1.9 M in aqueous solution.

Interestingly, in the aminotransferase reaction, the couples of amine donor/carbonyl co-product can be selected flexibly as the structure of the target product is determined by its amine acceptor. For instance, instead of L-Ala, isopropylamine (IPA) is considered frequently as an alternative amine donor for this type of reaction.[17,40] The equilibrium constant determined experimentally for Scheme 1 using IPA (instead of L-Ala) as the amine donor is 0.033.[7b] Although the equilibrium constant is increased significantly, perhaps surprisingly, neither IPA nor L-Ala is really a good choice of amine donor for the synthesis of such products if an excess of donor alone is used as the equilibrium shifting method. For IPA, still 240 molar equivalents are needed to push the equilibrium position to achieve 90% conversion (Figure 6). Although IPA requires a lower excess than L-Ala, the excess is still large, which generates waste caused by the unused reagent and creates separation problems downstream.[19a] Although the choice of the amine donor in this particular type of reaction plays a significant role to determine the equilibrium conversion of the target product, it may not be sufficient to enable such an approach. To understand this further, we measured the apparent equilibrium constant of several donor/acceptor combinations for the better implementation of such reactions.[41]

Alternatively, commercially available amine donors (e.g., *ortho*-xylylenediamine dihydrochloride[42] and 3-aminocyclohexa-1,5-dienecarboxylic acid[43]) that favour the tautomerisation process spontaneously could be used. This smart co-substrate approach can shift the equilibrium position successfully towards products in which the unstable co-product ketone is converted spontaneously to a more stable molecule, which gives >99% conversion to PEA. However, this approach is limited by the expensive amine donor that has to be added in equimolar amounts to achieve a high conversion.[44]

Interestingly, however, the use of IPA as an amine donor also allows the removal of its volatile co-product, acetone,[40a] by IScPR using technologies such as stripping,[33] sparging,[45] adsorbing resins[20] or membrane technologies.[46] In an analogous manner to the previous calculations, the maximum acetone concentration allowable in solution to give a required conversion, can be determined by K'. For example, if K' is 0.033 and if the target conversion is 95%, the required acetone concentration in solution should be less than 1 mM if the limiting reagent of 50 mM ACP is used (Figure 7a). It is also common to couple the use an excess of IPA

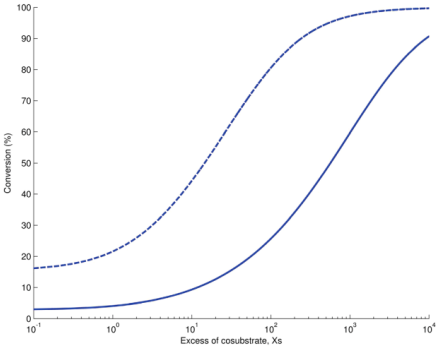

Figure 6. The equilibrium constant (K') determines the maximum theoretical conversion of a reaction. With an excess of co-substrate L-Ala ($K' = 4.03 \times 10^{-5}$, ——) or IPA ($K' = 0.033$, – – –).

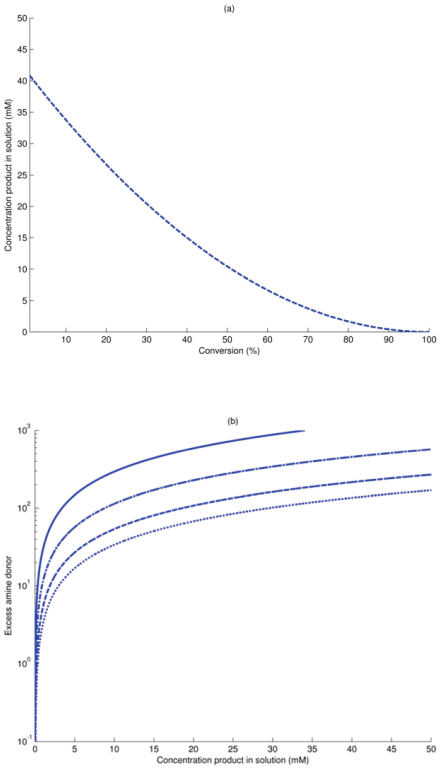

Figure 7. a) IScPR without excess IPA. ISPR gives the same trend (data not shown). b) IScPR or ISPR combine, with excess, at 85% (••••), 90% (– – –), 95% (–•–•) and 98% (——) conversion.

with IScPR to improve the calculation. For example, if the ACP concentration of 50 mM is used with a target of 95% conversion and the use of a 100-fold excess of IPA, the acetone in solution is 18.5 mM (Figure 7b). Still probably the 100-fold excess is unrealistic but in practice even more of a problem is that if IScPR and/or ISPR is used either with solvent or resin extraction because, in this example, the IPA competes with the PEA to bind onto the resins or to co-extract into the solvent, which results in ineffective ISPR.[20] Indeed, as mentioned previously, the selectivity of ISPR or IScPR is an essential requirement to shift the equilibrium using this technique.

For all these reasons, therefore, the use of co-substrate excess and/or co-product removal is limited using the techniques mentioned previously and this has driven the development of an alternative approach using coupling reactions. To date, several cascade reaction schemes to couple with ω-TA to overcome thermodynamic limitations have been proposed.[18] For instance, some cascade schemes to assist the synthesis of PEA have been reported (Scheme 2–4). Frequently, equilibrium-displacement reactions use secondary enzymes such as alanine dehydrogenase (AlaDH; EC 1.4.1.1),[37-39,47] lactate dehydrogenase (LDH; EC 1.1.1.27),[38,39,47,48] yeast alcohol dehydrogenase (YADH; EC 1.1.1.2),[40b] acetolactate synthase (ALS; EC 2.2.1.6),[49] and pyruvate decarboxylase (PDC; EC 1.2.4.1).[50] The reaction is coupled either to remove the co-product or re-generate the co-substrate, both with the objective to shift the equilibrium position towards the product. Notably, the amine donor L-Ala is used frequently in enzymatic cascades because of its selective reactivity towards other enzymes (e.g., AlaDH for re-generation) as well as its corresponding product pyruvate (e.g., LDH for IScPR).

In the same example, an approach of potentially even greater interest would be to use alcohols as the starting material rather than ketones to produce the corresponding amines using an alcohol dehydrogenase (AlcDH; EC 1.1.1.2).[51] However, both reactions (AlcDH and ω-TA) are reversible and need to be coupled with energetically favourable reactions to pull the reaction towards the target product.

In this example of a multi-enzyme cascade, LDH, AlaDH and YADH all require a co-factor (e.g., NADH), which is essential for the functionality of these enzymes. As a result of the cost of such co-factors, it is necessary to re-generate them in situ. To date, in the required direction, the most common co-factor re-generation systems are glucose dehydrogenase (GDH; EC 1.1.1.1) and formate dehydrogenase (FDH; EC 1.2.1.2). Both GDH and FDH are thermodynamically favourable in the required direction for which the apparent equilibrium constant is 3.1[52] and 420,[53] respectively. Other co-factor re-generation enzymes are also available, such as glucose-6-phosphate dehydrogenase (G6PH; EC 1.1.1.49)[54] and glutamate dehydrogenase (EC 1.4.1.2). A number of previous reviews have been published on the co-factor re-generation system.[55] Recently, a [Ni-Fe]-hydrogenase was coupled successfully with ω-TA/AlaDH using H_2 as the reducing equivalent to give high efficiency co-factor re-generation in comparison to the NH_3/formate or glucose systems.[56]

An alternative elegant method to overcome such problems is the use of a self-sufficient redox cascade[51a] (Scheme 4), in which AlaDH was used to shift both unfavourable reactions towards PEA and re-generate the amine donor L-Ala and nicotinamide co-factor (NAD^+) simultaneously in situ. Although the authors did not report the equilibrium constant or indicate that the equilibrium conversion was achieved, as the AlaDH reaction is energetically favourable ($K' = 1.30 \times 10^5$, pH 7.98), this

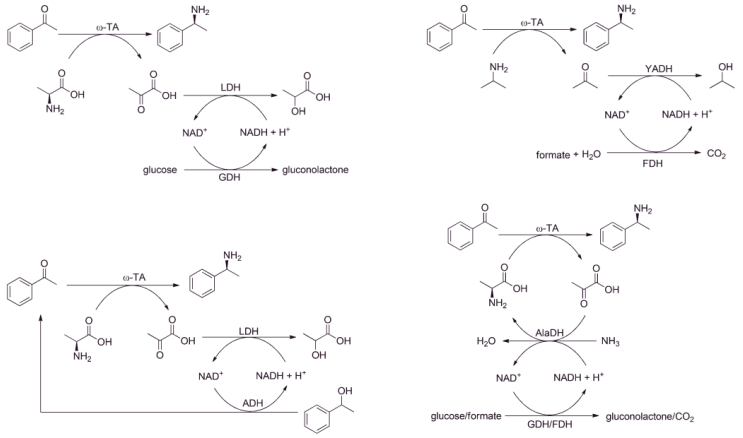

Scheme 2. Possible scheme of coupling reactions with aminotransferase in the synthesis of (*S*)-1-phenylethylamine. Equilibrium displacement reaction with co-factor regeneration system: ω-TA/AlaDH/FDH,[37,39,47] ω-TA/AlaDH/GDH,[38] ω-TA/LDH/GDH system,[20,38,39,47,48] ω-TA/YADH/FDH,[40b] system.

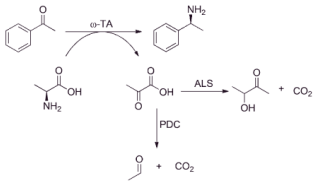

Scheme 3. Equilibrium displacement reaction without co-factor regeneration system: ω-TA/ALS system[49] or ω-TA/PDC system[50].

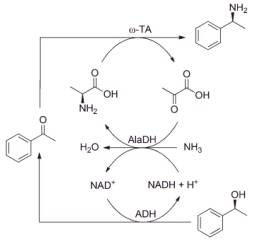

Scheme 4. Redox-neutral cascade: ADH/ω-TA/AlaDH system[51a]

in principle should provide the energy to make the reaction go forward.[57] Nevertheless, the extent to which such a reaction can drive the cascade is unknown. A final conversion of 25% was obtained. Nevertheless, such an elegant cascade might be beneficial for industrial practice, as the use of an external source of hydride can be eliminated and the co-substrate (ammonia) can also be used as a co-solvent, which would be beneficial from an environmental perspective.[19a]

Enzymatic cascades (rather than single reactions) have been operated experimentally with the use of an excess of co-substrate (Table 3). However, the effectiveness of such a strategy is not yet proven as a full thermodynamic analysis is not currently available. The key to maximise the equilibrium conversion of a cascade is determined by a single net reaction that controls the favourability of that cascade. For example, in the synthesis of PEA, 0.5 molar equivalents of pyruvate (co-substrate) were used in the ω-TA/AlaDH/GDH system and a conversion of 96% was achieved.[38] Interestingly, compared to the ω-TA/LDH/GDH system, 10 molar equivalents of L-Ala were required to achieve the same conversion.[38] This might be because of the net reaction that requires the excess to achieve the high conversion, and for the same system, 5 molar equivalents of L-Ala did not achieve such values.[48] Hence some enzymatic cascades coupled with an excess of co-substrate show good results, whereas others do not show significant improvements of the conversion (Table 3). Analysis of the thermodynamics should allow the excess of reagents to be minimised and the enzyme coupling to be used to its full potential.

In the use of coupling techniques that involve engineered enzymes, the substrate scope and kinetic profile of the en-

Table 3. Available experimental data for aminotransferase-catalysed reactions in the synthesis of PEA (kinetic conversion)

System	Process conditions	ACP [mM]	Ratio (co-substrate/ACP)	*ee* (conversion) [%]	Ref.
ω-TA/LDH/GDH	ω-TA (ATA-103), pH 7.5, 30 °C, 10 h	50	L-Ala (5 equiv.) glucose (~2 equiv.)	>99 (21)	[48]
	ω-TA (His-*Vibrio fluvialis*), pH 7, 30 °C, 24 h, 15% v/v DMSO	50	L-Ala (5 equiv.) glucose (~2 equiv.)	>99 (5)	[48]
	ω-TA (ATA-103), pH 7, 30 °C, 24 h, 15% v/v DMSO	50	L-Ala (10 equiv.) glucose (2 equiv.)	>99 (>96)	[38]
	ω-TA (ATA-113), pH 7, 30 °C, 24 h 15% v/v DMSO	50	L-Ala (5 equiv.) glucose (3 equiv.)	>99 (38)	[47]
ω-TA/AlaDH/FDH	ω-TA, (ATA-113), pH 7, 30 °C, 24 h	50	L-Ala (5 equiv.) NH_4HCO_2 (3 equiv.)	>99 (6)	[37]
	ω-TA (His-*Vibrio fluvialis*), pH 7, 30 °C, 24 h, 15% v/v DMSO	50	L-Ala (5 equiv.) NH_4HCO_2 (3 equiv.)	>99 (23)	[47]
	ω-TA (His-*Vibrio fluvialis*), pH 7, 30 °C, 24 h	50	L-Ala (5 equiv.) NH_4HCO_2 (3 equiv.)	>99 (65)	[47]
	ω-TA (His-*Vibrio fluvialis*), pH 7, 30 °C, 24 h	50	L-Ala (5 equiv.) NH_4HCO_2 (3 equiv.)	99 (97)	[47]
ω-TA/AlaDH/GDH	ω-TA (ATA-103), AlaDH (LAADH-117), pH 7.5, 30 °C, 48 h	50	Pyr (0.5 equiv.) NH_4Cl (2 equiv.) glucose (2 equiv.)	(96)	[38]
ω-TA/YADH/FDH	ω-TA (*Arthrobacter citreus*), YADH (*Saccharamyces* cerevisiae), FDH (*Candida boidinii*), pH 7, 30 °C, 24 h	1.8	IPA (311 equiv.)	>99 (99)	[40b]
ADH/ω-TA/AlaDH	ADH (*Rhodococcus ruber*), ω-TA (*Vibrio fluvialis*), AlaDH (*Rhodococcus ruber*), pH 7, 30 °C, 24 h	50[a]	L-Ala (5 equiv.) NH_4Cl (4 equiv.)	>98 (47, ACP; 25, PEA)	[51a]

[a] 1-Phenylethanol

zymes also need to be matched, which can be challenging for the conversion of a non-natural substrate. Nevertheless, protein engineers have made great progress to achieve workable cascades of non-natural pathways able to convert non-natural substrates. To control such systems carefully, it has been argued that in vitro systems are particularly attractive as the required enzyme activities can be manipulated relatively easily by altering protein concentration rather than by adjusting expression levels inside the cell. Regardless of the cascade system, the interactions and compatibility of each of the enzymes and their associated reagents need to be considered. For instance, the introduction of high concentrations of co-substrates (e.g., L-Ala, NH_3) is likely to affect the activity and stability of the other enzymes.

5. Obtaining Thermodynamic Properties of Biochemical Reactions

It is important to obtain meaningful thermodynamic properties to find the suitable operating strategies for biocatalytic processes. For example, the equilibrium constant is a critical parameter to make rational design choices to improve the conversion of a thermodynamically limited reaction (see Section 4). Several ways to obtain such properties are discussed here.

5.1. Thermodynamics database

The TECRDB is a data collection of in vitro apparent equilibrium constants K' determined experimentally and enthalpy changes $\triangle H'^{0}_{r}$ measured calorimetrically that can be found in the scientific literature.[6] To date, there are 400 biocatalytic reactions available in this database with various measurement conditions (temperature, pH, ionic strength, buffer(s) and co-factor(s)). Goldberg and co-workers (1993–2007)[6] have critically evaluated the quality of these data, and some were highly scattered. Therefore, process feasibility and economic viability for the reaction of interest could not be assessed directly because of data uncertainties. To some extent, the data can be used to identify the favourability of a reversible reaction under the given conditions.

However, the Alberty database has 131 biochemical compounds with thermodynamic properties such as $\triangle H^{0}_{f}$ and $\triangle G'^{0}_{f}$.[3] These properties are basically derived from the TECRDB with correlation with the K' values of various reaction conditions found in the TECRDB. The data of the Alberty database can be further used to calculate the standard molar transformed properties (e.g., enthalpies of reaction $\triangle H'^{0}_{r}$, Gibbs energy formations $\triangle G'^{0}_{f}$) under specified conditions of temperature, pH, pMg and ionic strength using the Legendre transformation.[58] This approach allows the calculation of K' values that are not available in the TECRDB. Interestingly, the mathematical function of Legendre transforms can be calculated quantitatively by using Mathematica (a computational software program).[59] However, the starting point of the Alberty database for the calculations is the TECRDB, in which the reliability of the experimental results is unknown, which is a clear disadvantage of this approach.

5.2. Experimental measurements

Thermodynamic properties can also be obtained through experimental measurements. To get more reliable and accurate

experimental data, Alberty and co-workers have developed guidelines and recommendations for data measurement and data presentation for biochemical thermodynamics.[60] However, to the best of our knowledge, there is no standard protocol available to measure such properties. One of the available methods (which can be found in the scientific literature) is to allow reactants to reach equilibrium from both directions of the reaction as, for example, in work done by Tewari et al.[7a,61] and Gundersen et al.[41] A recent approach was developed by Tufvesson and co-workers for the aminotransferase reaction.[7b] This method is based on the measurements of the reaction rate using a variety of substrate and product concentrations to find the point at which the forward and reverse reactions converge to a zero net reaction [Eq. (4)]. However, this method requires a lot of data points to reach a point at which the relative quotient (Q) at zero net reaction is equal to 1 and thus Q is assumed to be K'.

$$Q = \frac{[C][D]}{[A][B]} \xrightarrow{t = \infty} K' \quad (4)$$

The equilibrium constant can also be calculated by kinetic parameters determined experimentally by the Haldane relationship.[27a,36,62] This equation represents the kinetic parameters of a reversible enzymatic reaction. Each kinetic parameter is independent of the others and is limited by the thermodynamic equilibrium constant of the overall reaction.[63]

5.3. Property prediction methods

Not all thermodynamic properties are available for the compounds of interest in the scientific literature or databases. It is also unrealistic to measure the required data if time constraints are a major problem. Thus computational estimation methods, such as the group contribution (GC) method and quantum chemical calculations, are at best an interesting alternative or at worst a useful complement to experimental methods.

The GC method is the most commonly used computational tool to estimate the required properties quickly without a large computational effort. The method was developed to use the molecular structures of compounds in which the structure of a single compound is decomposed into a set of smaller molecular sub-structures (different sub-molecules for different GC methods), and each model parameter is associated with one of the constituent molecular sub-structures (or so-called "groups") that combine to form the compound. Mavrovouniotis was among the first to use the GC method to estimate the standard Gibbs free energies of the formation of biochemical compounds in aqueous solutions.[64]

However, this method has limited applicability because of an over-simplification of the represented molecular sub-structures, in particular for molecules that involve sulfur, nitrogen, and halogens. To build on this work, Jankowski and co-workers introduced these sub-structures in their GC method along with various new interaction factors (conjugated double bonds, thioester bonds and vicinal chlorine atoms) to give better accuracy.[65] However, we have found that the Jankowski GC method does not consider the stereochemistry of chiral compounds. For instance, in an aminotransferase reaction, the structural similarity between reactants and products may lead to the same energy value, which limits the applicability of this method. Recently, Noor and co-workers developed a new and updated version of the GC method that uses an integrated framework from TECRDB and the work of Alberty et al. and Jankowski et al. known as pseudo-isomeric group contribution (PGC).[66] In this approach, a biochemical compound is divided into its pseudo-isomers (e.g., L-Ala has three protonation states ($C_3H_5O_2$–HN_3^+, $C_3H_5O_2$–NH_2 and $C_3H_4O_2^-$–NH_3^+) given by its pK_a), and each pseudo-isomer has its own group contribution energy, which gives better predictions.

We have compared the properties of the standard Gibbs free energy of reaction $\triangle G_r'^0$ given by each of the GC methods discussed here and the corresponding concentration-based equilibrium constant K' calculated using Equation (3). Interestingly, there are significant deviations between the equilibrium constants determined experimentally and the predicted values from the various GC methods (Table 4). Additionally, the excellent GC method that is used to predict the pure and uncharged chemical compounds[67] cannot be used in such cases. For example, it was unable to estimate $\triangle G_f'^0$ accurately for such syntheses, which gives an energetically favourable value compared to the other GC methods. This might be because of the pH-dependent charges of biochemical compounds as biocatalytic reactions usually operate in aqueous solutions.[69] The properties of compounds in aqueous solutions deviate from the properties of the pure components in which the thermodynamic activity of the pure solvent is equal to 1.

Table 4. Comparison of thermodynamic properties using the different thermodynamic methods for the synthesis of PEA (see Scheme 1).

Methods	$\triangle G_r'^0$ [kJ mol^{-1}]	K'
experimental measurement[7b]	+25.50 ± 1.28	4.03×10^{-5}
Haldane relationship by kinetic measurement[68]	+17.73	8.81×10^{-4}
Mavrovouniotis GC[4a]	+0.42 ± 20.92	0.847
Jankowski GC[65]	+16.78 ± 5.22	1.28×10^{-3}
PGC[66]	+7.3 ± 8.12	5.52×10^{-2}
GC for pure compounds[67]	−27.76 ± 31.1	7.65×10^{5}

GC = group contribution.

Another emerging tool to estimate thermodynamic properties is the use of quantum mechanics (QM). This method solves the quantum mechanical Schrödinger equation[70] to predict the properties of the molecules. For instance, the quantum chemistry screening model for realistic solvents (COSMO-RS) is a QM-based method to calculate the chemical potential of a compound either in pure fluids or mixtures.[71] From this method, the values of $\triangle G_f'^0$ in any type of solvent, can be de-

termined.[72] Like COSMO-RS, ab initio QM can be used to predict the values of thermodynamic properties (e.g., standard molar enthalpies $\triangle H^0_{rx}$, entropies $\triangle S^0_{rx}$, Gibbs free energies G^0_{rx}) using the Hartree–Fock model of geometry-optimised structures.[72b] In this method, the total energies of reactions can be calculated based on the optimal energy of the molecular structure of the components involved. Recently, our group proposed a simple and fast approach to predict the thermodynamic favourability of a transaminase reaction.[73] This method is developed based on ab initio calculations of the total energies of the molecules involved and validated with the experimental values obtained from a review of the scientific literature and in our laboratory.

Through the use of an equation of state, such as electrolyte perturbed-chain statistical fluid theory (ePC-SAFT),[74] it is possible to estimate the activity coefficients of the biochemical compounds in an aqueous solution.[5,75] Interestingly, a recent study by Hoffmann and co-workers found that the activity coefficient correlates strongly with pH for a thermodynamically favourable reaction.[5] Clearly, further work is required especially as the kinetics of the aminotransaminase reaction is known to be affected by the protonation state of the amine reactant (which is itself dependent upon the pK_a).

6. Future Perspectives

An understanding the fundamental thermodynamics (e.g., thermodynamic equations) and properties (e.g., equilibrium constant) is important in the field of biocatalysis. Likewise, more accurate and reliable experimental data as well as reliable and robust predictive tools are needed urgently as these data and tools are required to find the suitable and effective equilibria shifting strategies to achieve sufficiently high conversions in thermodynamically limited reactions. Subsequently, the estimation of process feasibility of biocatalytic processes can be performed.

In this article, several options to shift the equilibrium position, such as the use of excess co-substrate, in situ product removal, in situ co-product removal and smart substrates/co-substrates, have been discussed. Nevertheless, each of these methods has practical limitations. Such challenges can be improved (at least) partly by the application of enzymatic cascades (the coupling of an energetically unfavourable reaction with a more favourable one) to achieve a sufficiently high conversion of an otherwise thermodynamically limited reaction. In the long term, it is clear that further examples of multi-enzyme cascades will be forthcoming as one of a number of new tools to help the synthetic and process chemist.

Acknowledgements

The authors gratefully acknowledge the Malaysian Ministry of Education (MoE) and Universiti Malaysia Pahang to support this research work.

Keywords: biocatalysis · computational chemistry · enzyme catalysis · kinetics · thermodynamics

[1] A. Liese, K. Seelbach, C. Wandrey, *Industrial Biotransformations, 2nd ed.*, Wiley-VCH, Weinheim **2006**.
[2] S. Riva, W. Fessner, *Cascade Biocatalysis Integrating Stereoselective and Environmentally Friendly Reactions*, Wiley-VCH, Weinheim, **2014**.
[3] R. A. Alberty, *Thermodynamics of Biochemical Reactions*, Wiley, Hoboken, NJ, **2003**.
[4] a) M. L. Mavrovouniotis, *J. Biol. Chem.* **1991**, *266*, 14440 – 14445; b) J. Villadsen, J. Nielsen, G. Lidén, *Bioreaction Engineering Principles*, Springer US, Boston, MA, **2011**.
[5] P. Hoffmann, M. Voges, C. Held, G. Sadowski, *Biophys. Chem.* **2013**, *173 – 174*, 21 – 30.
[6] R. N. Goldberg, Y. B. Tewari, T. N. Bhat, *Bioinformatics* **2004**, *20*, 2874 – 2877.
[7] a) Y. B. Tewari, R. N. Goldberg, J. D. Rozzell, *J. Chem. Thermodyn.* **2000**, *32*, 1381 – 1398; b) P. Tufvesson, J. S. Jensen, W. Kroutil, J. M. Woodley, *Biotechnol. Bioeng.* **2012**, *109*, 2159 – 2162.
[8] P. Tufvesson, J. Lima-Ramos, J. S. Jensen, N. Al-Haque, W. Neto, J. M. Woodley, *Biotechnol. Bioeng.* **2011**, *108*, 1479 – 1493.
[9] P. J. Halling, *Biotechnol. Bioeng.* **1990**, *35*, 691 – 701.
[10] J. M. Woodley, in *Enzyme Catalysis in Organic Synthesis, 3rd ed.* (Eds.: K. Drauz, H. Gröger, O. May), Wiley-VCH, Weinheim, **2012**, pp. 217 – 247.
[11] W. Kroutil, H. Mang, K. Edegger, K. Faber, *Adv. Synth. Catal.* **2004**, *346*, 125 – 142.
[12] a) U. T. Bornscheuer, G. W. Huisman, R. J. Kazlauskas, S. Lutz, J. C. Moore, K. Robins, *Nature* **2012**, *485*, 185 – 194; b) A. S. Bommarius, J. K. Blum, M. J. Abrahamson, *Curr. Opin. Chem. Biol.* **2011**, *15*, 194 – 200.
[13] K. M. Polizzi, A. S. Bommarius, J. M. Broering, J. F. Chaparro-Riggers, *Curr. Opin. Chem. Biol.* **2007**, *11*, 220 – 225.
[14] J. M. Woodley, M. Bisschops, A. J. J. Straathof, M. Ottens, *J. Chem. Technol. Biotechnol.* **2008**, *83*, 121 – 123.
[15] A. Freeman, J. M. Woodley, M. D. Lilly, *Biotechnologia* **1993**, *11*, 1007 – 1012.
[16] G. J. Lye, J. M. Woodley, *Trends Biotechnol.* **1999**, *17*, 395 – 402.
[17] N. Richter, R. C. Simon, W. Kroutil, J. M. Ward, H. C. Hailes, *Chem. Commun.* **2014**, *50*, 6098 – 6100.
[18] R. C. Simon, N. Richter, E. Busto, W. Kroutil, *ACS Catal.* **2014**, *4*, 129 – 143.
[19] a) Y. Ni, D. Holtmann, F. Hollmann, *ChemCatChem* **2014**, *6*, 930 – 943; b) S. Kara, D. Spickermann, J. H. Schrittwieser, C. Leggewie, W. J. H. van Berkel, I. W. C. E. Arends, F. Hollmann, *Green Chem.* **2013**, *15*, 330 – 335.
[20] M. D. Truppo, J. D. Rozzell, N. J. Turner, *Org. Process Res. Dev.* **2010**, *14*, 234 – 237.
[21] A. Bornadel, R. Hatti-Kaul, F. Hollmann, S. Kara, *ChemCatChem* **2015**, *7*, 2442 – 2445.
[22] A. Bruggink, R. Schoevaart, T. Kieboom, *Org. Process Res. Dev.* **2003**, *7*, 622 – 640.
[23] a) M. L. Mavrovouniotis, *Chem. Eng. Sci.* **1996**, *51*, 1495 – 1507; b) M. L. Mavrovouniotis, G. Stephanopoulos, G. Stephanopoulos, *Comput. Chem. Eng.* **1992**, *16*, 605 – 619; c) C. S. Henry, L. J. Broadbelt, V. Hatzimanikatis, *Biophys. J.* **2007**, *92*, 1792 – 1805; d) C. Efe, A. J. J. Straathof, L. A. M. van der Wielen, *Biotechnol. Bioeng.* **2008**, *99*, 1392 – 1406.
[24] a) E. Noor, A. Bar-Even, A. Flamholz, E. Reznik, W. Liebermeister, R. Milo, *PLoS Comput. Biol.* **2014**, *10*, e1003483; b) P. D. N. Pissarra, J. Nielsen, *Biotechnol. Prog.* **1997**, *13*, 156 – 165.
[25] a) M. I. García García, A. S. Carvajal, F. G. Carmona, Á. S. Ferrer, *J. Agric. Food Chem.* **2012**, *60*, 7450 – 7456; b) V. Zimmermann, H.-G. Hennemann, T. Daussmann, U. Kragl, *Appl. Microbiol. Biotechnol.* **2007**, *76*, 597 – 605.
[26] T. Miyazaki, H. Sato, T. Sakakibara, Y. Kajihara, *J. Am. Chem. Soc.* **2000**, *122*, 5678 – 5694.
[27] a) F. Parmeggiani, S. L. Lovelock, N. J. Weise, S. T. Ahmed, N. J. Turner, *Angew. Chem.* **2015**, *127*, 4691 – 4694; b) S. L. Lovelock, R. C. Lloyd, N. J. Turner, *Angew. Chem. Int. Ed.* **2014**, *53*, 4652 – 4656; *Angew. Chem.* **2014**, *126*, 4740 – 4744.
[28] Y. B. Tewari, *Appl. Biochem. Biotechnol.* **1990**, *23*, 187 – 203.
[29] H. Raj, W. Szymański, J. de Villiers, H. J. Rozeboom, V. P. Veetil, C. R. Reis, M. de Villiers, F. J. Dekker, S. de Wildeman, W. J. Quax, A.-M. W. H. Thun-

nissen, B. L. Feringa, D. B. Janssen, G. J. Poelarends, *Nat. Chem.* **2012**, *4*, 478 – 484.
[30] M. J. Abrahamson, J. W. Wong, A. S. Bommarius, *Adv. Synth. Catal.* **2013**, *355*, 1780 – 1786.
[31] S. Leuchs, S. Na'amnieh, L. Greiner, *Green Chem.* **2013**, *15*, 167 – 176.
[32] a) S. Gargiulo, D. J. Opperman, U. Hanefeld, I. W. C. E. Arends, F. Hollmann, *Chem. Commun.* **2012**, *48*, 6630 – 6632; b) N. Oberleitner, C. Peters, F. Rudroff, U. T. Bornscheuer, M. D. Mihovilovic, *J. Biotechnol.* **2014**, *192*, 393 – 399.
[33] K. Goldberg, K. Edegger, W. Kroutil, A. Liese, *Biotechnol. Bioeng.* **2006**, *95*, 192 – 198.
[34] C. K. Savile, J. M. Janey, E. C. Mundorff, J. C. Moore, S. Tam, W. R. Jarvis, J. C. Colbeck, A. Krebber, F. J. Fleitz, J. Brands, P. N. Devine, G. W. Huisman, G. J. Hughes, *Science* **2010**, *329*, 305 – 309.
[35] Y. Zhang, *J. Labelled Compd. Radiopharm.* **2000**, *43*, 1087 – 1093.
[36] J. S. Shin, B. G. Kim, *Biotechnol. Bioeng.* **1998**, *60*, 534 – 540.
[37] a) E.-S. Park, J.-Y. Dong, J.-S. Shin, *Org. Biomol. Chem.* **2013**, *11*, 6929 – 6933; b) K. E. Cassimjee, C. Branneby, V. Abedi, A. Wells, P. Berglund, *Chem. Commun.* **2010**, *46*, 5569 – 5571.
[38] M. T. Gundersen, R. Abu, M. Schürmann, J. M. Woodley, *Tetrahedron: Asymmetry* **2015**, *26*, 567 – 570.
[39] A. P. Green, N. J. Turner, E. O'Reilly, *Angew. Chem.* **2014**, *126*, 10890 – 10893.
[40] B. Wang, H. Land, P. Berglund, *Chem. Commun.* **2013**, *49*, 161 – 163.
[41] E.-S. Park, M. S. Malik, J.-Y. Dong, J.-S. Shin, *ChemCatChem* **2013**, *5*, 1734 – 1738.
[42] P. Tufvesson, C. Bach, J. M. Woodley, *Biotechnol. Bioeng.* **2014**, *111*, 309 – 319.
[43] a) S. Leuchs, J. Lima-Ramos, L. Greiner, N. Al-Haque, P. Tufvesson, J. M. Woodley, *Org. Process Res. Dev.* **2013**, *17*, 1027 – 1035; b) G. Rehn, P. Adlercreutz, C. Grey, *J. Biotechnol.* **2014**, *179*, 50 – 55.
[44] M. Höhne, S. Kühl, K. Robins, U. T. Bornscheuer, *ChemBioChem* **2008**, *9*, 363 – 365.
[45] D. Koszelewski, I. Lavandera, D. Clay, G. M. Guebitz, D. Rozzell, W. Kroutil, *Angew. Chem.* **2008**, *120*, 9477 – 9480.
[46] M. D. Truppo, J. D. Rozzell, J. C. Moore, N. J. Turner, *Org. Biomol. Chem.* **2009**, *7*, 395 – 398.
[47] F. G. Mutti, C. S. Fuchs, D. Pressnitz, J. H. Sattler, W. Kroutil, *Adv. Synth. Catal.* **2011**, *353*, 3227 – 3233.
[48] H. Yun, B.-G. Kim, *Biosci. Biotechnol. Biochem.* **2008**, *72*, 3030 – 3033.
[49] a) K. Tauber, M. Fuchs, J. H. Sattler, J. Pitzer, D. Pressnitz, D. Koszelewski, K. Faber, J. Pfeffer, T. Haas, W. Kroutil, *Chem. Eur. J.* **2013**, *19*, 4030 – 4035; b) J. H. Sattler, M. Fuchs, K. Tauber, F. G. Mutti, K. Faber, J. Pfeffer, T. Haas, W. Kroutil, *Angew. Chem. Int. Ed.* **2012**, *51*, 9156 – 9159; *Angew. Chem.* **2012**, *124*, 9290 – 9293.
[50] N. G. Brink, J. K. Miettinen, J. Olsen, A. I. Virtanen, N. A. Sörensen, *Acta Chem. Scand.* **1953**, *7*, 1081 – 1089.
[51] U. Rusching, U. Müller, P. Willnow, T. Höpner, *Eur. J. Biochem.* **1976**, *70*, 325 – 330.
[52] M. Hall, C. Stueckler, B. Hauer, R. Stuermer, T. Friedrich, M. Breuer, W. Kroutil, K. Faber, *Eur. J. Org. Chem.* **2008**, 1511 – 1516.
[53] a) A. Weckbecker, H. Gröger, W. Hummel, in *Biosystems Engineering I Vol. 120: Advances in Biochemical Engineering/Biotechnology,* Springer, Heidelberg, **2010**, pp. 195 – 242; b) W. Hummel, H. Gröger, *J. Biotechnol.* **2014**, *191*, 22 – 31; c) S. Kara, J. H. Schrittwieser, F. Hollmann, M. B. Ansorge-Schumacher, *Appl. Microbiol. Biotechnol.* **2014**, *98*, 1517 – 1529; d) R. Wichmann, D. Vasic-Racki in *Technology Transfer in Biotechnology* (Ed.: U. Kragl), Springer, Heidelberg, **2005**, pp. 225 – 260.
[54] A. K. Holzer, K. Hiebler, F. G. Mutti, R. C. Simon, L. Lauterbach, O. Lenz, W. Kroutil, *Org. Lett.* **2015**, *17*, 2431 – 2433.
[55] A. Piérard, J. M. Wiame, *Biochim. Biophys. Acta* **1960**, *37*, 490 – 502.
[56] D. Koszelewski, I. Lavandera, D. Clay, D. Rozzell, W. Kroutil, *Adv. Synth. Catal.* **2008**, *350*, 2761 – 2766.
[57] F. G. Mutti, C. S. Fuchs, D. Pressnitz, N. G. Turrini, J. H. Sattler, A. Lerchner, A. Skerra, W. Kroutil, *Eur. J. Org. Chem.* **2012**, 1003 – 1007.
[58] R. N. Goldberg, Y. B. Tewari, T. N. Bhat, *J. Phys. Chem. Ref. Data* **2007**, *36*, 1347 – 1397.
[59] R. A. Alberty, *Biochemical Thermodynamics: Applications of Mathmatica*, Wiley, Hoboken, **2006**.
[60] R. A. Alberty, A. Cornish-Bowden, R. N. Goldberg, G. G. Hammes, K. Tipton, H. V. Westerhoff, *Biophys. Chem.* **2011**, *155*, 89 – 103.
[61] Y. B. Tewari, E. Gajewski, R. N. Goldberg, *J. Phys. Chem.* **1987**, *91*, 904 – 909.
[62] J.-H. Seo, D. Kyung, K. Joo, J. Lee, B.-G. Kim, *Biotechnol. Bioeng.* **2011**, *108*, 253 – 263.
[63] V. Leskovac, *Comprehensive Enzyme Kinetics*, Kluwer Academic Publishers, New York, **2004**.
[64] M. L. Mavrovouniotis, *Biotechnol. Bioeng.* **1990**, *36*, 1070 – 1082.
[65] M. D. Jankowski, C. S. Henry, L. J. Broadbelt, V. Hatzimanikatis, *Biophys. J.* **2008**, *95*, 1487 – 1499.
[66] a) J. Marrero, R. Gani, *Fluid Phase Equilib.* **2001**, *183 – 184*, 183 – 208; b) A. S. Hukkerikar, B. Sarup, A. Ten Kate, J. Abildskov, G. Sin, R. Gani, *Fluid Phase Equilib.* **2012**, *321*, 25 – 43.
[67] U. von Stockar, L. A. M. van der Wielen, *Adv. Biochem. Eng./Biotechnol.* **2003**, *80*, 1 – 17.
[68] W. J. Hehre, *A Guide to Molecular Mechanics and Quantum Chemical Calculations*, Wavefunction, Irvine, **2003**.
[69] T. M. Letcher, *Thermodynamics, Solubility, and Environmental Issues*, Elsevier, Amsterdam, **2007**.
[70] a) M. F. Eckstein, M. Peters, J. Lembrecht, A. C. Spiess, L. Greiner, *Adv. Synth. Catal.* **2006**, *348*, 1591 – 1596; b) M. F. Eckstein, J. Lembrecht, J. Schumacher, W. Eberhard, A. C. Spiess, M. Peters, C. Roosen, L. Greiner, W. Leitner, U. Kragl, *Adv. Synth. Catal.* **2006**, *348*, 1597 – 1604.
[71] J. S. Shin, B. G. Kim, *Biotechnol. Bioeng.* **1999**, *65*, 206 – 211.
[72] E. Noor, A. Bar-Even, A. Flamholz, Y. Lubling, D. Davidi, R. Milo, *Bioinformatics* **2012**, *28*, 2037 – 2044.
[73] R. J. Meier, M. T. Gundersen, J. M. Woodley, M. Schürmann, *ChemCatChem* **2015**, *7*, 2594 – 2597.
[74] L. F. Cameretti, G. Sadowski, J. M. Mollerup, *Ind. Eng. Chem. Res.* **2005**, *44*, 3355 – 3362.
[75] C. Held, L. F. Cameretti, G. Sadowski, *Ind. Eng. Chem. Res.* **2011**, *50*, 131 – 141.

Received: July 29, 2015
Published online on September 11, 2015

Tetrahedron: *Asymmetry* 26 (2015) 567–570

Contents lists available at ScienceDirect

Tetrahedron: *Asymmetry*

journal homepage: www.elsevier.com/locate/tetasy

Amine donor and acceptor influence on the thermodynamics of ω-transaminase reactions

Maria T. Gundersen [a], Rohana Abu [a], Martin Schürmann [b], John M. Woodley [a,*]

[a] Department of Chemical and Biochemical Engineering, Technical University of Denmark, 2800 Lyngby, Denmark
[b] DSM Chemical Technology R&D B.V./DSM Innovative Synthesis, Urmonderbaan 22, NL-6167RD Geleen, The Netherlands

ARTICLE INFO

Article history:
Received 2 March 2015
Accepted 10 April 2015
Available online 23 April 2015

ABSTRACT

In recent years biocatalytic transamination using ω-transaminase has become established as one of the most interesting routes to synthesize chiral amines with a high enantiomeric purity, especially in the pharmaceutical sector where the demand for such compounds is high. Nevertheless, one limitation for successful implementation and scale-up is that the thermodynamics of such conversions are frequently found unfavourable. Herein we report experimental measurements of apparent equilibrium constants for several industrially relevant transamination reactions in a systematic manner to better understand the effect of amine acceptor and donor choice. For example, we have found that *ortho*-substitution of acetophenone like molecules, had a significant impact on the thermodynamic equilibrium. Likewise, the effect of cyclic amine acceptors was evaluated and compared to similar non-cyclic structures. It was found that an aliphatic six membered ring was favourable and a conjugated bicyclic five membered ring structure, unfavourable. Finally, we evaluated and compared the use of five different donor molecules, and calculated their ΔG^{app} values. This is particularly important in the further implementation of such reactions because it may be used to help select suitable donor/acceptor combinations. The results presented here give guidance, with respect to thermodynamics, in order to further extend the application of biocatalytic transamination.

1. Introduction

Biocatalysis, where one or more synthetic chemical reactions are catalysed by enzymes, has over recent decades proved to be a particularly powerful complement to conventional approaches for the synthesis of chiral molecules, as illustrated by numerous commercial processes.[1] In particular the synthetic application of biocatalysis capitalizes upon the excellent stereo- and regioselectivity and mild reaction conditions of enzymes,[2,3] implying a potentially attractive synthesis of valuable chiral products.

One particularly interesting group of chiral products is optically active amines, which are amongst the most important groups of chiral molecules from a commercial perspective, with many interesting pharmaceutical applications.[3,4] There are several biocatalytic methods to produce optically active amines and one of the most established methods uses the enzyme ω-transaminase (ω-TA) (EC.2.6.1.18).[5] The enzyme catalyses the transfer of an amine group from an amine donor to an amine acceptor, yielding an optically active amine target product and a non-chiral carbonyl co-product (see Scheme 1).

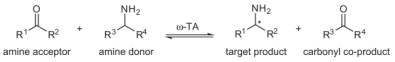

Scheme 1. Generalized scheme of biocatalytic transamination.

Despite its applicability, the utilization of this enzyme is frequently hampered by low reaction yields, often stemming from the unfavourable thermodynamics of the respective couples of substrates (amine acceptor and amine donor) and products (target product and carbonyl co-product). Additionally, low yields can be the result of biocatalyst related issues, such as enzyme inhibition or instability of the enzyme. Such limitations can be overcome by enzyme modification through protein engineering.[6] However, the thermodynamics of the reaction, which are very often found to be the primary limitation, is independent of the enzyme used to catalyse the reaction and therefore alternative solutions need to be sought.[7]

* Corresponding author. Fax: +45 4525 2885.
E-mail address: jw@kt.dtu.dk (J.M. Woodley).

http://dx.doi.org/10.1016/j.tetasy.2015.04.006
0957-4166/

The thermodynamic yield of a reaction is influenced by the structural and energetic differences between the couples of amine donor/amine acceptor and the target product/carbonyl co-product, respectively. Since the structure of the target product is determined by the structure of the acceptor molecule, chemical flexibility in the reaction is provided by the choice of amine donor alone. Although in principle this means that a plethora of possible compounds could be used as the donor, in practice, to date only a few selected compounds have been used, or even tested, in large part due to limited availability and poor enzyme specificity. With this in mind, we reasoned that it would be useful to evaluate a wider range of donors and in particular establish their effect on the reaction thermodynamic yield. At the same time it is clear that the influence of donor selection on the thermodynamic equilibrium is dependent upon the given acceptor molecule to be converted. Hence we have also sought to understand the effect of using different acceptors on the thermodynamics, with a given donor molecule.

Although it is clear that overcoming thermodynamic constraints is paramount for the successful implementation of ω-transaminase-based processes,[8,9] remarkably little information about reaction thermodynamics has been reported in the scientific literature, with a few exceptions.[10,11] Herein, we report experimentally determined concentration-based equilibrium constants (K_{eq}^{app}) for a variety of ω-transaminase catalysed reactions. In each reaction, we have chosen amine acceptor molecules in such a way as to explore the influence of both substitution and the effect of ring strain. Likewise various donors have been selected, for transamination with a given acceptor, to also understand the effect of different donors on thermodynamic equilibrium. In Table 1 the various donors and target products of all the reactions used herein are listed. The corresponding amine acceptors can be derived from these.

In order to simplify the interpretation of the results throughout, we have kept either the donor, or the acceptor, molecule fixed and changed the other reactant. Hence we have compared variable half reactions. The alteration to a given molecule occurs on both the reactant and product side. Hence, we are comparing a certain structural change and the effect that has on both the reactant and product side. For example, when comparing the reaction of **1b**/**2b** with **1c**/**2c**, substituting the fluorine for an alcohol has an overall negative effect on the thermodynamic equilibrium of that of half reaction, but does not indicate that **1b** is more stable than **1c** in isolation.

Table 1
Structures of amine donors

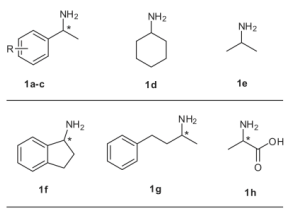

(**1a**) R = H, (**1b**) *o*-F, (**1c**) *o*-OH, (**1d**) cyclohexylamine, (**1e**) isopropylamine, (**1f**) aminoindane, (**1g**) 3-amino-1-phenylbutane, (**1h**) alanine. The corresponding amine acceptors are named with the designation 2 followed by the same letter.

2. Results and discussion

2.1. Influence of amine acceptor

In initial experiments we sought to determine the effects of two types of acceptor modification on the thermodynamic equilibrium. In the first type we examined the effect of substituted aryl compounds similar to those of acetophenone, by *ortho*-substitution to investigate the effect of the substituent group. In the second type, we explored the effect of ring strain between cyclohexane and indane, compared to similar compounds in the absence of the ring or just one ring, respectively.

2.1.1. Substitution in the acceptor molecule

Several acceptors **2a**, **2b**, **2c** (see Table 1) were chosen to test in ω-transaminase catalysed reactions in order to understand the effects of substitution at the *ortho*-position of the amine acceptor on the measured apparent equilibrium constant.

The reaction equilibrium at completion was measured using both **1a** and **1e**, as the amine donor, and variously substituted acetophenone molecules as the acceptor.

We found the K_{eq}^{app} of **2a** with **1a** and **1e** to be 1 and 0.006. In comparison the *ortho*-substituted compounds **2b** and **2c** gave K_{eq}^{app} of **2b**: 1.8 and 0.1 and **2c**: 0.3 and 0.01 with the same donors **1a** and **1e**, respectively. The results indicate that fluorine substitution gives a higher apparent equilibrium constant than hydroxyl substitution in the *ortho*-position, and therefore is more favourable for product formation. We postulate there is a higher fraction of one of the stable un-reactive tautomers of the molecule, resulting in a lower conversion. Previous work supports that a significant fraction of such tautomers may exist in solution.[5]

Talwar et al.[12] have used a cyclometallated iridium catalyst to carry out the transfer reaction reporting 14 reactions with substituted acetophenones, where all of the substituted reactants have either the same or higher isolated yields than acetophenone itself. No strong electron donating substituents were used. Likewise, Paul et al.[13] report similar trends. Finally Tufvesson et al. have shown that substitution may significantly impact thermodynamics of acetophenone-like compounds.[14] These published studies are qualitative, support the results presented here.

2.1.2. Ring strain in the amine acceptor

A further aspect of interest in the acceptor molecules is the effect of ring strain. Here the effect on the thermodynamic equilibrium might in some cases be easier to predict, since there is an observed difference in the bond angles of the ketone of the amine acceptor and the amine in the amine donor; approximately 120° to 109°, respectively. In order to test this, we measured the apparent equilibrium constant using **2d** and **2f** where we predict conversion to **1d** to be favourable and **1f** to be unfavourable in comparison to the respective non-cyclic structure, **2e**, and monocyclic structure, **2a**. In all cases, **1a** was used as the amino donor.

In the reaction between **2d**/**1d**, compared to **1e**/**2e**, the ring has a positive effect on the measured apparent equilibrium constant: in this case the ring of the target product is less strained. We suggest that this is caused by the formation of the cyclohexane with six sp^3 carbons, the most stable saturated hydrocarbon conformation, compared to the starting material with five sp^3 carbons and one sp^2 carbon.

Likewise, **2f** can be compared with **2a**, with an additional five-membered ring. Since the angle strain of the sp^2 is stipulated to be more favourable than the sp^3 carbon of the product, this would result in increased strain. However the amino donor in the reaction pair **2f**/**1f** would be less flexible and therefore more susceptible to steric hindrance. We therefore considered that these two acceptors

would give similar apparent equilibrium values. Interestingly, the results (Table 2) indicate that **2f** gives an apparent equilibrium constant of merely one hundredth of the value for **2a**. These results are also partially supported by the low observed conversion yields in another study by Fesko et al.[15]

Table 2
Effect on ring strain, using five- and six- membered rings, all using **1a** as the donor

Acceptor	K_{eq}^{app}
2d	213
2e[11]	30
2f	0.01
2a	1

2.2. Influence of amine donor

Finally, we have compared the data from the experiments here with some other data previously published to investigate the effect of donor choice. As mentioned, the ω-transaminase reaction is used to produce a chiral amine, thus the structure of the amino acceptor is determined solely by the structure of the desired product. However, the amine donor may be freely selected and this will clearly influence the apparent thermodynamic constant. Here we have compared the measured apparent equilibrium constant of five different donors (using acetophenone as the acceptor molecule). Using these values, the ΔG^{app} of each reaction couple was calculated. This is particularly interesting, because by comparing the half reaction between each of these donor choices, it is possible to use ΔG^{app} to estimate the impact of changing the donor in any given reaction, where the ΔG^{app} or K_{eq}^{app} is known for either one of the donors listed in the table. The results are presented in Table 3.

Table 3
K_{eq}^{app} and ΔG^{app} for the acceptor **2a** coupled to the donors; **1a**, **1d**, **1e**, **1f**, **1g** or **1h**

Donor	K_{eq}^{app}	ΔG^{app} (kJ/mol)
1a	1	0
1d	$6.0 * 10^{-3}$	13
1e[11]	$3.3 * 10^{-2}$	8.6
1g	0.18	4.3
1h[11]	$4.0 * 10^{-5}$	26

Out of the five compounds selected for testing, we found that the K_{eq}^{app} of the selected reaction varies by five orders of magnitude from the most beneficial donor, **1a** to the worst case alanine **1h**. Another reaction with alanine using **2f** as the acceptor likewise gave a very poor equilibrium constant of $<10^{-4}$. These data clearly indicate the strong influence of donor selection. Interestingly, two of the donors are achiral **2d** and **2e**, offering an advantage economically (higher concentrations and less expensive starting material) by avoiding an enantiomerically pure starting material.

3. Conclusion

The data reported here show interesting patterns for selection of the amine acceptor and donor couples. The data presented in Table 3 are potentially the basis for at least initial calculations of reaction feasibility. Nevertheless the effects of substitution and ring strain on the acceptor molecules reported here are not supported by all published data. For example, for ring strain, the opposite trend was found by Talwar et al.[12] This indicates not only the difficulty of making effective measurements but also the need to report a wider dataset.

The use of data such as those measured in the experiments reported here are to enable an estimate of process feasibility, and to establish if supplementary methods are required to achieve sufficiently high reaction yields. For example, an excess of the amine donor can be used (provided it is not inhibitory to the enzyme or difficult to separate downstream). Other possibilities include in situ product removal or in situ co-product removal. Nevertheless, all such schemes have operational limitations. For example, using an in situ co-product removal approach to reach high reaction yields by 'pulling' reactions towards the target product through removal of the carbonyl co-product, by evaporation under reduced pressure[2] or extraction into a second, organic solvent phase,[9] is limited to those cases in which the carbonyl co-product is significantly more volatile or hydrophobic, respectively, than the amine acceptor. Indeed, high selectivity in in situ product removal or in situ co-product removal approaches is a prerequisite for effectively shifting equilibrium. For this reason, careful choice of the amine donor and acceptor pair, considering not just kinetics, but also thermodynamics are important for further applications of the ω-transaminase reaction.

4. Experimental

4.1. Materials

All chemicals were of reagent grade or higher and purchased from a chemical vendor and used without further alteration. Enzymes ATA-42/ATA-81, were provided from c-LEcta GmbH (Leipzig, Germany), ATA-42 was used for reactions 4 and 8 all other reactions were carried out with ATA-81.

4.2. Reactions

All reactions were carried out in duplicate with a minimum of 3 different donor/acceptor concentrations between 2 mM and 10 mM, thus a minimum of 6 reactions for each reaction. All were carried out at a 0.4 mL scale in 1.5 mL Eppendorf tube with: 1 mg/mL lyophilized ω-transaminase, 1 mM pyridoxal-5′-phosphate, 2 to 10 mM substrate, 5% (v/v) DMSO in 0.1 M Tris–HCl buffer, pH 7. Equilibrium was reached by 48 h incubation in a thermoshaker (HCL, Bovenden, Germany) at 30 °C with constant agitation (400 rpm). Each reaction was carried out in duplicate, with duplicate blank samples where enzyme activity was quenched by NaOH before substrate addition, see analytical analysis below.

4.3. Analytical

After 48 h, the reaction was quenched by adding the aqueous NaOH (5 M, 100 μL). 0.02 mL eternal standard solution (150 mM 4-bromo-acetophenone in DMSO) was added. An extraction was carried out with 400 μL ethyl acetate. After separation the sample was dried in magnesium sulfate. Furthermore 0.15 mL of the ethyl acetate was transferred to a GC vial and derivatized by the addition of 15 μL triethylamine and 10 μL acetic anhydride. Conversion was measured by Gas chromatography on a Clarus 500 (Perkin–Elmer) with a 25 m * 0.25 mm CP-Chirasil-Dex CB column (Agilent J&W GC scientific). 2 μL sample was injected, with a thermal gradient from 120 to 200 °C for 13 min, 1.4 mL/min He was used as a carrier gas. FID detection was carried out at 250 °C.

4.4. Experimental set up for reactions: 1f/2f and 1 h/2 h

4.4.1. Materials

All chemicals were of reagent grade or higher and purchased from a chemical vendor and used without alteration. The ω-

transaminases from *Vibrio fluvialis* and *Aspergillus terreus* as described and produced by Meadows et al.[16] and Fesko et al.[17] were used as cell-free *Escherichia coli* extracts.

4.4.2. Reactions

All reactions were carried out on a 5.0 mL scale in 10 mL screw-capped glass vials containing 5 mM of the respective acceptor substrate and amine donor in 50 mM potassium phosphate buffer pH 7.5 containing 0.1 mM pyridoxal-5′-phosphate. As biocatalyst 1.25 mL cell-free extract containing the respective transaminase was added resulting in final total protein concentrations of approximately 10 mg/mL. The reactions were incubated on an IKA KS130 basic shaker at 28 °C with constant agitation (480 rpm). The reactions were followed in time until the equilibrium was reached by taking 250 μL samples, diluting and stopping by addition into 750 μL of a 1:1 mixture of acetonitrile and 0.5% (v/v) formic acid.

4.4.3. Analytical

All samples were analysed by HPLC on a Hypersil BDS C18 column (250 × 4.0 mm, I.D. 5 μm) and eluted with a gradient of Eluent A (0.1% formic acid in water) and Eluent B (0.1% formic acid in acetonitrile) from 97.5% A/2.5% B to 30% A/70% B in 10 min with a flow of 1.0 mL/min at 40 °C and an injection volume of 5 μL. Substrates and products were detected by UV at 256 nm and 210 nm and quantified based external standards of the respective substrate and product compounds.

Acknowledgements

The support of AMBIOCAS financed through the European Union 7th Framework Programme (Grant agreement no: 245144) is gratefully acknowledged. The authors would also like to thank Mette Joan Nielsen (DTU), Kasper Israelsen (DTU) and Natascha Smeets (DSM) for expert experimental work and Robert Meier (DSM) for fruitful discussions and support.

References

1. Science of Synthesis. In *Biocatalysis in Organic Synthesis*, Faber, K.; Fessner, W.-D.; Turner, N. J., Eds.; Thieme, Stuttgart, Germany, 2014; Vol. 3.
2. Ma, S. K.; Gruber, J.; Davis, C.; Newman, L.; Gray, D.; Wang, A.; Grate, J.; Huisman, G. W.; Sheldon, R. A. *Green Chem.* **2010**, *12*, 81–86.
3. Savile, C. K.; Janey, J. M.; Mundorff, E. C.; Moore, J. C.; Tam, S.; Jarvis, W. R.; Colbeck, J. C.; Krebber, A.; Fleitz, F. J.; Brands, J.; Devine, P. N.; Huisman, G. W.; Hughes, G. J. *Science* **2010**, *329*, 305–309.
4. Koszelewski, D.; Tauber, K.; Faber, K.; Kroutil, W. *Trends Biotechnol.* **2010**, *28*, 324–332.
5. Kohls, H.; Steffen-Munsberg, F.; Höhne, M. *Curr. Opin. Chem. Biol.* **2014**, *19*, 180–192.
6. Bornscheuer, U. T.; Huisman, G. W.; Kazlauskas, R. J.; Lutz, S.; Moore, J. C.; Robins, K. *Nature* **2012**, *485*, 185–194.
7. Woodley, J. M. *Curr. Opin. Chem. Biol.* **2013**, *17*, 310–316.
8. Tufvesson, P.; Lima-Ramos, J.; Nordblad, M.; Woodley, J. M. *Org. Process Res. Dev.* **2011**, *15*, 266–274.
9. Lima-Ramos, J.; Neto, W.; Woodley, J. M. *Top. Catal.* **2013**, *57*, 301–320.
10. Tufvesson, P.; Bach, C.; Woodley, J. M. *Biotechnol. Bioeng.* **2013**.
11. Tufvesson, P.; Jensen, J. S.; Kroutil, W.; Woodley, J. M. *Biotechnol. Bioeng.* **2012**, *109*, 2159–2162.
12. Talwar, D.; Salguero, N. P.; Robertson, C. M.; Xiao, J. *Chem. Eur. J.* **2014**, *20*, 245–252.
13. Paul, C.; Rodríguez-Mata, M.; Busto, E.; Lavandera, I.; Gotor-Fernández, V.; Gotor, V.; García-Cerrada, S.; Mendiola, J.; de Frutos, O.; Collado, I. *Org. Process Res. Dev.* **2013**, *18*, 788–792.
14. Tufvesson, P.; Bach, C.; Woodley, J. M. *Biotechnol. Bioeng.* **2014**, *111*, 309–319.
15. Fesko, K.; Steiner, K.; Breinbauer, R.; Schwab, H.; Schürmann, M.; Strohmeier, G. a. *J. Mol. Catal. B: Enzym.* **2013**, *96*, 103–110.
16. Meadows, R. E.; Mulholland, K. R.; Schurmann, M.; Golden, M.; Kierkels, H.; Meulenbroeks, E.; Mink, D.; May, O.; Squire, C.; Straatman, H.; Wells, A. S. *Org. Process Res. Dev.* **2013**, *17*, 117–122.
17. Fesko, K.; Steiner, K.; Breinbauer, R.; Schwab, H.; Schürmann, M.; Strohmeier, G. A. *J. Mol. Catal. B: Enzym.* **2013**, *96*, 103–110.

Krist V. Gernaey, Jakob K. Huusom and Rafiqul Gani (Eds.), 12th International Symposium on Process Systems Engineering and 25th European Symposium on Computer Aided Process Engineering.
31 May – 4 June 2015, Copenhagen, Denmark

Thermodynamic Calculations for Systems Biocatalysis

Rohana Abu, Maria T. Gundersen, John M. Woodley*

Department of Chemical and Biochemical Engineering, Technical University of Denmark, Søltofts Plads Building 229, Kgs. Lyngby, Denmark.
**jw@kt.dtu.dk*

Abstract

'Systems Biocatalysis' is a term describing multi-enzyme processes *in vitro* for the synthesis of chemical products. Unlike *in-vivo* systems, such an artificial metabolism can be controlled in a highly efficient way in order to achieve a sufficiently favourable conversion for a given target product on the basis of kinetics. However, many of the most interesting non-natural chemical reactions which could potentially be catalysed by enzymes, are thermodynamically unfavourable and are thus limited by the equilibrium position of the reaction. A good example is the enzyme ω-transaminase, which catalyses the transamination of a pro-chiral ketone into a chiral amine (interesting in many pharmaceutical applications). Here, the products are often less energetically stable than the reactants, meaning that the reaction may be thermodynamically unfavourable. As in nature, such thermodynamically-challenged reactions can be altered by coupling with other reactions. For instance, in the case of ω-transaminase, such a coupling could be with alanine dehydrogenase. Herein, the aim of this work is to identify thermodynamic bottlenecks within a multi-enzyme process, using group contribution method to calculate the Gibbs free energy change, $\Delta G_r^{o\prime}$, of the overall cascade. The findings show that unfavourable reactions in the cascade can be improved by coupling to a favourable reaction giving more energetically stable products.

Keywords: Systems Biocatalysis, multi-enzyme, thermodynamics, group contribution

1. Introduction

Servi and co-workers (2013) recently introduced the term 'Systems Biocatalysis' to describe the science associated with multi-enzyme cascades via the use of isolated enzymes *in-vitro* for the synthesis of chemical products. To date, several promising multi-enzyme processes have been reported in the scientific literature and no doubt many more examples will be forthcoming in the future as such systems are established as a useful approach for industrial synthesis (Riva, 2014). In an example of a multi-enzyme processes (Figure 1), the primary enzyme (E1) is the main enzyme that determines the synthesis of the target product (P1) while a second enzyme (E2) is added to the system to assist the main reaction. This secondary enzyme acts in such a way as to aid the primary enzyme to achieve the desired product in a high enough yield. In this representative example, the second enzyme requires a cofactor (X) which is crucial for the functionality of the secondary enzyme. Addition of a cofactor is frequently expensive and it must therefore be re-generated *in-situ*, and thus a third enzyme (E3) is introduced to the system. In this way, the multi-enzyme system is built.

The production of methylbenzylamine from acetophenone using ω-transaminase (EC.2.6.1.18) as a catalyst provides a good example of such a scheme. In this chiral amine synthesis, the equilibrium constant of $4.03*10^{-5}$ has been determined

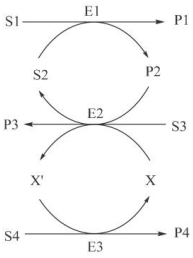

Figure 1: Representative scheme of multi-enzyme processes. E: enzyme, S: substrate, P: product, and X: cofactors.

determined experimentally where alanine was employed as the amine donor (Tufvesson et al., 2012). The value shows that the reaction alone is thermodynamically unfavourable and thus the maximum achievable conversion is only 0.63 %. Interestingly, a sufficiently favorable conversion of methylbenzylamine can be achieved, when transaminase is coupled with secondary enzymes. Using alanine as the same amine donor, the transamination achieved >70 % conversion (Truppo et al. 2009). The secondary enzymes were lactate dehydrogenase, LDH (EC 1.1.1.27) and glucose dehydrogenase, GDH (E.C.1.1.1.1). The LDH was added to remove the co-product pyruvate that hinders the formation of the target amine while GDH was used to re-generate cofactor *in situ* required by the LDH. An alternative option could be to use transaminase coupled with alanine dehydrogenase, AlaDH (EC.1.4.1.1), which was used to achieve 96 % conversion. In this system, alanine was re-generated *in situ* by recycling the pyruvate. As well as LDH, the AlaDH requires cofactors, in which the third enzyme (GDH) was also added to complete the multi-enzyme system. Even though the study claimed that the role of LDH and AlaDH was to drive the reaction to completion, there was no thermodynamic analysis to support this. Likewise, for many other multi-enzyme processes reported in the scientific literature (Simon et al., 2014), there is remarkably little thermodynamic background. Herein, this work is aimed to identify thermodynamic bottleneck in multi-enzyme processes, using the group contribution method to calculate the Gibbs free energy change $\Delta G_r^{o\prime}$. Such thermodynamic evaluation is fundamental to successfully apply systems biocatalysis.

2. Thermodynamic analysis

The thermodynamic favourability of biocatalytic reactions can be quantified by the standard Gibbs free energy change of reaction, $\Delta G_r^{o\prime}$, using Eq. 1. The data on thermodynamic properties, the standard Gibbs free energy of formation, $\Delta G_f^{o\prime}$, of reactants and products, are thus required. These data can be obtained from group contribution (GC) methods developed by Jankowski and co-workers (2008). To date, the Jankowski-GC method is established tools for estimating such properties of

biochemical molecule. It has a large training set that allows for accurate estimation of $\Delta G_f^{o\prime}$.

$$\Delta G_r^{o\prime} = \sum_j^p n_j \, \Delta G_{f,j}^{o\prime} - \sum_i^r n_i \, \Delta G_{f,i}^{o\prime} \tag{1}$$

Usually, $G^{o\prime}$ is used to denote the standard Gibbs free energy of biochemical compounds (pH 7, a temperature of 298 K, and zero ionic strength), while G^o refers to the standard state for chemical compounds. However, in practice, biocatalytic reactions are not operated at the standard state conditions. Therefore, the Eq. 2 is used to calculate the Gibbs free energy change of reaction under different conditions, which is termed as ΔG. R is the gas constant, T is the temperature, c is the concentration of component i in reactant r and component j in product p which obtained from experiments, and n is the stoichiometric coefficient of component i and j.

$$\Delta G = \Delta G_r^{o\prime} + RT \ln \frac{\prod_j^p c_j^{n_j}}{\prod_i^r c_i^{n_i}} \tag{2}$$

The sign of ΔG shows the favourability of a reaction; a minus ΔG means that the reaction will proceed towards the products, whereas, a positive ΔG means the opposite direction. When the reaction is at equilibrium, the value of ΔG is equal to zero, which in turn gives the apparent (concentration-based) equilibrium constant, K' of a reaction can be determined (Eq. 3).

$$\Delta G_r^{o\prime} = -RT \ln K' \tag{3}$$

3. Case study

In this paper, we have chosen one interesting case study from the scientific literature in order to demonstrate a suitable thermodynamic analysis for a multi-enzyme processes (Tauber et al., 2013). In this case, the artificial multi-enzyme process is constructed for the transformation of 4-phenyl-2-butanol (**a**) to a chiral amine, 4-phenyl-2-butanamine (**b**). Figure 2 illustrates the reaction scheme of the ADH/ωTA/AlaDH coupled system to produce the chiral amine. The first step is on oxidation step catalysed by an alcohol dehydrogenase (ADH), consuming cofactor (NAD+) leading to the formation of an intermediate product, 4-phenyl-2-butanone (**b**). Secondly, ω-transaminase (ωTA) catalyses the intermediate product and alanine (amine donor) to produce the desired product. In this system, alanine and the cofactor NAD+ are re-generated *in situ* through alanine dehydrogenase (ADH). The system reportedly gave 25 % conversion of the ketone (**b**) and 47 % conversion of the amine (**c**).

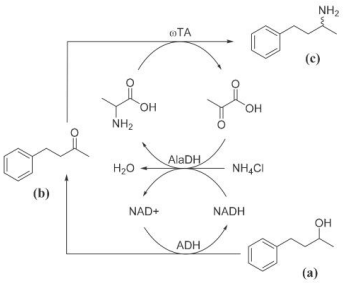

Figure 2: ADH/ωTA/AlaDH coupled system. Reaction conditions: NADH (1 mM), alanine (250 mM), NH_4Cl (200 mM) and 4-phenyl-2-butanol, (**a**) (50 mM). ADH: alcohol dehydrogenase (EC1.1.1.1), ωTA: ω-transaminase (EC2.6.1.18), and AlaDH: alanine dehydrogenase (EC1.4.1.1).

4. Results and discussion

In principle, a favourable reaction proceeds spontaneously towards the minimum energy level state (equilibrium). In the case of ADH/ωTA/AlaDH coupled system, the thermodynamic feasibility was determined and used to make the energy profile as shown in Figure 3. This diagram describes the free energy content between reactants and products (vertical axis) through the progress of reaction steps (horizontal axis) from starting material (**a**) to the final product (**c**).

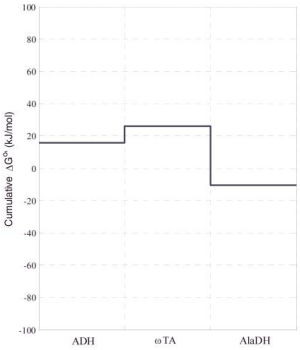

Figure 3: The energy profile represents the cumulative energy $\Delta G_r^{o'}$ at the standard state conditions for producing 4-phenyl-2-butanamine through pathways of ADH, ωTA and AlaDH. ADH: alcohol dehydrogenase, ωTA: ω-transaminase and AlaDH: alanine dehydrogenase.

In the standard state conditions, it was found that ωTA-catalyzed reaction is the thermodynamic bottleneck within the ADH/ωTA/AlaDH coupled system which is shown by the uphill reaction in the cumulative energy of $\Delta G_r^{o\prime}$. However, a positive $\Delta G_r^{o\prime}$ does not necessarily indicate a bottleneck within the system. In the ADH and ωTA reactions, both have the $\Delta G_r^{o\prime}$ constraint of positive values of 15.73 kJ/mol and 10.29 kJ/mol respectively. The values signify that the reactions are unfavourable since both products (**b** and **c**) are energetically unstable which contribute to the positive values of $\Delta G_r^{o\prime}$. The overall $\Delta G_r^{o\prime}$ for the ADH/ωTA/AlaDH coupled system is thermodynamically downhill where AlaDH is identified as a thermodynamic driving force to push the equilibrium system to completion and ending with a negative $\Delta G_r^{o\prime}$ value (-10.33 kJ/mol). At equilibrium, the apparent equilibrium constant, K' of ADH/ωTA/AlaDH system is 60.4, calculated using Eq. 3. The GC-method can be useful to determine the feasibility of the cascades when experimental thermodynamic data is not available. To date, very few data on equilibrium constants are available from experiments, in particular for multi-enzyme cascades.

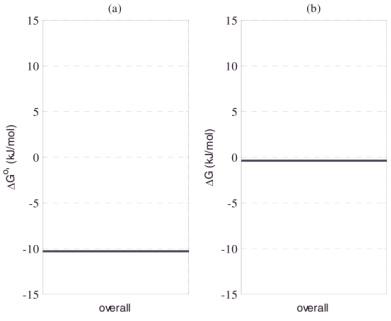

Figure 4: The free energy difference in ADH/ωTA/AlaDH coupled system. (a) $\Delta G_r^{o\prime}$ (Reaction conditions: pH 7, 298 K) and (b) ΔG (Reaction conditions: pH 7.5, 303 K, $C_{10}H_{14}O$ (37.5 mM), $C_{10}H_{15}N$ (5.9 mM), NH_4Cl (194.1 mM), and water (55.6 M)).

A system is rarely operated at standard state conditions and thus it is interesting to find the thermodynamic feasibility of ADH/ωTA/AlaDH system using the actual ΔG which calculated as a function of concentration of products and reactants (Eq. 4). From the calculation, the ΔG of the system has changed from -10.33 kJ/mol to -0.75 kJ/mol. Here, the concentration of pure water is 55.6 M and the regeneration system of NAD+ and alanine is assumed run efficiently using AlaDH. The results show that the system is thermodynamically feasible and the value of ΔG describes how far the free energy has changed from the standard state conditions. In most cases, biocatalytic reactions are controlled at pH >7. However, in this ΔG calculation, the pH value is not taken into account. Recently, Hoffmann and coworkers (2013) has found that the activity coefficient strongly correlates with pH in which the $\Delta G_r^{o\prime}$ changed accordingly. Further study on activity effect is currently carried out as more data is needed to confirm such an effect.

$$\Delta G = \Delta G_r^{o\prime} + RT \ln \frac{[C_{10}H_{15}N][H_2O]}{[NH_4^+][C_{10}H_{14}O]} \quad (4)$$

5. Conclusions

In conclusion, multi-enzyme system can be a useful approach for biocatalytic processes, but it requires fundamental knowledge of the thermodynamics. The thermodynamic bottlenecks can be identified through the energy profile of reaction steps in the overall reactions. It is, however, it is necessary to obtain values for the thermodynamic properties of Gibbs free energy of formation of a compound to draw the diagram. For an unfavourable reaction such as transaminase, it can be improved by coupling with thermodynamically favourable reactions to drive the system to completion. Such multi-enzyme processes if successfully designed can yield high conversions of unfavourable transformation. Likewise, high conversion of the multi-enzyme processes is also attractive in the downstream processes since fewer unit operations are required to remove intermediates/by-products within the reaction step. Nevertheless, more work should be done to evaluate the multi-enzyme systems in term of economics, determine whether designed cascades can reduce the downstream cost.

References

P. Hoffmann, M. Voges, C. Held, and G. Sadowski, 2013, The role of activity coefficients in bioreaction equilibria: thermodynamics of methyl ferulate hydrolysis. Biophysical Chemistry, 173-174, 21–30.

M. D. Jankowski, C. S. Henry, L. J. Broadbelt and V. Hatzimanikatis, 2008, Group contribution method for thermodynamic analysis of complex metabolic networks, Biophysical Journal, 95(3), 1487–1499.

S. Servi, R. Wohlgemuth and W. D. Fessner, 2013, CMST COST Action CM1303: Systems Biocatalysis, Retrieved August 26, 2014, from http://www.cost.eu/domains_actions/cmst/Actions/CM1303.

S. Riva, 2014, Cascade biocatalysis integrating stereoselective and environmentally friendly reactions. Wiley-Vch.

R. C. Simon, N. Richter, E. Busto and W. Kroutil, 2014, Recent developments of cascade reactions involving ω-transaminases, ACS Catalysis, 4(1), 129–143.

K. Tauber, M. Fuchs, J. H. Sattler, J. Pitzer, D. Pressnitz, D. Koszelewski, K. Faber, J. Pfeffer, T. Haas and W. Kroutil, 2013, Artificial multi-enzyme networks for the asymmetric amination of sec-alcohols. Chemistry (Weinheim an Der Bergstrasse, Germany), 19(12), 4030–4035.

M. D. Truppo, J. D. Rozzell, J.C. Moore, and N. J. Turner, 2009. Rapid screening and scale-up of transaminase catalysed reactions. Organic & Biomolecular Chemistry, 7(2), 395–398.

P. Tufvesson, J. S. Jensen, W. Kroutil, and J. M. Woodley, 2012, Experimental determination of thermodynamic equilibrium in biocatalytic transamination, Biotechnology and Bioengineering, 109(8), 2159–2162.

ARTICLE

BIOTECHNOLOGY and BIOENGINEERING

Enzymatic Network for Production of Ether Amines From Alcohols

Cyntia M. Palacio,[1] Ciprian G. Crismaru,[1] Sebastian Bartsch,[1] Vaidotas Navickas,[2] Klaus Ditrich,[2] Michael Breuer,[2] Rohana Abu,[3] John M. Woodley,[3] Kai Baldenius,[2] Bian Wu,[1] Dick B. Janssen[1]

[1]Department of Biochemistry, Groningen Biomolecular Sciences and Biotechnology Institute (GBB), University of Groningen, Nijenborgh 4, Groningen 9747AG, The Netherlands; telephone: +31-50-3634008; fax: 31-50-3634165; e-mail: d.b.janssen@rug.nl

[2]White Biotechnology Research, BASF SE, Ludwigshafen, Germany

[3]Department of Chemical and Biochemical Engineering, Technical University of Denmark, Lyngby, Denmark

ABSTRACT: We constructed an enzymatic network composed of three different enzymes for the synthesis of valuable ether amines. The enzymatic reactions are interconnected to catalyze the oxidation and subsequent transamination of the substrate and to provide cofactor recycling. This allows production of the desired ether amines from the corresponding ether alcohols with inorganic ammonium as the only additional substrate. To examine conversion, individual and overall reaction equilibria were established. Using these data, it was found that the experimentally observed conversions of up to 60% observed for reactions containing 10 mM alcohol and up to 280 mM ammonia corresponded well to predicted conversions. The results indicate that efficient amination can be driven by high concentrations of ammonia and may require improving enzyme robustness for scale-up.

Biotechnol. Bioeng. 2016;113: 1853–1861.

KEYWORDS: biocatalysis; alcohol dehydrogenase; aminotransferase; amination; ether amines

Introduction

Ether and polyether amines are valuable synthetic compounds with applications in diverse areas such as surface chemistry, colloid chemistry, and bioconjugate chemistry (Bayat and Akarsu, 2002; Hedberg, 1970; Mongondry et al., 2003). Polyether amines may be used as curing agents, silica deposition agents, in paintings, or as intermediates in the synthesis of polyamides or polyureas (Brandl et al., 2010; Harris et al., 1984; Lin et al., 2010). Ether amines can be produced chemically by a reaction of haloalkyl ethers with ammonia or diamines at high pH and high temperature (Buckmann et al., 1981), or by the cyanoethylation of ether alcohols with acrylonitrile followed by hydrogenation of the corresponding cyanoethers (Froimowicz et al., 2005). A more cost-effective process would be the direct conversion of an ether alcohol, using ammonia as the amine donor. Chemical manufacturing processes have been developed for such conversions employing metal catalysts (Lafrance et al., 2012) or by making use of other well-known chemical reactions (Swamy et al., 2009). However, the lack of enantio- and regioselective control often hampers these processes by formation of undesired side-products. Furthermore, the catalysts are toxic and the reactions typically require harsh conditions involving high energy use and environmental costs (Imm et al., 2011). Hence, a biocatalytic process would be an attractive alternative if it affords high efficiency and selectivity with a low energy consumption and little use of raw materials.

As there is no enzyme known to catalyze the conversion of an alcohol to the corresponding amine in a single step, multi-enzyme routes have been considered to access amines (Kohls et al., 2014; Kroutil et al., 2013; O'Reilly and Turner, 2015; Simon et al., 2014; Villegas-Torres et al., 2015). One attractive solution emulates a short metabolic pathway via an enzymatic network process that oxidizes an alcohol to an aldehyde or ketone catalyzed by an alcohol dehydrogenase (ADH), and subsequent transamination of the carbonyl compound to an amine by an aminotransferase (AT). If L-alanine is used as amino donor and NAD as electron-accepting cofactor for the dehydrogenase, their recycling is required for an efficient process. This can be done with an alanine dehydrogenase (AlaDH), which oxidizes the reduced cofactor and synthesizes alanine from pyruvate (Sattler et al., 2012). Theoretically, the recycling would allow the use of only low concentrations of NAD and alanine. In practice, a large excess of alanine has been used

Sebastian Bartsch's present address is c-LEcta GmbH, 04103 Leipzig, Germany.
Bian Wu's present address is CAS Key Laboratory of Microbial Physiological and Metabolic Engineering, Institute of Microbiology, and State Key Laboratory of Transducer Technology, Chinese Academy of Sciences, China.
Correspondence to: D.B. Janssen
Contract grant sponsor: BioNexGen
Contract grant number: 266025
Received 5 October 2015; Revision received 11 February 2016; Accepted 15 February 2016
Accepted manuscript online 23 February 2016;
Article first published online 9 March 2016 in Wiley Online Library (http://onlinelibrary.wiley.com/doi/10.1002/bit.25954/abstract).
DOI 10.1002/bit.25954

(Sattler et al., 2012), which makes it possible to overcome equilibrium or product inhibition (Shin and Kim, 2002) issues that might prevent efficient cycling in the network.

Variations of this network have been described, including, the use of other enzymes for cofactor recycling (Klatte and Wendisch, 2014, 2015; Klatte et al., 2014; Kroutil et al., 2013). For example, Tauber et al. (2013) examined regeneration of the reduced nicotinamide cofactor formed during alcohol oxidation by an NADP-dependent alcohol dehydrogenase and an NADPH oxidase, while the NADH required by alanine dehydrogenase was recycled by a formate dehydrogenase. The same group investigated the use of a lactate dehydrogenase to reduce pyruvate to lactate in order to shift the conversion of the aminotransferase step to completion. Such modifications can increase yields, but conversion becomes dependent on auxiliary reactions, that is, formate oxidation and pyruvate reduction. The two-step transformation of an alcohol to the corresponding amine has also been applied for the conversion of caprolactone to 6-aminohexanoic acid (Sattler et al., 2014), in which case a methyl ester was transiently generated to prevent formation of 6-hydroxyhexanoic acid. Recently, a variation of such a network was described in which an engineered amine dehydrogenase rather than an aminotransferase was used for direct incorporation of ammonia into ketones (Mutti et al., 2015). These studies indicate that various measures can be undertaken to improve conversion in an amination network, and raise the questions which factors restrict conversion by a self-sufficient network when no auxiliary reactions are included for recycling of intermediates.

To examine the suitability of a self-sufficient network for ether amine formation and study the factors that determine conversion, we investigated a biocatalytic process that uses ether alcohols and ammonia as the substrates to produce the ether amines. For this purpose, a redox-neutral enzymatic network of three enzymes was used (Sattler et al., 2012). Different alcohol dehydrogenases, aminotransferases, and alanine dehydrogenases were tested, and the characteristics of the system were studied by measurement of reaction equilibria, which are important parameters for the design and optimization of such biocatalytic networks (Tufvesson et al., 2012). Only few equilibrium constants for amination and alcohol oxidation reactions have been reported in the literature (Goldberg and Tewari, 1994; Goldberg et al., 2004, 2007; Tufvesson et al., 2011). We selected a primary ether alcohol (butyldiglycol, **1a**) and a secondary ether alcohol (1-butoxy-2-propanol, **2a**) as model substrates, as both the alcohols and amines are miscible with water and ether amines derived from similar compounds are used in industrial products. From experimentally determined conversion curves and reaction equilibria, it appeared that very high concentrations of ammonia can drive conversion toward effective synthesis.

Materials and Methods

Substrates and Chemicals

Butyldiglycol (**1a**), nicotinamide adenine dinucleotide (NAD), reduced nicotinamide adenine dinucleotide (NADH), L-alanine, ammonium carbamate, and sodium carbonate were purchased from Sigma–Aldrich (Zwijndrecht, the Netherlands). Compounds **1b,c** and **2a–c** were prepared by BASF (Ludwigshafen, Germany; see Supporting Information). Substrate **2a** was the (*S*)-enantiomer, in agreement with the enantioselectivity of the ADH that was selected. Pyridoxal phosphate (PLP) was purchased from Fisher Scientific (Landsmeer, the Netherlands) and pyruvic acid was acquired from Acros Organics (Geel, Belgium).

Enzymes

Enzymes tested as catalysts for the enzymatic network were alcohol dehydrogenases from *Geobacillus stearothermophilus* 1 (*Gs*ADH1, accession number BAA14411), *G. stearothermophilus* 2 (*Gs*ADH2, CAA80989), *Pseudomonas putida* (*Pp*ADH, ADR59556), or *Rhodococcus jostii* RHA1 (*Rj*ADH, ABG94302.1). Aminotransferases were from *Chromobacterium violaceum* (*Cv*AT, NP_901695), *Vibrio fluvialis* (*Vf*AT, AEA39183), and *Escherichia coli* putrescine aminotransferase (*Ep*TA, NP_417544). The two alanine dehydrogenases examined were from *Archeoglobus fulgidus* (*Af*AlaDH, AIG98665.1) and *Vibrio proteolyticus* (*Vp*AlaDH, AF070716). The coding DNA segments were obtained by gene synthesis or PCR and cloned into the expression vector pET28b or pBAD to add a hexahistidine tag (Table I). The constructs were confirmed by DNA sequencing.

The enzymes were produced in *E. coli* C41(DE3) or *E. coli* TOP10 (Table I). For this, cells were grown at 37°C in TB medium with 50 μg/mL kanamycin. Expression was induced by addition of 0.8 mM isopropyl-β-D-thiogalactopyranoside (IPTG; pET system) or 0.02% arabinose (pBAD system) when the optical density (OD_{600}) reached ca. 0.6. Cultivation was continued for 16 h at 28°C and 135 rpm. Cells were obtained by centrifugation and disrupted by sonication at 4°C, followed by centrifugation for 45 min at 15,000 rpm to obtain the cell-free extract. The enzymes were purified in a two-step procedure using metal affinity chromatography (HisTrap HP column; 5 mL; GE Healthcare, Eindhoven, the Netherlands) and a desalting step (HiPrep 26/10 column, 53 mL, GE Healthcare). The enzymes were stored frozen at −20°C in 50 mM potassium phosphate, pH 8.0.

Alcohol Dehydrogenase Reactions

Activities of different alcohol dehydrogenases were measured by following NAD reduction at 340 nm ($\varepsilon_{NADH} = 6.22 \times 10^3\,M^{-1}\,cm^{-1}$). The reaction mixtures of 1 mL contained ammonium carbamate (40 mM, pH 9), alcohol dehydrogenase (1 mg/mL), NAD^+ (1 mM) and alcohol **1a** or **2a** (10 mM). For estimating reaction equilibria, the assay system consisted of the same buffer, a suitable amount of *Gs*ADH (ca. 0.1 mg/mL), NAD^+ (0.4 mM), and alcohols **1a** (5 mM) or **2a** (0.4 mM) in a final volume of 1 mL. For the reverse reaction, the same enzyme concentration and buffer system were used with NADH (0.4 mM) and aldehyde **1b** (5 mM) or ketone **2b** (0.4 mM). The formation or depletion of NADH was followed at 340 nm at 30°C. Equilibria were calculated from Equation (2), assuming stoichiometric relationships between the change in NADH and alcohol or aldehyde.

Aminotransferase Reactions

Activities of different aminotransferases were determined by following acetophenone formation at 245 nm ($\varepsilon = 12\,mM^{-1}\,cm^{-1}$)

Table I. Expression and catalytic activities of enzymes for use in amination network.

Reaction	Enzymes	Gene[a]	Expression system	Expression (mg/L)	Activity[c] (mU/mg) **1a**/**1b**/L-Ala	Activity[c] (mU/mg) **2a**/**2b**/L-Ala
ADH	*Rhodococcus jostii* RHA1	PCR	pET/C41(DE3)	6	<1	<1
	Geobacillus stearothermophilus 1	PCR	pET/C41(DE3)	100	74	834
	Geobacillus stearothermophilus 2	PCR	pET/C41(DE3)	200	55	483
	Pseudomonas putida	Syn[b]	pET/C41(DE3)	10	12	46
AT	*Vibrio fluvialis*	Syn[b]	pET/C41(DE3)	160	3	62
	Chromobacterium violaceum	PCR	pET/C41(DE3)	200	5	78
	E. coli putrescine AT	Syn[b]	pET/C41(DE3)	80	<1	<1
AlaDH	*Archeoglobus fulgidus*	PCR	pBAD/TOP10	20	2×10^4	
	Vibrio proteolyticus	PCR	pBAD/TOP10	300	1×10^4	

[a]Gene obtained by PCR amplification of genomic DNA or as synthetic gene.
[b]Synthetic gene.
[c]One unit of enzyme activity corresponds to a conversion of 1 μmole/min under the assay conditions used. Data represent averages of measurements done in duplicate or triplicate. Average standard deviations estimated from multiple duplicate measurements were less than 10% of the reported values.

as described by Schätzle et al. (2010). The reaction mixtures contained 1-phenylethylamine (2 mM), **1b** or **2b** (10 mM), sodium phosphate (50 mM, pH 7), and aminotransferases (0.2 mg/mL).

Equilibria were estimated by incubating purified enzyme in ammonium (sodium) carbamate buffer (40 mM, pH 9) with *Cv*AT (0.35 mg/mL), L-Ala (10 mM), ketone **2b** (1 mM), and PLP (0.35 mM). Samples (1350 μL) were taken and quenched by adding NaOH (150 μL, 10 N) and ethyl acetate (500 μL). The mixture was stirred with a Vortex mixer for 30 s, sonicated, centrifuged for 1 min at 13,200 rpm and analyzed. The concentrations of the ketone **2b** and amine **2c** were determined by GC analysis, whereas the concentrations of pyruvate and L-Ala were calculated from the stoichiometry. Equilibria were calculated with Equation (3).

Alanine Dehydrogenase Reactions

Reaction mixtures contained enzyme (0.002 mg/mL), ammonium carbamate (40 mM, pH 9), NADH (0.2 mM), pyruvate (10 mM), and ammonium carbonate (125 mM). Activities were calculated from the rates of pyruvate-dependent NADH oxidation, measured at 340 nm.

The assay system for establishing the equilibrium of the alanine recycling reaction consisted of sodium carbonate (40 mM, pH 9), NAD (0.4 mM), *Vp*AlaDH (0.004 mg/ml), and L-alanine (2.5 mM) in a final volume of 1 mL. The conversion was followed by monitoring the formation of NADH at 340 nm, while the concentrations of the other components were calculated from the reaction stoichiometry.

Network Reaction Conditions

Three-enzyme conversions were routinely performed in reaction mixtures (15 mL) containing ammonium carbamate buffer (40 mM, pH 9), alcohol **1a** or **2a** (10 mM, final concentration), NAD^+ (1 mM), L-Ala (0.5 mM), PLP (0.35 mM), *Gs*ADH (0.1 mg/mL), *Vp*AlaDH (0.004 mg/mL for **1a** and 0.04 mg/mL for **1b**) and *Cv*AT (0.064 mg/mL). The mixtures were incubated in 50 mL glass bottles at 30°C, and samples were taken at different times for analysis by gas chromatography (GC). Apparent equilibrium constants (K′) were calculated with Equation (1). For these calculations and in Tables and Figures, we used nominal concentrations of ammonia representing the sum of protonated and unprotonated species and assuming complete dissociation of carbamate to 2 equivalents of ammonia (Wang et al., 1972).

Optimization was studied by individually varying concentrations of ammonium (80 mM, 200 mM, 400 mM, 1 M, or 2 M), alcohol **1a** (5, 10, 20, 50, and 100 mM), L-Ala (0.5, 1, 2.5, and 5 mM), and NAD^+ (0.125, 0.25, 0.5, and 1 mM). PLP was kept at 0.35 mM and enzyme concentrations were *Gs*ADH at 0.1 mg/mL, *Vp*AlaDH at 0.004 mg/mL, and *Cv*AT at 0.064 mg/mL.

Results and Discussion

Enzyme Production and Selection

To establish a three-enzyme network for alcohol to amine conversion, we first examined several enzymes for each reaction step. We cloned and expressed four alcohol dehydrogenases for the oxidation of **1a** and **1b**, three transaminases for the transamination of the corresponding aldehyde (**1b**) and ketone (**2b**), and two alanine dehydrogenases for the recycling of the cofactors and amino donors (Table I). All enzymes were expressed in soluble form and were purified by His-tag affinity chromatography.

Activity assays with the purified enzymes were performed as described under Materials and Methods to select suitable enzymes for the designed network. The results in Table I show that the thermostable ADH from *G. stearothermophilus* 1 (*Gs*ADH1) and the aminotransferase from *C. violaceum* (*Cv*AT) had the highest activity toward **1a** and **2a**, and **1b** and **2b**, respectively. These were, therefore, selected for further use. The thermostable and highly active AlaDH from *V. proteolyticus* (*Vp*AlaDH) was used for cofactor recycling because of its high activity and high overexpression in *E. coli*.

Network Reactions

Having selected suitable enzymes, we tested the possibility for a network reaction with **1a** and **2a** as substrates (10 mM) in the presence of all three enzymes (Fig. 1). In the initial tests, eight

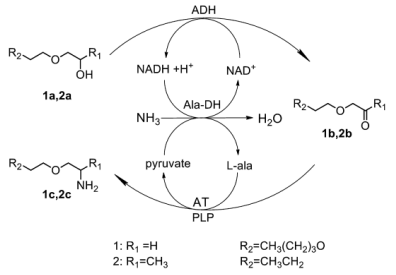

Figure 1. Enzymatic network with **1a** and **2a** as substrates. The proposed enzymatic cycle encompasses three enzymes: an alcohol dehydrogenase (*Gs*ADH1) that converts the alcohol to a ketone or an aldehyde; a transaminase (*Cv*AT) that converts the ketone or the aldehyde to the amine with L-Ala as the amino donor; and an alanine dehydrogenase (*Vp*AlaDH) that converts pyruvate to L-Ala with simultaneous recycling of NADH to NAD^+.

equivalents of ammonia and one equivalent of L-Ala were added (final concentrations 80 and 10 mM, respectively). For both substrates, conversion of ether alcohol to ether amine reached a promising 40%, using the network reaction conditions described in Materials and Methods.

We next examined the effect of varying concentration of substrates on the conversion, aiming at a higher yield of the ether amines. For this, we performed time course experiments in which supposedly important conditions were varied, especially the concentrations of alcohol substrate, cofactor (NAD^+), L-Ala, and ammonium. First, different concentrations of alcohol **1a** were tested in the range from 5 to 100 mM. The highest yields and conversions rates were observed with the lower concentrations of **1a** (Fig. 2A). The highest accumulation of product **1b** was obtained with 50 mM alcohol, but the conversion of substrate to amine decreased at the highest concentration of **1a** almost to zero. Further reactions were carried out with alcohol concentrations in the range of 5 to 10 mM because these gave the best conversion (Fig. 2A).

Next, the effect of increasing ammonium concentrations was measured as this might shift the equilibrium of the reaction. However, increasing the concentration by adding different level of ammonium (80 mM, 200 mM, and 1M) did not improve the percentage of conversion of **1a–c**, and conversion was significantly reduced above 200 mM ammonia while precipitation of enzymes was observed. The best conversion was observed at 80 mM of ammonia (Fig. 2B).

We also examined the effect of varying L-Ala concentrations. The conversion to amine **1c** was only slightly affected by the level of L-Ala added (Fig. 2C). Importantly, at a low concentration of L-Ala (0.5 mM) conversion to amine already reached 30%, and conversion was not better at higher levels. Furthermore, L-Ala was indeed recycled, as the level of amine produced (3 mM) was sixfold higher than the level of L-Ala added (0.5 mM). Subsequent experiments on the amination of **1a** and **2a** were carried out with 0.5 mM L-Ala.

Finally, the level of NAD was varied. Good conversion was obtained with 1 mM NAD added (Fig. 2D), whereas conversion was reduced when the cofactor concentration was lower. As the final concentration of product **1c** (4 mM) was higher than that of cofactor (1 mM), also AlaDH-mediated cofactor recycling was working properly. Further experiments were carried out with 1 mM NAD^+.

A series of optimization measures were tested, in which substrate, amino donor, ammonium, and cofactor concentrations were varied in different combinations. These attempts did not lead to identification of reaction conditions that improved conversion beyond 40% for **1a–c** and conversion also did not exceed 40% for **2a–c**. This suggests that equilibrium factors, in combination with effects of ammonia on enzyme activity, were limiting the degree of conversion.

Reaction Equilibria

In agreement with observations on other reactant systems (Höhne et al., 2008), the thermodynamic equilibrium was postulated to limit conversion in the three-enzyme amination network. To examine this possibility, we measured the apparent equilibrium constants of the three-enzyme network and of separate reactions. Following the notation of Goldberg (2014), the equilibrium for the overall conversion of alcohol to amine (K'_N) is given by Equation (1), while Equation (2) gives the apparent equilibrium constant for alcohol oxidation (K'_o), Equation (3) for the aminotransferase reaction, and K'_r in Equation (4) stands for the recycling step or alanine dehydrogenase reaction. The numbers are pH-dependent. All measurements were done at pH = 9.0.

$$K'_N = \frac{[Ami]}{[Alc][NH_4^+]} \quad (1)$$

$$K'_o = \frac{[NADH][Ald]}{[NAD^+][Alc]} \quad (2)$$

$$K'_t = \frac{[Pyr][Ami]}{[Ala][Ald]} \quad (3)$$

$$K'_r = \frac{[NAD^+][Ala]}{[Pyr][NH_4^+][NADH]} \quad (4)$$

In these equations, [Ami] stands for the equilibrium concentrations of amines **1c** or **2c**, [Alc] stands for the alcohols **1a** or **2a**, [Ald] stands for aldehyde **1b** or ketone **2b**, [Pyr] for pyruvate, and $[NH_4^+]$ is the total nominal concentration of ammonia. The other abbreviations have their usual meaning. By convention, water is fixed at 1 and does not appear in the equilibrium constants (Goldberg, 2014). All concentrations are lumped for different protonation states, which are obviously pH dependent.

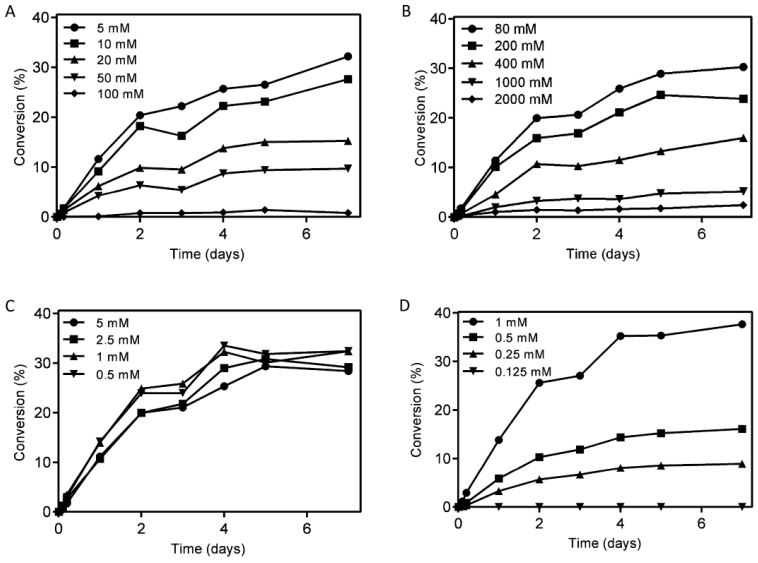

Figure 2. Time course of ether amine formation under different reaction conditions. Panels: **A**, varying substrate alcohol **1a**; **B**, varying ammonium; **C**, varying amino donor (L-alanine); **D**, varying cofactor (NAD) concentration.

The apparent equilibrium constant of the whole network should match the equilibrium constants of the separate reactions (Equation (5)).

$$K'_N = K'_o \cdot K'_t \cdot K'_r \qquad (5)$$

Although prior studies have shown that the equilibrium of transamination reactions with a ketone or aldehyde as substrate and L-Ala as amino donor is in the direction of the amino acid (Koszelewski et al., 2010), little is known about the equilibrium of the oxidation reaction of ether alcohols to ether ketones or ether aldehydes. Some equilibrium data of alcohol/ketone redox reactions have been reported in the literature (Goldberg et al., 1993, 2007), but the equilibrium constants were calculated at different temperatures, buffer conditions, and with different compounds. In order to establish the position of the various equilibria, reactions with the three enzymes were performed separately as described in Materials and Methods.

All the equilibrium constants (K'_N, K'_o, K'_r and K'_t) shown in the Table II were calculated from experimental measurements, except for the value of K'_t for the reaction of **1b–c**. Due to the reactivity of **1b** with product **1c** under the conditions of sample preparation, the analysis of **1c** was not reliable. A value for K'_t was estimated from the other experimentally measured constants.

The apparent equilibrium constants K'_o calculated with Equation (2) from conversion data (Fig. 3A) showed that alcohol oxidation is unfavorable for substrates **1a** and **2a** (Table II). Similar equilibrium constants were reported for 1-butanol ($1.8 \cdot 10^{-3}$) and for 1-octanol oxidation ($1.1 \cdot 10^{-3}$) confirming that NAD-coupled alcohol oxidation is thermodynamically rather unfavorable (Goldberg et al., 1993). Especially for ether alcohol **1a**, the equilibrium is strongly in the direction of the alcohol.

The aminotransferase equilibrium (Equation (3)) of **2b** and **2c** was estimated by GC analysis (Fig. 3B). The equilibrium constants appeared to be highly unfavorable both for ether aldehyde and ether ketone amination (Table II). Especially the K'_t value for conversion of ether ketone **2b** to amine **2c** illustrates poor acceptance of an amino group. The observed unfavorable equilibrium of the aminotransferase reaction is in agreement with the equilibrium constant reported for the transamination of 2-oxoglutarate and L-Ala ($2.9 \cdot 10^{-3}$; Goldberg and Tewari, 1994). Additionally, the equilibrium constant of the transamination of acetophenone with alanine to produce 1-phenylethylamine is reported to be $8.81 \cdot 10^{-4}$ (Koszelewski et al., 2010), which is also strongly favorable toward the

Table II. Experimental equilibrium constants at 30°C and pH 9.0. Mean values are reported ± the standard error of the mean.

				K'_N (M^{-1})	
Substrate	K'_o (ADH)	K'_t (AT)	K'_r (M^{-1}) AlaDH	Experimental	Calculated
1a, 1b	$2.6 \times 10^{-4} \pm 2.9\ 10^{-6}$	6.1×10^{-2a}	$8.23 \times 10^{+5} \pm 4.23\ 10^{+4}$	13.1 ± 0.45	–
2a, 2b	0.14 ± 0.004	$4.0 \times 10^{-4} \pm 4.7\ 10^{-6}$		12.1 ± 1.28	46[b]

[a]This value was calculated from the experimental values of K'_o, K'_r, and K'_N, from Equation (5).
[b]This value was calculated with Equation (5).

substrates. Obviously, transfer of the charged (at neutral pH) amino group from the zwitterionic L-Ala to an apolar acceptor is not favored.

The alanine dehydrogenase equilibrium was measured by following NADH formation (Fig. 3C). The equilibrium constant appeared highly favorable for recycling of alanine as amine donor and NAD^+ as electron acceptor for alcohol oxidation, and predicts an L-alanine/pyruvate ratio of 82,000 per M of ammonia present at equal concentrations of NAD^+ and NADH. The equilibrium constants obtained here are in the same range as those reported for similar substrates by Goldberg et al. (1993, 2007).

From these individual equilibria, it appears that conversion of **1a–c** and of **2a–c** are both thermodynamically feasible (Table II), mainly due to the alanine recycling reaction, which strongly favors alanine and NAD^+ formation thereby driving the alcohol oxidation and aminotransferase reactions.

Implications for Network Reactions

The relationship between the overall reaction equilibrium K'_N and the theoretical maximal conversion in the three-enzyme network was examined. As a very low concentration of NAD^+ was used, the accumulation of aldehyde or ketone is negligible in Equation (1), and ammonia-dependent conversion of alcohol to amine is given by

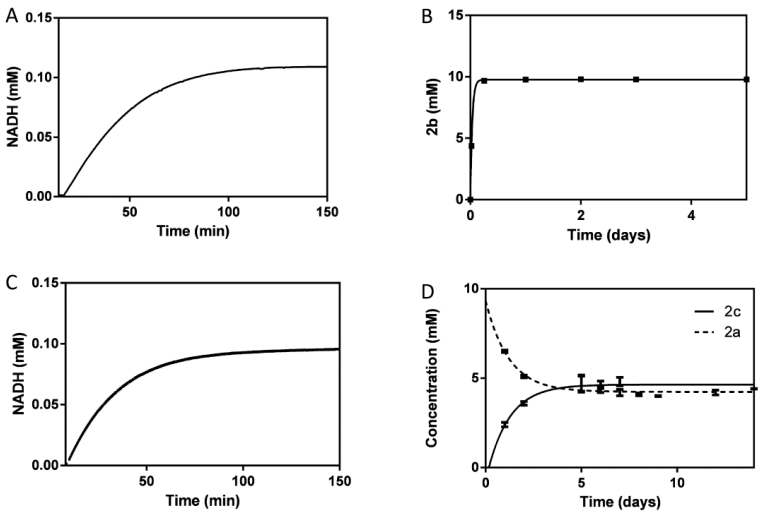

Figure 3. Estimation of reaction equilibria. **Panel A**: Formation of NADH by *Gs*ADH acting on the oxidation of alcohol **2a**. **Panel B**: Production of ketone **2b** catalyzed by *Cv*AT. **Panel C**: NADH formation in the conversion of L-Ala to pyruvate, catalyzed by *Vp*AlaDH. **Panel D**: Progress curves for alcohol **2a** consumption and amine **2c** production in the complete enzymatic network. Reaction conditions are described in Materials and Methods. Curves are representative examples of experiments that were performed in duplicate.

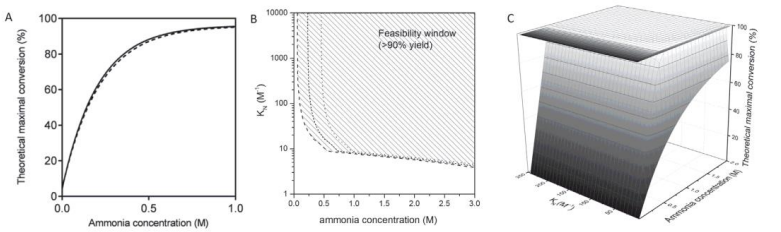

Figure 4. Maximal conversion in amination networks based on equilibria. **Panel A**: Predicted maximal conversion of 10 mM ether alcohol to the corresponding ether amine with different concentrations of ammonia. The solid line represents $K'_N = 13.1$ for reaction **1a–c**. The dashed line represents $K'_N = 12.1$ for reaction **2a–c**. **Panel B**: Feasibility of operation window of the amination network as a function of K'_N and ammonia concentration. Lines: dotted line, $[alcohol]_0 = 0.1$ M; short dashed line, $[alcohol]_0 = 0.5$ M; long dash, $[alcohol]_0 = 1$ M. **Panel C**: Surface representing the theoretical maximal conversion (%) dependent on the ammonia concentration and the K'_N of the network.

$$K'_N = \frac{[\mathrm{Ami}]}{\left([\mathrm{Alc}]_0 - [\mathrm{Ami}]\right)\left([\mathrm{NH_4^+}]_0 - [\mathrm{Ami}]\right)} \qquad (6)$$

where $[\mathrm{Alc}]_0$ is the initial concentration of the ether alcohol and $[NH_4^+]_0$ is the initial concentration of ammonia (sum of ionization states). Conversion in the whole network can be calculated from

Equation (7) describes the theoretical maximal conversion as a function of the overall reaction equilibrium K'_N and the initial substrate concentrations, and was used to calculate the maximum conversion at different concentrations of ammonia (Fig. 4A). To visualize the conditions at which amination becomes feasible, we also plotted the >90% conversion window as a function of K'_N and the initial ammonia loading (Fig. 4B). The plot shows that K'_N should be at least 10–100 to obtain a product yield exceeding 90%.

$$c = \frac{[\mathrm{Ami}]}{[\mathrm{Alc}]_0} = \frac{\left([\mathrm{Alc}]_0 + [\mathrm{NH_4^+}]_0 + \frac{1}{K'_N}\right) - \sqrt{\left([\mathrm{Alc}]_0 + [\mathrm{NH_4^+}]_0 + \frac{1}{K'_N}\right)^2 - 4[\mathrm{Alc}]_0[\mathrm{NH_4^+}]_0}}{2[\mathrm{Alc}]_0} \qquad (7)$$

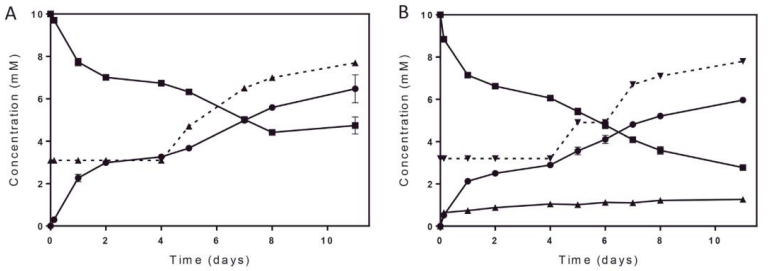

Figure 5. Time course of alcohol to amine conversion by a three-enzyme network. **Panel A**: Observed conversion of alcohol **1a** (squares) to amine **1c** (closed circles) as compared to predicted maximum conversion (inverted triangles, calculated using Equation (7)). The concentration of aldehyde **1b** remained below the detection limit (<0.03 mM). **Panel B**: observed conversion of alcohol **2a** (squares) to ketone **2b** (triangles) and amine **2c** (closed circles) and theoretical maximum conversion (inverted triangles). The reactions were carried out at 30°C in ammonium carbamate buffer (40 mM, pH 9), substrate alcohol (**1a**) or (**2a**) (10 mM), NAD^+ (1 mM), PLP (0.35 mM), L-Ala (0.5 mM), *Gs*ADH (0.1 mg/mL), *Vp*AlaDH (0.004 mg/mL), and *Cv*ωAT (0.064 mg/ml). Pulses of ammonium and re-addition of enzyme took place after sampling at 4 days (40 mM ammonium), 6 days (80 mM), 7 days (40 mM), and 8 days (80 mM) for 1a and 2a. Samples were analyzed in duplicate. Data show a representative example of an experiment carried out in duplicate.

The dependence of the yield on K'_N and ammonia concentration is further plotted in Figure 4C, again illustrating the requirement of a high K'_N (>10) and high ammonium concentrations (>0.5 M) for effective amination.

These results show that the conversion of the three-enzyme amination networks can be limited by an unfavorable equilibria of the final amination steps yielding amines **1c** and **2c** and of the formation of the intermediates aldehyde **1b** and ketone **2b**. The use of a high ammonium concentration can drive the equilibrium to product formation.

Reaction Optimization

Using Equation (7) as a guide, we attempted to further improve conversion of alcohol to amine. For reactions **1a–c** and **2a–c**, at least 0.7 M of ammonia is predicted to be required for a good conversion (>95% yield, Fig. 4A). Therefore, conversion was tested with a range of ammonia concentrations varying from 80 mM to 1 M. However, addition of ammonia to concentrations exceeding 200 mM caused precipitation of the enzymes, as indicated by visual turbidity and SDS–PAGE analysis of the precipitate. The latter indicated that all three enzymes formed precipitating aggregates (data not shown). Therefore, reactions were run with repeated addition of smaller amounts of ammonia (concentration 80 mM) and of enzyme (*Gs*ADH [0.1 mg/mL], *Vp*AlaDH [0.004 mg/mL] and *Cv*AT [0.064 mg/mL]), and the production of ether amine was followed over time. This strategy resulted in improved yields. The highest conversion was found with stepwise addition of a total 280 mM ammonium, which afforded a conversion of 60% for **1a–c** and for **2a–c** (Fig. 5). To the best of our knowledge, these are the highest conversions reached in such a three-enzyme network for secondary amine production using purified enzymes as catalysts (Tauber et al., 2013).

The time course experiment with stepwise addition of ammonium and enzyme showed that the accumulation of amine correlated reasonably well with predictions for maximum conversion based on reaction equilibria (Fig. 5), suggesting that conversions indeed became equilibrium-limited. The final product concentrations of amines **1c** and **2c** were 6 mM, exceeding the level of added nicotinamide cofactor (1 mM NAD^+) and L-Ala (0.5 mM for **1a**), again indicating effective recycling in the alanine dehydrogenase reaction. This is in agreement with the equilibrium calculations, which showed that cofactor recycling is an essential component of the network since it drives the overall conversion toward amine synthesis.

Although cofactor recycling networks were reported earlier (Findrik and Vasic-Racki, 2009; Kragl et al., 1996; Yun et al., 2003), amination networks are usually operated in the presence of an excess of L-Ala, which may be added up to a 25-fold excess (Klatte and Wendisch, 2014; Sattler et al., 2012). Alternatively, amination is driven by an additional redox reactions, such as the conversion of NADH to NAD^+ by an NADH oxidase (Findrik et al., 2008), or the conversion of pyruvate to lactate (Koszelewski et al., 2010). For example, Klatte and Wendisch (2014) used whole cells expressing the three enzymes of the network with addition of cofactors, amino donor, ammonia source, and substrates. They described a conversion of 100% with 1,10-diaminodecane (10 mM) with addition of 250 mM (25 equivalents) of L-alanine. Equimolar concentrations of alanine and alcohol substrate were effective when transamination was stimulated by oxidase-mediated conversion of the produced pyruvate (Klatte and Wendisch, 2015).

In conclusion, the biocatalytic conversion of ether alcohols to the corresponding amines with ammonia as the sole additional substrate would be an attractive process. In the current study, we describe an amination cycle using an alcohol dehydrogenase, an aminotransferase, and an alanine dehydrogenase that recycles both the nicotinamide cofactor (NAD^+) for the alcohol dehydrogenase and the amine donor alanine (L-Ala) for the aminotransferase. Equilibrium measurements showed that conversion of alcohol to aldehyde or ketone is disfavored, as is the amination of aldehyde and ketone. The overall conversion of alcohol to amine is based on the alanine dehydrogenase-mediated formation of L-Ala and NAD^+. Using measured and computed equilibrium constants, theoretical maximum conversions and feasible operation windows were calculated. High ammonia concentrations can drive the overall reaction, giving conversions of up to 60%, in agreement with equilibria. The results further suggest that enzyme robustness, especially resistance and maintenance of activity at high concentrations of ammonia and high pH, is a key factor when pursuing practical application of the suggested amination network.

C.M.P. was supported by an Eurotango fellowship 2012. This research also received funding from the European Union's Seventh Framework Programme for research, technological development and demonstration under grant agreement 266025 (BioNexGen).

References

Bayat O, Akarsu H. 2002. Evaluation of new collectors for silica/glass sand and statistical analysis of plant trials. Miner Eng 15:293–296.

Brandl FP, Seitz AK, Teßmar JK V, Blunk T, Göpferich AM. 2010. Enzymatically degradable poly(ethylene glycol) based hydrogels for adipose tissue engineering. Biomater Sci 31:3957–3966.

Buckmann AF, Morr M, Johansson G. 1981. Functionalization of poly(ethy1ene glycol) and monomethoxy-poly(ethy1ene glycol). Makromol Chem 1384:1379–1384.

Findrik Z, Šimunović I, Vasić-Rački D. 2008. Coenzyme regeneration catalyzed by NADH oxidase from *Lactobacillus brevis* in the reaction of l-amino acid oxidation. Biochem Eng J 39:319–327.

Findrik Z, Vasic-Racki D. 2009. Overview on reactions with multi-enzyme systems. Chem Biochem Eng Q 23:545–553.

Froimowicz P, Gandini A, Strumia M. 2005. New polyfunctional dendritic linear hybrids from terminal amine polyether oligomers (Jeffamine): Synthesis and characterization. Tetrahedron Lett 46:2653–2657.

Goldberg RN. 2014. Standards in biothermodynamics. Perspect Sci 1:7–14.

Goldberg RN, Tewari YB. 1994. Thermodynamics of enzyme catalyzed reactions transferases. J Phys Chem Ref Data 23:547–617.

Goldberg RN, Tewari YB, Bell D, Fazio K. 1993. Thermodynamics of enzyme-catalyzed reactions: Part 1. Oxidoreductases. J Phys Chem Ref Data 22:515–582.

Goldberg RN, Tewari YB, Bhat TN. 2004. Thermodynamics of enzyme-catalyzed reactions-a database for quantitative biochemistry. Bioinformatics 20:2874–2877.

Goldberg RN, Tewari YB, Bhat TN. 2007. Thermodynamics of enzyme-catalyzed reactions: Part 7. J Phys Chem Ref Data 36:1347–1397.

Harris JM, Struck EC, Case MG, Paley MS, Yalpani M, van Alstine JM, Brooks DE. 1984. Synthesis and characterization of poly(ethylene glycol) derivatives. J Polym Sci Polym Chem Ed 22:341–352.

Hedberg MC. 1970. Cationic flotation of silica from magnetic iron-ore concentrates. J Am Oil Chem Soc 47:177–179.

Höhne M, Kühl S, Robins K, Bornscheuer UT. 2008. Efficient asymmetric synthesis of chiral amines by combining transaminase and pyruvate decarboxylase. Chembiochem 9:363–365.

Imm S, Bähn S, Zhang M, Neubert L, Neumann H, Klasovsky F, Pfeffer J, Haas T, Beller M. 2011. Improved ruthenium-catalyzed amination of alcohols with ammonia: Synthesis of diamines and amino esters. Angew Chem Int Ed Engl 123:7741–7745.

Klatte S, Lorenz E, Wendisch VF. 2014. Whole cell biotransformation for reductive amination reactions. Bioengineered 5:56–62.

Klatte S, Wendisch VF. 2014. Redox self-sufficient whole cell biotransformation for amination of alcohols. Bioorg Med Chem 22:5578–5585.

Klatte S, Wendisch VF. 2015. Role of L-alanine for redox self-sufficient amination of alcohols. Microb Cell Factories 14:9.

Kohls H, Steffen-Munsberg F, Höhne M. 2014. Recent achievements in developing the biocatalytic toolbox for chiral amine synthesis. Curr Opin Chem Biol 19: 180–192.

Koszelewski D, Tauber K, Faber K, Kroutil W. 2010. Omega-transaminases for the synthesis of non-racemic alpha-chiral primary amines. Trends Biotechnol 28:324–332.

Kragl U, Vasic-Racki D, Wandrey C. 1996. Continuous production of L-*tert*-leucine in series of two enzyme membrane reactors. Bioprocess Eng 14:291–297.

Kroutil W, Fischereder E, Fuchs CS, Lechner H, Mutti FG, Pressnitz D, Rajagopalan A, Sattler JH, Simon RC, Siirola E. 2013. Asymmetric preparation of *prim*-, *sec*-, and *tert*-amines employing selected biocatalysts. Org Process Res Dev 17: 751–759.

Lafrance M, Roggen M, Carreira EM. 2012. Direct, enantioselective iridium-catalyzed allylic amination of racemic allylic alcohols. Angew Chem Int Ed Engl 51:3470–3473.

Lin J-J, Chan Y-N, Chan W-H. 2010. N-Amphiphilic poly(oxyalkylene)-amines interacting with layered clays: Intercalation, exfoliation, and new applications. In: Geckeler KR, Nishide H, editors. Advanced nanomaterials. Weinheim, Germany: Wiley-VCH Verlag. p 459–478.

Mongondry P, Bonnans-Plaisance C, Jean M, Tassin JF. 2003. Mild synthesis of amino-poly (ethylene glycol) s. Application to steric stabilization of clays. Macromol Rapid Commun 24:681–685.

Mutti FG, Knaus T, Scrutton NS, Breuer M, Turner NJ. 2015. Conversion of alcohols to enantiopure amines through dual-enzyme hydrogen-borrowing cascades. Science 349:1525–1529.

O'Reilly E, Turner NJ. 2015. Enzymatic cascades for the regio- and stereoselective synthesis of chiral amines. Perspect Sci 4:55–61.

Sattler JH, Fuchs M, Mutti FG, Grischek B, Engel P, Pfeffer J, Woodley JM, Kroutil W. 2014. Introducing an in situ capping strategy in systems biocatalysis to access 6-aminohexanoic acid. Angew Chemie Int Ed Engl 53:14153–14157.

Sattler JH, Fuchs M, Tauber K, Mutti FG, Faber K, Pfeffer J, Haas T, Kroutil W. 2012. Redox self-sufficient biocatalyst network for the amination of primary alcohols. Angew Chem Int Ed Engl 51:9156–19459.

Schätzle S, Höhne M, Robins K, Bornscheuer UT. 2010. Conductometric method for the rapid characterization of the substrate specificity of amine-transaminases. Anal Chem 82:2082–2086.

Shin JS, Kim BG. 2002. Substrate inhibition mode of ω-transaminase from *Vibrio fluvialis* JS17 is dependent on the chirality of substrate. Biotechnol Bioeng 77:832–837.

Simon RC, Richter N, Busto E, Kroutil W. 2014. Recent developments of cascade reactions involving ω-transaminases. ACS Catal 4:129–143.

Swamy KCK, Kumar NNB, Balaraman E, Kumar KVPP. 2009. Mitsunobu and related reactions: Advances and applications. Chem Rev 109:2551–2651.

Tauber K, Fuchs M, Sattler JH, Pitzer J, Pressnitz D, Koszelewski D, Faber K, Pfeffer J, Haas T, Kroutil W. 2013. Artificial multi-enzyme networks for the asymmetric amination of *sec*-alcohols. Chem Eur J 19:4030–4035.

Tufvesson P, Jensen JS, Kroutil W, Woodley JM. 2012. Experimental determination of thermodynamic equilibrium in biocatalytic transamination. Biotechnol Bioeng 109:2159–2162.

Tufvesson P, Lima-Ramos J, Jensen JS, Al-Haque N, Neto W, Woodley JM. 2011. Process considerations for the asymmetric synthesis of chiral amines using transaminases. Biotechnol Bioeng 108:1479–1493.

Villegas-Torres MF, Martinez-Torres RJ, Cazeres A, Hailes H, Baganz F, Ward J. 2015. Multi-step biocatalytic strategies for chiral amino alcohol synthesis. Enz Microb Technol 81:23–30.

Wang TT, Bishop SH, Himoe A. 1972. Detection of carbamate as a product of the carbamate kinase-catalyzed reaction by stopped flow spectrophotometry. J Biol Chem 247:4437–4440.

Yun H, Yang Y-H, Cho B-K, Hwang B-Y, Kim B-G. 2003. Simultaneous synthesis of enantiomerically pure (*R*)-1-phenylethanol and (*R*)-alpha-methylbenzylamine from racemic alpha-methylbenzylamine using omega-transaminase/alcohol dehydrogenase/glucose dehydrogenase coupling reaction. Biotechnol Lett 25: 809–814.

Supporting Information

Additional supporting information may be found in the online version of this article at the publisher's web-site.

CAPEC-PROCESS Research Center
Department of Chemical and Biochemical Engineering
Technical University of Denmark
Building 229
DK – 2800 Kgs. Lyngby
Denmark

Phone: +45 45 25 28 00
Web: capec-process.kt.dtu.dk